HYDROLOGIC, NUTRIENT, AND SEDIMENT RESPONSES OF RESTORED PERENNIAL VEGETATION/WETLAND COMPLEXES IN SOUTHERN MINNESOTA

A THESIS
SUBMITTED TO THE FACULTY OF THE GRADUATE SCHOOL
OF THE UNIVERSITY OF MINNESOTA
BY

GREG DAVID FRANSEN

IN PARTIAL FULFILLMENT OF THE REQUIREMENTS
FOR THE DEGREE OF
MASTER OF SCIENCE

Kenneth N. Brooks, Ph. D, Advisor

March, 2012

Acknowledgements

I would like to thank my adviser, Ken Brooks, and my committee members, Hobie Perry and Brandy Toner, for their intelligence, humor, enthusiasm, and patience; Peter Ffolliott and the Ffolliott Fellowship for financial support; the property owners of our research sites for their generosity in allowing us access to their land; and the faculty and staff of the University of Minnesota Department of Forest Resources for their commitment to the University's mission of research and education.

Dedication

This thesis is dedicated to my family members, who have faithfully supported me in all my endeavors.

Abstract

The Blue Earth River basin, located in the prairie pothole region of northern Iowa and southern Minnesota, is intensively ditched and drained to improve agricultural production. Agricultural drainage systems increase watershed drainage density and can efficiently transport easily leachable agricultural contaminants, such as nitrate, to receiving water bodies. This thesis examines the hydrologic and water quality benefits provided by two restored perennial vegetation-wetland complexes in the Elm Creek subwatershed of the Blue Earth River basin. Flow measurements and water quality samples were collected at the wetland outlets and at drain tiles and surface channels flowing into the wetlands. Four years of flow data showed that the wetlands reduced the magnitude of peak flows to Elm Creek, but that they did not significantly reduce water yield compared to the agricultural watersheds. The restored wetlands decreased nitrate export by 85 percent during the months of April to June, the period when nitrate from agricultural drainage water contributes to formation of the "dead zone" in the Gulf of Mexico. The wetlands did not significantly decrease phosphorus or sediment export to Elm Creek. Water quality benefits attained by trapping phosphorus and sediment from surface runoff were offset by internal phosphorus loading, algal blooms, and sediment resuspension. Empirical modeling of one wetland basin showed that wind speed and wind direction could explain 60 percent of the suspended sediment concentration within the wetland. Active management of water levels and wetland vegetation are presented as strategies to reduce sediment and phosphorus export from restored wetland basins.

Table of Contents

List of Tables

List of Figures

Introduction and Problem Statement

Wetlands are among the most endangered ecosystems in the world. Occurring in myriad forms on many landscapes, wetlands contribute ecological services by mitigating floods, trapping nutrients and sediments, and providing wildlife habitat. However, loss of wetlands through land use conversion has resulted in increased flooding, degraded water quality, and decreased the biodiversity of many watersheds.

South-central Minnesota was once characterized by tallgrass prairie vegetation and a groundwater-flow dominated system of depressional wetlands, or "prairie potholes". These wetlands were part of a landscape known as the prairie pothole region (PPR), which stretched northwest from central Iowa through southern and western Minnesota, eastern South Dakota, central North Dakota, and into Canada. Over the last century, the major land use of the southern prairie pothole region (PPR) in Minnesota and Iowa has been changed to corn and soybean row crop agriculture. Much of this region has been drained by networks of surface ditches and subsurface tile lines to increase arable land area and improve crop yields; in some watersheds greater than 80% of the wetlands were drained (Quade 2000).

The importance of wetlands to ecological functioning is now widely recognized. Remnant wetlands in U.S. agricultural landscapes are protected by the 'Swampbuster' provisions of the Food Security Act of 1985 (United States Congress 1985). Restoration of damaged or destroyed wetlands has become an important objective for both private and governmental organizations. Drained or degraded wetlands have been restored by non-profit organizations such as Ducks Unlimited and the Nature Conservancy, by federal and state wildlife agencies, and by conservation-minded landowners, often with support from government conservation programs.

One government program, the Minnesota River Conservation Reserve Enhancement Program (CREP I), combined USDA funding dedicated to the protection of soil resources with state funding dedicated to the preservation of critical wildlife habitat. Administered by the Minnesota Board of Water and Soil Resources (BWSR), CREP I

was designed to restore habitat and improve water quality in the Minnesota River and its tributaries by restoring wetlands and converting adjacent erosion-sensitive lands from row-crop agriculture to perennial vegetation. The program met its goal of 100,000 acres (~40,500 hectares) of grasslands and wetlands enrolled in the five year period between 1998 and 2002, at a cost of $244 million (Minnesota Board of Water and Soil Resources 2004c).

Experience with past restoration projects has shown that care must be taken in order to produce wetlands that provide ecological benefits while remaining within site and budgetary constraints. Restoration projects that lie along existing public drainage systems are required to maintain drainage for croplands lying "upstream" and should not increase the risk of flooding to adjacent fields. Therefore, restored wetlands in the southern PPR rarely duplicate the original hydrology of the site and their potential to improve water quality or other ecological benefits is limited (Galatowitsch and Van der Valk 1998).

This thesis examines the hydrologic and water quality benefits provided by two restored perennial vegetation-wetland complexes in south-central Minnesota. The wetlands were restored in 2004-2005 under the CREP-I program using a flow-through strategy. Existing drain tile lines were redirected to the surface and then cut to fill the basins, and water control structures were installed to allow excess water to discharge to outflowing tile lines. From 2005 to 2008, wetland inlets and outlets were monitored continuously during the growing season to measure discharge, while grab samples were taken at intervals to determine concentrations of total suspended solids (TSS), ortho-phosphate (OP), total phosphorus (TP) and nitrate+nitrite-N (NN). Data from 2005, 2006 and early 2007 were collected by other members of the University of Minnesota Forest Hydrology group. Results for 2005-2006 have been published previously (Lenhart 2008).

The thesis is organized into two chapters:

1. Hydrologic and water quality response to restoration of perennial vegetation/wetland complexes.
2. A wind-based model to estimate the contribution of wind-aided sediment resuspension to TSS export.

Chapter 1 Watershed Response

1.1 Literature Review

1.1.1 Introduction

Chemical characteristics of fresh water are directly related to the climate, vegetation, geology, topography, and land use of the watershed from which the water flows. The Blue Earth River basin (BER), located in the prairie pothole region of northern Iowa and southern Minnesota, is intensively farmed due to its favorable climate and rich soils. Before European settlement of North America, the wetlands of the BER provided storage for snowmelt and precipitation events, thereby delaying the delivery of stormwater to nearby creeks and rivers by intercepting surface runoff and converting it to subsurface flow. During the past century, the drainage density of the BER and other basins of the southern PPR has increased through installation of subsurface drain tiles, wetland area has decreased through drainage, and land cover has been converted from perennial grasses and forbs to annual summer season row crops.

Global population growth promises to put increasing pressure on natural resources even as public awareness of land use and water quality issues grows. In this context, it is important that watershed managers make choices that provide local ecological benefits while maintaining agricultural productivity and minimizing negative impacts to downstream areas. Because the interactions between water yield, peak flows, and nutrient and sediment loading are complex, a reading of relevant literature is required to understand the integrated response of a watershed to land use changes such as restoration of perennial cover and wetlands.

1.1.2 Water Yield

Water yield increases due to agricultural influences within the Mississippi River basin have been reported at both large and small scales. Using alkalinity as a proxy for discharge, Raymond et al. analyzed 100 years of streamflow records from the Mississippi River basin and found that in subwatersheds with high (>70%) proportions of croplands, discharge in response to average precipitation had increased by approximately 40 mm per year(Raymond and others 2008). In a more localized study (Schilling 2005), three river basins of the southern PPR ranging from 1362 km^2 to 4193 km^2 showed increases in baseflow of 79 mm to 130 mm over 60 to 70 year periods that ended in 2000. This increase coincided with the approximate doubling of the proportion of row crop land use to greater than 80% in the river basins. Finally, in a study of small watersheds in the Minnesota River basin, flood frequency analysis showed an increase in the peak discharge of frequent events within the last 100 years (Magner and Steffen 2004).

When the flows of frequent return interval events are increased, the greater stream power results in channel down-cutting. This process cuts off the channel from its historic floodplain, and higher magnitude flows are consequently contained within the deepened stream channel. As a result, stream banks are undercut and bank slumping occurs, causing damage to adjacent property and increased turbidity in the stream through high suspended sediment loads. Land use conversion has been shown to increase runoff, bankfull discharge, and mass wasting in forested watersheds (Riedel, Verry, Brooks 2005). These effects are also evident within the southern PPR, where tributary streams in the BER showed increased entrenchment ratios (the ratio of channel depth to channel width) in recent years (Lenhart 2008).

Little of the original southern PPR landscape remains intact; therefore, it is difficult to directly compare the difference in water yield between drained, cultivated conditions and undrained, uncultivated conditions at a watershed scale. However, several studies have examined individual factors that can influence the magnitude of the response. A Kansas study (Hutchinson, Koelliker, Knapp 2008) estimated water usage coefficients

for fully watered tallgrass prairie versus an alfalfa reference crop with a water use coefficient of 1.0. The average prairie water use coefficient for the period from June 1 to September 30 was 0.90, lower than the reference crop in part because the warm season grasses studied (Big Bluestem, Little Bluestem, Indiangrass, and Switchgrass) used less water than alfalfa during the spring and late summer. The authors also anecdotally reported that the soil profile was nearly always at or near field capacity from May 1 to June 1 due to slow growth of the warm season grasses during a period of ample precipitation. Corn and soybean plots were not included for comparison in this study. A southern Minnesota study modeling evapotranspiration (ET) did include both a perennial grass-forb mix (Big Bluestem and Illinois bundleflower) and corn-soybean row crop field plots (Hinck 2008). A Penman-Monteith ET model calibrated on field measurements of soil moisture predicted that during the time period from April 1 to July 1, water usage by the perennial mix was slightly higher than the row crops. The model showed that during this period, both the grass mix and row crops had lower ET than alfalfa. Over the entire season, the predicted ET was about equal for all the vegetation types.

Other groups have taken simulation approaches to assess water yield response to land use change. Using the IBIS global-scale land surface/ecosystem model to analyze a western Wisconsin location, Twine et al. (Twine, Kucharik, Foley 2004) estimated total evapotranspiration (ET) changes for conversion of grasslands to summer crop (corn), winter crop (winter wheat), or spring crop (spring wheat). The simulation showed that conversion from grassland to summer crops caused ET to increase by 17% (73 $mm \cdot yr^{-1}$) due to greater soil evaporation during bare soil conditions and higher transpiration rates during late summer. However, the researchers suggested that estimates of grassland ET may have been too low because the IBIS model did not take into account the contribution of the grassland residue layer to ET flux. Another group (Mao and Cherkauer 2009) used the Variable Infiltration Capacity (VIC) large scale hydrology model to investigate the response of the Great Lakes region to land use changes from pre-settlement conditions. When grassland to cropland change was simulated for the

southern Minnesota region, the result was a predicted annual increase in ET of 10-16% (40-80 mm·yr^{-1}, with a corresponding decrease in annual runoff.

Drain tile systems remove a significant amount of water from the soil profile, particularly during early season periods that are characterized by low transpiration and high soil moisture. While the previously mentioned studies illustrate general water budget relationships, it is important to note that none of the modeling scenarios specifically considered the presence of subsurface drainage tile.

A field scale simulation of subsurface drainage using an 85 year climatic period for southern Minnesota showed that, for a corn-soybean rotation, artificial drainage represented approximately 37% (283 mm) of annual precipitation(Jin and Sands 2003). The majority of this drainage occurred during the March to June period, which accounted for 27% (209 mm) of annual precipitation. In a five year field plot study in Waseca, Minnesota, the same group found that 17% (150 mm) of annual precipitation was converted to sub-surface drainage, and that the majority of the sub-subsurface drainage (101 mm) occurred during the April to June period (Sands and others 2008).

1.1.3 Nitrogen

Nitrogen compounds in soil or water are part of a complex set of interactions known as the nitrogen biogeochemical cycle. The natural entry points into the nitrogen biogeochemical cycle are the processes of fixation and mineralization, which produce ammonia (NH_3) from nitrogen gas (N_2) and organic compounds, respectively. Modern farming practices have added a third ammonia source: nitrogen-based fertilizers, which are necessary to maintain the high productivity of agricultural soils. In soil, ammonia is rapidly protonated to form ammonium (NH_4^+) and adsorbed onto negatively charged soil particles; this is the form taken up by plant roots and incorporated into plant tissues. However, NH_3 is also used directly by certain soil microorganisms that obtain energy by oxidizing it to NO_3^- by the process of nitrification. Nitrogen as NO_3^- is less able to adsorb to soil particles, and is therefore easily leached from the soil, finding its way into groundwater through percolation or to surface water through runoff or subsurface

drainage systems. Once NO_3 reaches a low redox environment, such as shallow groundwater, standing surface water, or wet soils, it becomes an energy source for a second class of microorganisms that reduce it to N_2 through a process known as denitrification. Nitrogen as N_2 diffuses through water and is returned to the atmosphere.

The chemical reactions for the N cycle are summarized below:

Mineralization	Organic N	=>	NH3⇔NH_4^+
Fixation	N_2	=>	NH3⇔NH_4^+
Fertilization	(Various)	=>	NH3⇔NH_4^+
Nitrification	$NH_3⇔NH_4^+=>NH_2OH=>N_2O=>NO_2=>NO_3^-$		
Denitrification	$NO_3^-=>NO_2=>NO=>N_2O=>N_2$		

Drain tiles efficiently transport easily leachable agricultural amendments, such as nitrate (Lowrance, Todd, Asmussen 1984),(Kladivko and others 1999). These nutrient loads have far-reaching effects on downstream ecosystems. Nitrate+nitrite-N (NN) from the Mississippi River leads to high primary productivity in the Gulf of Mexico, increasing the magnitude of algal blooms at the river mouth during the spring NN pulse (Atwood and others 1994). Later in the summer, these phytoplankton decay, creating a "dead zone" of hypoxic water on the continental shelf which kills fish and crustacea. Recent analyses of historical data have shown that the area of the hypoxic zone measured in July roughly doubled in size from 1980 to 2000. The July size was directly correlated with the May NN load at the mouth of the Mississippi (Turner, Rabalais, Justic 2008).

Within Minnesota, the Minnesota River basin is of particular concern for NN export, because it drains a landscape of intensively ditched, drained and fertilized lands. A USGS analysis found that the greatest contributors of NN to the Gulf of Mexico were river basins in southern Minnesota, Iowa, Illinois and Ohio that drained agricultural areas. It was suggested that tile drains contributed to high nitrate concentrations by

'short-circuiting' the flow of ground water to streams. The study found that during the period from 1980 to 1996, an average of 1200 kg/km^2 of nitrate was transported annually past the Minnesota River monitoring site at Jordan, MN (Goolsby and others 1999).

The contribution of subsurface drainage systems to high NN in streams of the MRB is supported by small and large scale studies. A five year study of nitrate concentration in drainage from corn/soybean test plots (Sands and others 2008) showed that annual flow weighted mean concentration (FWMC) of nitrate in subsurface drainage tile varied between 10.2 and 20.4 mg·L^{-1} , with a five year mean of 13.6 mg·L^{-1}. This represented a mean leaching loss of 6.2 kg·ha^{-1}·yr^{-1} to 34.4 kg·ha^{-1}·yr^{-1}. Tributaries of the Minnesota River are heavily influenced by subsurface tile drainage; a study of water chemistry and isotopic concentrations in the BER showed that 90% of river water originated as subsurface tile drainage, and that nitrate-N in drain tiles and rivers was elevated by 10 times to 1000 times that of nitrate-N in groundwater (Magner, Payne, Steffen 2004).

1.1.4 Phosphorus

The phosphorus biogeochemical cycle differs from the nitrogen cycle because there is not a major atmospheric pool of phosphorus. Phosphorus is found in several forms in surface waters and soils (Reddy 2008). Dissolved phosphorus includes the inorganic phosphate anion in the form of H2PO$_4^-$, HPO$_4^{2-}$, or PO$_4^{3-}$, known collectively as orthophosphate (OP), along with organic phosphorus in the form of biomolecules such as DNA or lipids. Particulate phosphorus (PP) is also divided into inorganic and organic forms; inorganic PP includes phosphorus bound to clay soil particles or precipitated with calcium, magnesium, aluminum, or iron, while organic PP includes living zooplankton and phytoplankton as well as detritus derived from plants and animals.

Phosphorus is an essential nutrient for plant growth, and is generally considered to be the limiting nutrient for freshwater aquatic systems. Indeed, the trophic state of freshwater lakes is often classified by the total phosphorus (TP) concentration (Wetzel 1975):

- Oligotrophic (<0.010 $mg \cdot L^{-1}$)
- Mesotrophic (0.010-0.030 $mg \cdot L^{-1}$)
- Eutrophic (0.030-0.100 $mg \cdot L^{-1}$),
- Hypereutrophic (>0.100 $mg \cdot L^{-1}$).

Phosphorus originating in the MRB is important on a more local scale than nitrogen because of its deleterious effect on freshwater systems rather than saltwater,. High concentrations of phosphorus can stimulate nuisance blooms of algae, resulting in poor water clarity. Dying algae sink to the bottom of lakes and slow-flowing rivers, where its decomposition contributes to biological oxygen demand (BOD). When high BOD leads to oxygen depletion, fish and invertebrate kills can result. In 1992, Minnesota Governor Arne Carlson requested state agencies to come up with a 10 year plan to make the Minnesota River fishable and swimmable. Phosphorus was identified as a pollutant of major concern, key to achieving the 10 year goal (Senjem 1997).

The Blue Earth River (BER) contributes a disproportionate amount of phosphorus to the Minnesota River compared to its flow contribution. The Minnesota River Assessment Project (MRAP) showed that orthophosphate-phosphorus (OP) exceeded 0.100 $mg \cdot L^{-1}$ in 30% of BER samples, and that total phosphorus (TP) exceeded 0.100 $mg \cdot L^{-1}$ in 74% of the samples (Payne 1994). Sources of phosphorus loading in the BER can be divided into point sources, such as municipal and industrial waste-water plants, and non-point sources, such as agricultural fields. In low-flow years, 72 percent of the Minnesota River phosphorus load at Jordan originated from point sources, while during average-flow and high-flow years, non-point sources dominated, comprising 74 percent and 90 percent of the total load, respectively (Minnesota Pollution Control Agency 1998).

Non-point source phosphorus originates from both natural and anthropogenic sources. Agricultural soils tend to build up soil phosphorus from years of fertilizer application (Randall, Iragavarapu, Evans 1997). This soil phosphorus pool can be divided into the following three fractions, which maintain equilibrium over long time periods (Busman and others 1997):

- Solution P, available for uptake by plants and release to surface runoff waters, under most conditions in the form of HPO_4^{2-} and $H_2PO_4^-$.
- Active P, adsorbed to soil via weak reactions with cations; a form that is easily dissolved.
- Fixed P, reacted with Fe, Al, Mn, Ca, or humic compounds; a form that is more slowly dissolved.

In unsaturated soil, solution P maintains a relatively constant concentration through equilibrium with the weakly bound active P fraction. The weakly bound active P can also partition to fixed P. Additions to the fixed P fraction first form simple complexes with amorphous iron and calcium, but over time these simple complexes can transform to more stable, crystalline forms (Reddy 2008).

Phosphorus is transported from agricultural lands to river systems by surface runoff and tile flow. The highest P concentrations result from surface runoff during high intensity precipitation events. These events mobilize particulate P in the form of entrained soil particles and organic matter. This was demonstrated in an Illinois study of three streams flowing through agricultural lands, where researchers found a positive correlation between streamflow and particulate phosphorus concentrations (Gentry and others 2007).

Phosphorus loading from tile drains is much less predictable than nitrate loading. High density monitoring on seven tile drains in Ontario showed that total phosphorus ranged from 0.044 $mg \cdot L^{-1}$ to 1.553 $mg \cdot L^{-1}$ over the course of the study. The variability was influenced by storm/melt events, season, and management practices; attempts to build discharge-concentration relationships were largely unsuccessful (Macrae and others 2007). However, this study and others (Gachter, Ngatiah, Stamm 1998; Stamm and others 1998) suggested that the highest flows were associated with intense precipitation or snowmelt events that resulted in rapid phosphorus transport through the soil profile via macropores.

1.1.5 Suspended solids

Rivers typically carry a "suspended load" of small particles of organic and inorganic origin. The concentration of total suspended solids (TSS) is typically used to quantify the suspended particle load of surface waters. While the suspended load is a natural property of streamflow, excess loads negatively impact water quality by decreasing light penetration and increasing diffusion of nutrients from inorganic particles to the water column (Sondergaard, Kristensen, Jeppesen 1992). Imbalances of sediment input with stream power also cause rapid, undesirable changes in stream morphology. Loading of solids in excess of the channel's capacity to transport those solids can cause aggradation of the stream channel, filling navigation channels and silting in fish spawning grounds.

The Blue Earth River and its tributaries flow through soils of poorly cohesive, easily erodible silty clay glacial till, and as a result these streams are prone to problems associated with fine sediment. The problem of excess sediment carrying capacity has been exacerbated in Elm Creek by construction of agricultural drainage networks and by channel straightening to accommodate road construction (Lenhart 2008). Surface ditches and subsurface drainage tile increase drainage density of the watershed, connecting upland sources directly to the creek that previously contributed to streamflow only through slow groundwater movement (baseflow). Channel straightening increases the slope of the stream, thereby raising stream power and increasing the potential for downcutting and bank erosion.

Wetlands are also affected by suspended sediment loading. The loss of wetland volume through in-filling with sediment is a particular concern for isolated wetland basins. In a Texas study, it was shown that playa wetlands located in cropland 8.5 times more sediment than rangeland playas. In fact, 90% of the cropland playas in the study had lost all their original volume to sedimentation (Luo and others 1997). Because a major emphasis of wetland restoration in the PPR is to enhance wildlife habitat, restoration sites are often associated with conversion of adjacent cropped uplands to perennial grasses, shrubs or forests. These surrounding lands act as buffers to slow movement of

overland water flow, preventing erosion and trapping sediment during high intensity precipitation events. Trapping sediment before it can reach the wetland also decreases the influx of phosphorus attached to soil particles (Magette and others 1989).

Turbidity, a measure of water clarity, is positively correlated with TSS concentration. The Minnesota Pollution Control Agency (MPCA) has declared portions of Elm Creek, the Blue Earth River, and the Minnesota River impaired by turbidity (Minnesota Pollution Control Agency 2008); therefore, it is important to identify and quantify the suspended solids contribution of restored flow-through wetlands to Elm Creek and similar tributaries of Minnesota River Basin.

1.1.6 Wetland restoration

Wetlands in agricultural settings, particularly those sites that are restored as treatment wetlands for agricultural drainage, typically receive a large proportion of their annual inflow from drain tile discharge. Research has suggested that wetlands should be sited to receive a large proportion of flow from the watershed in order to remove significant amounts of nitrate. Modeling showed that wetlands sited to intercept 50% of the flow from a watershed could remove approximately 35% of the nitrate load, and would significantly reduce nitrate exports even under high flow conditions (Crumpton 2001). The Iowa CREP program recommended that enrolled wetlands fall within a 0.5% to 2% wetland to watershed area ratio to maximize their benefit (Crumpton and others 2006).

1.2 Site Description

1.2.1 Climate and geology

The study location is in the Elm Creek watershed in southern Minnesota, the westernmost subwatershed of the Blue Earth basin. The site lies in the flat to slightly rolling Des Moines Lobe Till plain, which has a poorly defined natural drainage network, characteristic of recently de-glaciated areas. Soils are primarily fine-textured loams and clay loams, according to the SSURGO soils database (USDA). The most widespread soil types at the study sites include the Nicollet-Crippin complex, Clarion loam, Webster clay loam, the Canisteo-Glencoe depressional complex, and the Clarion-Storden complex on steep slopes. The site lies along a stagnation moraine that is slightly steeper than the surrounding area, resulting in more rapid subsurface drainage and surface runoff (Perrine and Meschke, 2006). Hydric soils have formed in depressional areas (Figure 1.1)

The site lies southwest of the prairie/forest boundary where annual evaporation exceeds annual precipitation of 79.8 cm (31.4 inches) per year at Fairmont, Minnesota (USDA, 1989). Surface water runoff averages 11.4 cm (4.5 inches) per year in western Martin County ((Lorenz, G.H. Carlson, C.A. Sanocki 1997)).

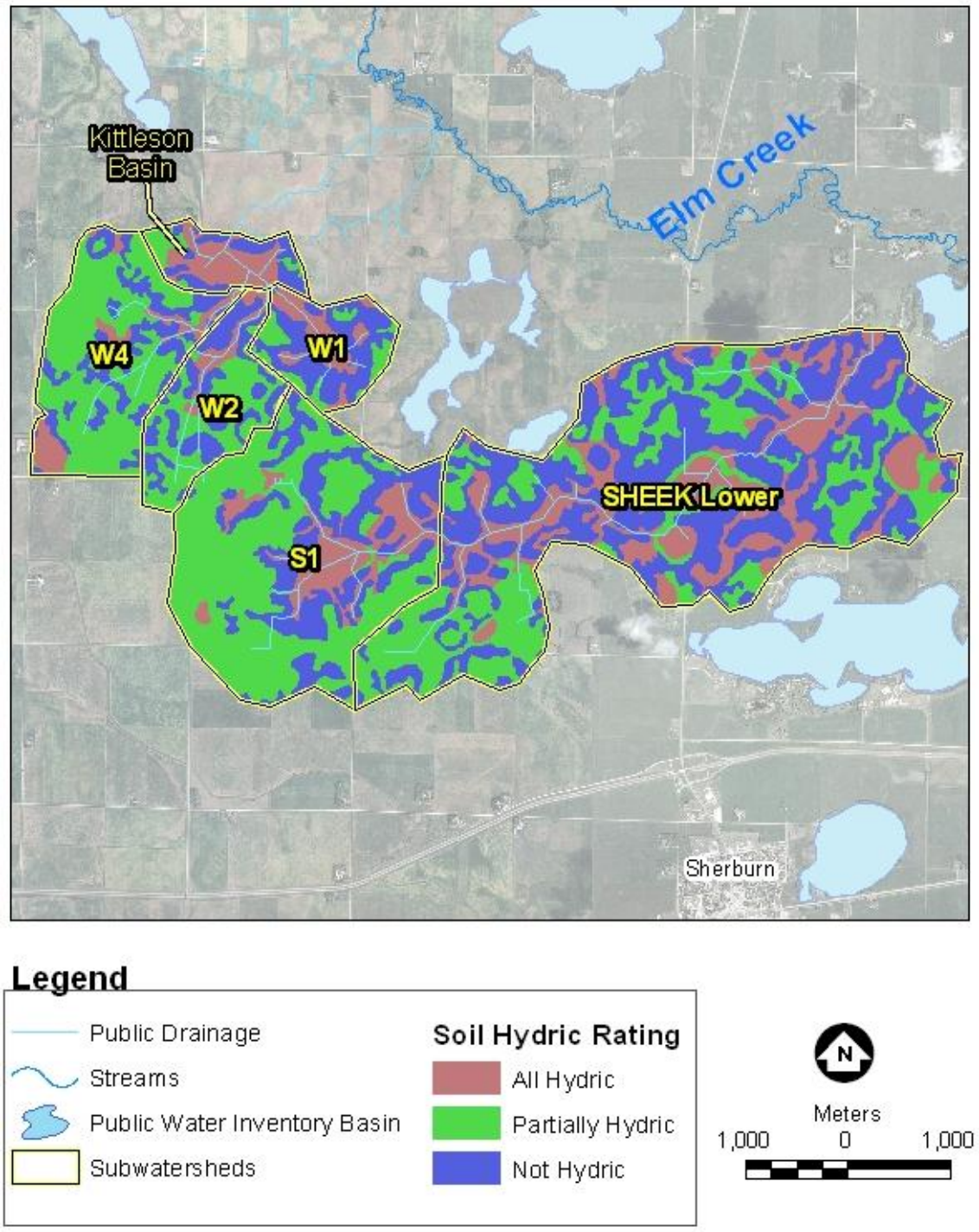

Figure 1.1 Hydric soil rating.
Imagery source is 2009 FSA aerial photography. Soil data is from the SSURGO database.

1.2.2 Restoration design

Two wetland complexes were restored in 2004-2005. Drain tile lines that passed beneath the sites were rerouted to daylight on steep slopes surrounding the former wetland basins. Riprap was installed to prevent erosion at the tile outlets. The tile lines beneath the basin were abandoned, and outlet control structures were installed to return excess water to the municipal drainage system.

The northern complex, known as the 'Kittleson' site, has 42 hectares of water surface area at its design elevation of 1252 feet, divided among three connected basins flowing in a northwesterly direction. These wetlands drain a watershed of approximately 652 hectares that is underlain by a subsurface tile system designated Judicial Ditch #73-2 (JD73-2). The most upstream basin has a 14 hectare open water area with maximum depth of 3.0 feet (0.9 meters) and average depth of 2.3 feet (0.7 meters) at normal water elevation (NWE). The pond outlets through a culvert with invert 1252 feet into a small (4 hectare) basin to the northwest. A short channel connects the small basin to a 24 hectare basin with maximum depth four feet (1.2 meters) and average depth 2.3 feet (0.7 meters) at NWE. The elevation of the large basin is controlled by a stoplog structure with a sharp-crested rectangular weir opening 24 inches in length, installed at the northwestern shore (Figure 1.2). The inlet pipe for the structure runs under the basin to permit draining of the pond. Discharge from the wetland is returned to JD73-2, which drains approximately 260 hectares downstream of the wetland outlet before discharging into Elm Creek approximately 2.6 kilometers to the northeast. The wetland basins and flow directions are shown in Figure 1.3.

Figure 1.2 Outlet structure installation.
Photos show the stoplog structure just after placement (left) and the completed outlet (right). Photos were taken from the future site of the pond, facing north.

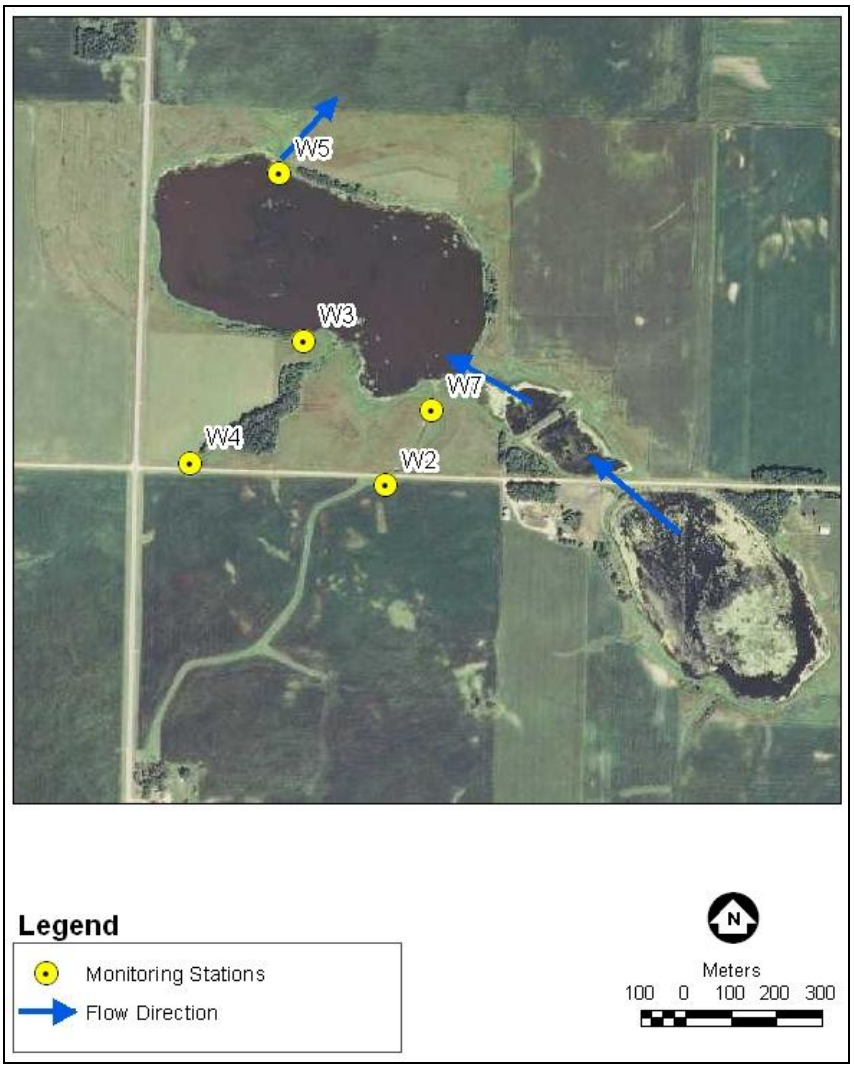

Figure 1.3 Kittleson restoration site flow direction.
Imagery source is 2009 FSA aerial photography.

The south wetland complex, known as the 'SHEEK' site, has 35 hectares of open water surface at design elevation. It consists of a 20-hectare upper basin with maximum depth eight feet and average depth 4.6 feet at its design elevation of 1257 feet, and a 15-hectare lower basin with maximum depth five feet and average depth 2.8 feet at its design elevation of 1255 feet. Taken together, the two basins drain a 560-hectare watershed. Approximately 360 hectares are drained by branches of Judicial Ditch #37

(JD37) in subwatersheds ranging from 36 to 101 hectares, while the remaining 200 hectares drain directly to the ponds.

A dike at the east end of the upper basin separates the two wetlands. A culvert outlet with an inlet invert of 1257 feet was constructed as the principal spillway to allow discharge to the lower wetland. In addition, an outlet control structure with the stoplog elevation routinely set above 1257 feet provides additional discharge capacity and allows the water elevation to be lowered below 1255 feet. The lower pond level is controlled by a stoplog water control structure installed in a dike at the eastern end of the wetland, through which excess water is discharged to JD37. Downstream of the wetland outlet, JD37 drains approximately 1090 hectares before discharging into a surface drainage ditch. The ditch then flow into Lake Seymour, a small (~20 hectare) lake with an outlet to Elm Creek. The wetland basins and flow directions are shown in Figure 1.4.

Figure 1.4 SHEEK restoration site flow direction.
Imagery source is 2009 FSA aerial photography.

1.2.3 Subwatershed descriptions

The watershed draining to the outlet structure of the Kittleson site was named “W5". This watershed was further divided into four subwatersheds, based on topography and the known extent of subsurface drainage systems (Figure 1.5).

The Kittleson Basin subwatershed represents surface runoff and interception received by the northernmost wetland, as well as subsurface flow from two unmonitored drain

tiles to the west and northeast, each draining approximately 8 hectares. The wetland outlet structure was monitored for flow and water quality at station W5.

The W2 and W4 subwatersheds are defined by two major branches of Judicial Ditch 73-2. The eastern branch (subwatershed W2) drains approximately 162 hectares, while the western branch (subwatershed W4) drains approximately 291 hectares. During the restoration, both branches were rerouted to the surface and daylighted at the southern side of the Kittleson basin. The drain tile lines draining subwatersheds W2 and W4 were monitored for flow and water quality at stations W7 and W3, respectively. Under most conditions flows from these subwatersheds is conveyed to the Kittleson basin only through the subsurface drains. However, during major precipitation events excess surface runoff is conveyed by channels that follow paths roughly overlying the main drain tile lines. Surface runoff from subwatershed W4 passes under the road south of the Kittleson basin through a 30-inch reinforced concrete pipe (RCP) culvert and a 36-inch corrugated metal pipe (CMP) culvert, then overland through a steep, highly eroded surface channel which outlets to the wetland. Surface flow from subwatershed W2 is carried by a grass channel to the road south of the Kittleson basin, then passes under the road through a 36-inch CMP culvert. The W2 culvert and one of the W4 culverts were monitored for flow and water quality at stations W2 and W4, respectively.

The W1 subwatershed is approximately 117 hectares in area and drains into the two smaller basins that flank the road southeast of the Kittleson basin. Approximately 81 hectares are drained by subsurface tile lines that empty into the larger of the two basins. These subsurface lines were not monitored for discharge or water quality. An attempt was made during the 2006 season to measure the discharge of the larger basin through its culvert outlet, but this proved difficult due to low velocity flow, sediment buildup in the culvert, and a tendency for the flow to reverse under certain conditions (Lenhart, personal communication).

The nested watershed drained by JD37 was divided into two subwatersheds (Figure 1.5). The S1 subwatershed drains approximately 560 hectares and outlets at the outlet structure of the lower basin. This outlet was monitored for flow and water quality at

station S1. Subwatersheds were not delineated for individual tile drain inlets to the basins, nor were these inlets monitored for flow or water quality. The lower subwatershed represents the remaining 1090 hectares of S2 drained by JD37 downstream of the wetlands. Flow and water quality were measured at station S2, located at the road culvert outlet, approximately 50 feet downstream from the point where JD37 daylights. In the autumn of 2007, the Martin County Soil and Water Conservation District (SWCD) installed a branch outlet on the JD37 main line, downstream from the SHEEK wetland complex that effectively diverted a portion of the flow to another wetland basin approximately 1.5 miles north of the city of Sherburn. This discharge was not measured due to equipment restraints; therefore, discharge and water quality results for the S2 watershed were affected in an unpredictable fashion during the 2008 monitoring year.

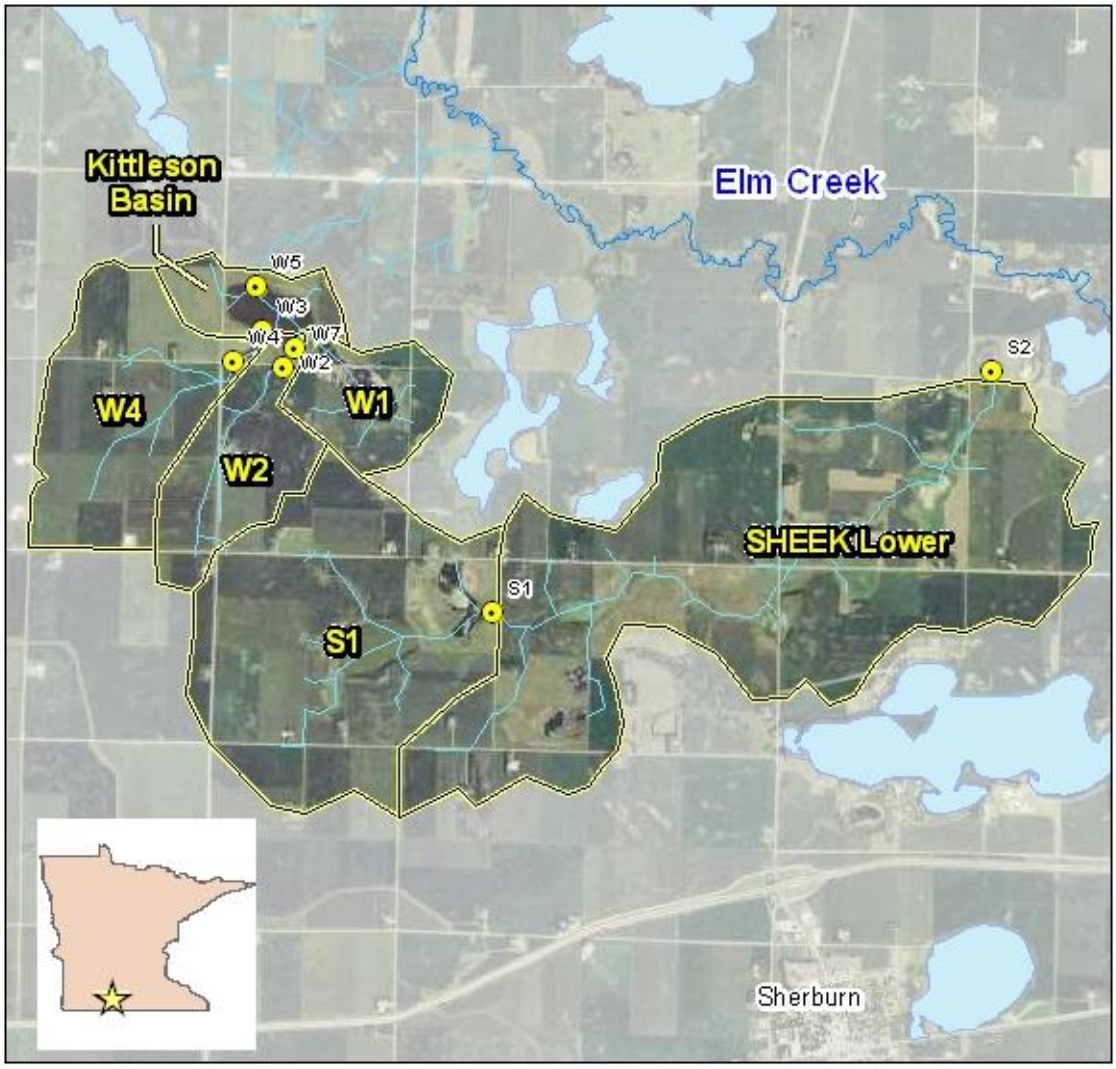

Legend

- Monitoring Stations
- Public Drainage
- Streams
- Subwatersheds

N

Meters

1,000 0 1,000

Figure 1.5 Subwatersheds and Monitoring Stations
Imagery source is 2009 FSA aerial photography.

1.2.4 Land Use

The predominant land use for the region was row crop, corn-soybean rotational agriculture. Field boundaries were defined in GIS using aerial imagery. Land cover for the years 2007 to 2009 was determined by ground surveys during the growing season of each year. Cover was classified as perennial cover, row crop, or surface water basin. Areas classified as perennial cover included grass pasture, alfalfa, restored prairie grassland and cattail marsh, while areas classified as row crop were predominantly planted to corn and soybeans. Building sites and roads were not classified. The proportion of unclassified land was assumed to remain unchanged throughout the study. The land cover class proportions for each subwatershed for the 2007-2009 crop seasons are shown in Table 1.1 and the land cover is shown graphically in Figure 1.6. The data show that there were not significant changes in land use during the three years that the survey was run. Land use during the 2005 and 2006 crop seasons was not recorded, but was reportedly similar to the land use during 2007-2009 (Lenhart, personal communication).

The W2 and W4 subwatersheds were 87% and 92% row crop, respectively, and each contained less than 5% perennial cover. In contrast, the S1 and S2 subwatersheds had lower proportions of row crop (approximately 70%) with 17-19% perennial cover. The variation of land use on neighboring subwatersheds presented an opportunity to compare their water yield and water quality.

Table 1.1 Land use by subwatershed, 2007-2009

Subwatershed	Area (ha)	Row			Perennial			Open Water		
		2007	2008	2009	2007	2008	2009	2007	2008	2009
S1	563	69.1%	72.9%	72.8%	17.5%	13.8%	13.8%	6.3%	6.2%	6.2%
S2 (includes S1)	1654	70.5%	69.8%	70.4%	19.1%	20.5%	20.1%	2.6%	2.6%	2.6%
W1	117	59.4%	61.1%	61.1%	15.1%	15.0%	15.0%	16.1%	16.1%	16.1%
W2	164	87.0%	87.0%	87.0%	4.1%	4.1%	4.1%	1.3%	1.2%	1.2%
W4	290	92.2%	92.1%	92.1%	2.5%	2.5%	2.5%	0.0%	0.0%	0.0%
W5 (includes W1, W3, W4)	652	77.6%	77.8%	77.8%	9.3%	9.2%	9.2%	6.9%	6.9%	6.9%

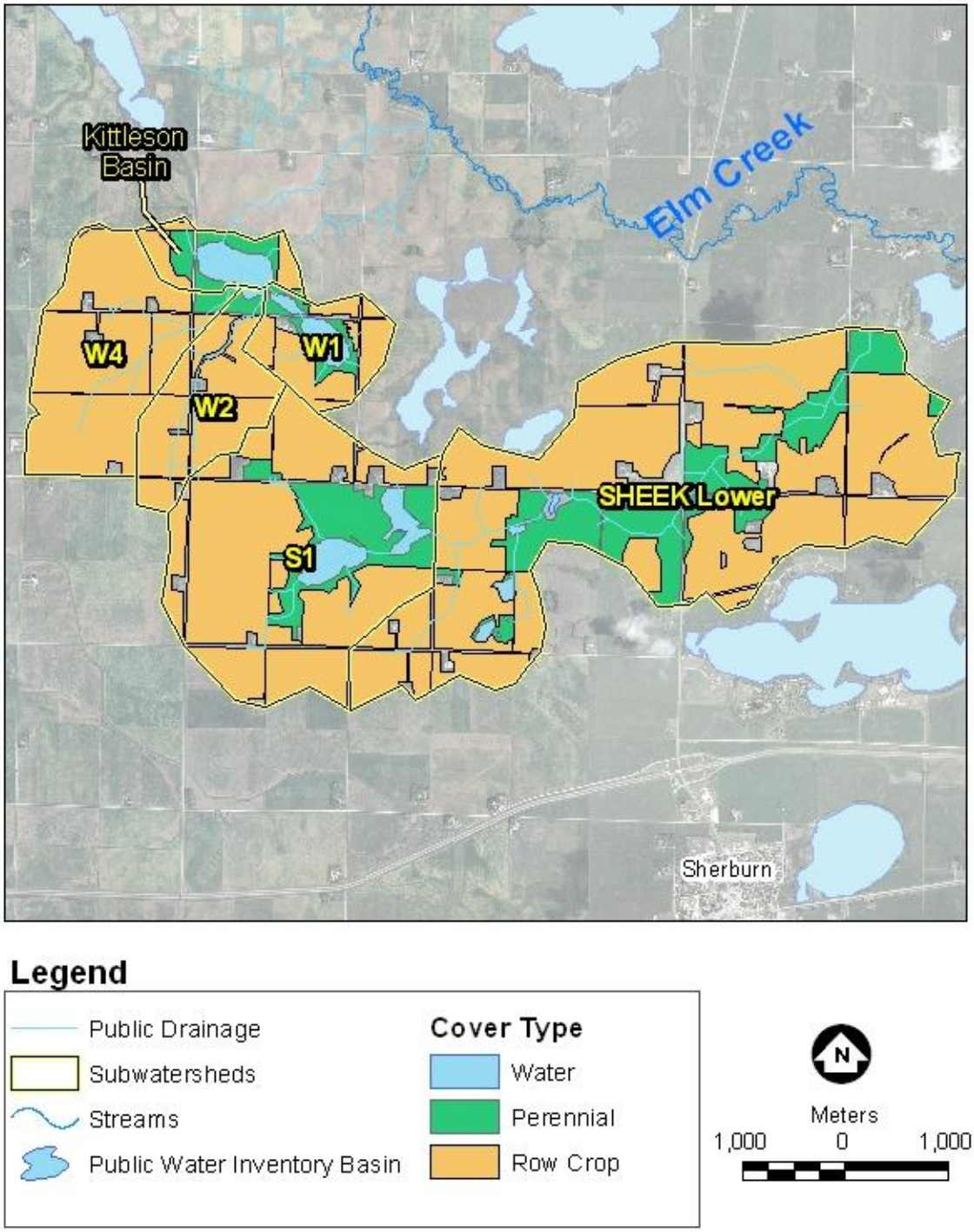

Figure 1.6 Land use (2008 season).
Imagery source is 2009 FSA aerial photography.

1.3 Methods

1.3.1 Flow Monitoring Methods

Teledyne Isco model 4150 Area Velocity flow meters were used to monitor discharge from the W2 and W4 subwatershed drain tiles and culverts. Level and velocity readings were monitored continuously, and the average flow was calculated internally and recorded at 15 minute intervals.

A Teledyne Isco model 4120 submerged probe flow meter was used to monitor discharge from the Kittleson wetland. The level was measured continuously, and the average level was recorded at 15 minute intervals. Because the elevation of the top of the water control structure was 1253 feet, only one foot higher than NWSE, it often became submerged after precipitation events. Modeling by a BWSR consultant showed that submerged conditions resulted in a complex flow regime involving orifice flow, weir flow and pipe flow that would not be accurately estimated by placing a probe in the structure to measure head behind the weir, and it was recommended that the probe be placed in the wetland itself (Minnesota Board of Water and Soil Resources 2004b). Therefore, under most conditions the probe was placed in a vertical three inch diameter PVC pipe that was connected to the wetland by a horizontal pipe. In early spring, when ice formation within the PVC pipes prevented installation of the probe, and in 2009, when the free end of the horizontal pipe became buried in sediment, the probe was placed in the upstream portion of the water control structure, directly behind the weir. Stage-discharge tables were provided by the BWSR consultant to convert level measurements to discharge for either position.

For part of the 2006 and all of the 2007 monitoring season, improper programming of the datalogger caused repeated gaps of approximately 10 days between download dates throughout the season. A water budget method was used to replace the gaps, where precipitation and inflow from the W2 and W4 subwatersheds were considered inputs, and evaporation and outflow from the wetland were considered outputs.

Discharge from smaller drain tiles emptying into the SHEEK site basins was not measured due to equipment limitations. The discharge from the SHEEK complex was measured using a Teledyne Isco 4120 submerged probe flow logger. Modeling showed that this stoplog structure would not become submerged during extreme events (Minnesota Board of Water and Soil Resources 2004a), so the pressure transducer was installed directly in the box behind the weir. A stage-discharge table was used to convert water level to flow.

Flow was measured at the downstream outlet of JD37 using a Teledyne Isco 4150 area-velocity flow logger, with the transducer installed in the outlet of a 36 inch diameter CMP culvert passing under a road approximately 50 feet below the JD37 outlet. Under most conditions the discharge from the drain tile outlet flowed directly to the culvert through a channel, but during peak events the water often backed up and the channel overflowed into a small basin upstream of the road. The culvert switched between inlet control and outlet control depending on the water level of the downstream channel. Under outlet control conditions the flow velocity was often too slow for accurate measurement by the velocity probe. Velocity measurements taken with a current meter were used to develop a culvert outlet stage-discharge relationship which was applied during these periods.

1.3.2 Water Quality Methods

Manual grab samples were taken every 7 to 14 days to determine concentrations of total suspended solids (TSS), orthophosphate-P (OP), total phosphorus (TP) and nitrate+nitrite-N (NN). Fresh single-use plastic sample bottles were provided by Minnesota Valley Testing Laboratories (MVTL). A one liter sample bottle was filled for the TSS, OP, and NN samples, while a 500 mL bottle containing one mL of concentrated sulfuric acid as a preservative was filled for the TP sample. Samples were immediately placed on ice and transported to the MVTL laboratory within 24 hours, where samples were immediately filtered and preserved. OP testing was completed within 48 hours. TP and OP testing were by method EPA 365.1, NN testing was by method 353.2, and TSS sampling by USGS I-3765-85. Beginning in 2006, suspended volatile solids concentrations were also regularly measured, by method EPA 160.4. In 2008 and 2009, one liter amber sample bottles were filled from the wetland discharges or surface water for chlorophyll-a determination by method 10200H. Turbidity was also measured on-site in 2008 and 2009, using a portable turbidimeter.

During 2008 and 2009, *in situ* measurements were performed within the Kittleson and the SHEEK wetlands using a YSI Professional Plus multiparameter meter. Linear transects were set up across the basins, with approximately 100 meter spacing between stations. The stations were marked with buoys and their positions were recorded by GPS. Paired measurements of oxidative-reductive potential (ORP), dissolved oxygen (DO), temperature, and pH were taken from a canoe at depths of one foot below the water surface and approximately one inch above the wetland bottom. A two point calibration of the pH probe with pH 7 and pH 10 reference solutions and a one point calibration of the ORP probe with Zobell's solution were done before each use. The DO probe was calibrated against air at 100% saturation before each use.

1.4 Results

1.4.1 Precipitation

Monthly precipitation totals measured at the study sites and mean precipitation for 1991-2008 measured at Fairmont, MN (U.S. Historical Climate Network) are shown in Table 1.2. Mean precipitation during the drainage season for the years 1991-2008 was 326 mm, measured at Fairmont, MN (U.S. Historical Climate Network). During the study period of 2005-2008, mean precipitation at the study site was 303 mm. While monthly precipitation varied greatly from year to year, seasonal precipitation was more stable; only the 2007 drainage season total of 162 mm was much less than the long term average. Mean precipitation during the ET season for the years 1991-2008 was 286 mm. Precipitation during the ET season for the study years was extremely variable. The 2005 ET season was very wet, while the 2006 and 2007 seasons were about normal and the 2008 was extremely dry.

Table 1.2 Monthly precipitation

Period	**Precipitation (mm)**					
	April	**May**	**June**	**July**	**Aug**	**Sept**
2005	99	178	83	108	99	212
2006	197	49	100	56	152	63
2007	39	85	38	41	201	61
2008	137	134	73	17	10	46
1991 - 2008 Mean	**93**	**110**	**124**	**101**	**101**	**84**

1.4.2 Water Yield

The hydrograph for 2008 shows the typical seasonal behavior (Figure 1.7). The wetlands were recharged in early spring by snowmelt and in the late fall (following senescence of vegetative cover) by precipitation rains. By the end of March, the wetlands had usually filled to their design elevations and begun to discharge, and the tile drains had begun to flow at increasing rates as frost left the ground. Prior to crop

emergence and perennial vegetation green-up, all subwatersheds remained saturated and primed for discharge, and were very responsive to precipitation. Once the growing season started, the subwatersheds became less responsive to precipitation as the soil water was depleted by evapotranspiration. During the months of July through September, the subwatersheds became very unresponsive to precipitation as evapotranspiration reached its peak. At this time the wetlands typically fell below their design elevations due to low inflow, evaporative losses, and possibly seepage to groundwater.

Figure 1.7 also shows differences in the typical responses to precipitation of the individual subwatersheds. The tiled subwatershed (W2) exhibited 'flashy' surface flow that occurred only during high intensity precipitation events. Subsurface flow from the W2 subwatershed also exhibited sharp peaks during precipitation events, probably due to percolation of soil water directly above the tile lines, followed by a rapid drop to 'baseflow' conditions where discharge was driven by lateral flow of water to the tile. Baseflow diminished slowly as the shallow water table fell. The W5 subwatershed outlet shows a steadier discharge rate, particularly in the receding limbs of stormflow peaks, due to the routing of the hydrograph through the pond.

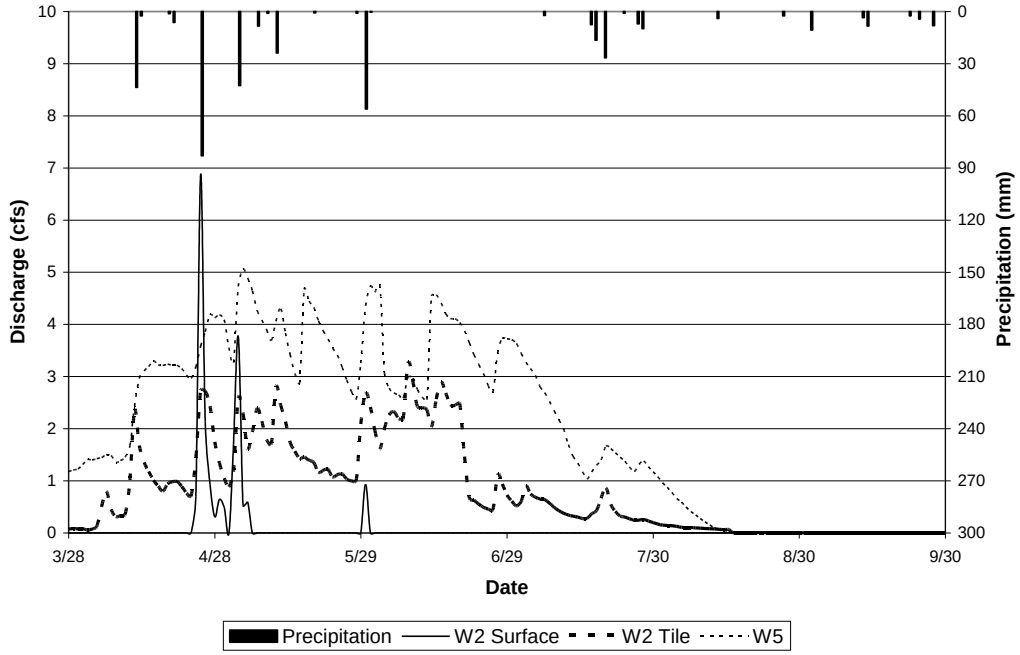

Figure 1.7 2008 hydrographs for subwatersheds W2 and W5

The seasonal pattern was used to divide each monitoring season into two periods for flow and loading analysis: the 'drainage season', from April 14 to June 30, and the 'ET season', from July 1 to September 30. These ranges were modified slightly from previous studies (Helmers and others 2005; Jin and Sands 2003) to fit our records. In 2005 the flow monitoring equipment was not installed until April 14; therefore, that date was selected as the beginning date for the water yield analysis.

Water yield was evaluated by quantifying the watershed response to precipitation in the form of the Q/P ratio. The flow logger 15 minute readings were used to calculate a daily average flow, then the total water volume was calculated by:

$$Q = \frac{\sum_{i=1}^{n} \overline{Q_i} * \Delta t}{A}$$ **Equation 1**

Where Q = Depth in meters, Q_{bar} = Daily flow average, in $m^3 \cdot s^{-1}$, Δt = time interval of 86,400 seconds, n = number of days, and A = subwatershed area in m^2. For subwatersheds where both drain tile flow and surface flow were measured, the two flows were summed to calculate a total response. Total precipitation was calculated by summing the depths of precipitation measured by the tipping bucket rain gauge at station W5.

The seasonal Q/P ratios of each subwatershed were first compared to test the alternative hypothesis (H_a) that watersheds were more responsive to precipitation in the drainage season than in the ET season. The mean of the Q/P ratios for 2005 – 2008 were calculated and compared for subwatershed W2, W5, and S1. Using the Student's t-test and $\alpha = 0.10$, W2 ($p = 0.022$), W5 ($p = 0.025$) and S1 ($p = 0.074$) were all found to be significantly different. This result confirmed the decision to analyze the data by dividing the year into two seasons.

A box and whisker plot shows that the Q/P data varies considerably from year to year (Figure 1.8). Some of the variation was due to the initial restoration; in 2005 the S1 Q/P ratio was abnormally low because the SHEEK basins had not yet filled after restoration and did not reach their design depth and begin discharging until May 14. The plot shows upward skewness for every subwatershed in the ET season, caused by high Q/P ratios during the 2008 year. This was mainly the result of the extremely low precipitation recorded during the 2008 ET season and not high flows (Table 1.2). S1 was further influenced in 2008 by a planned release that dropped the water level of the lower SHEEK wetland well below NWSE to facilitate bank repair work.

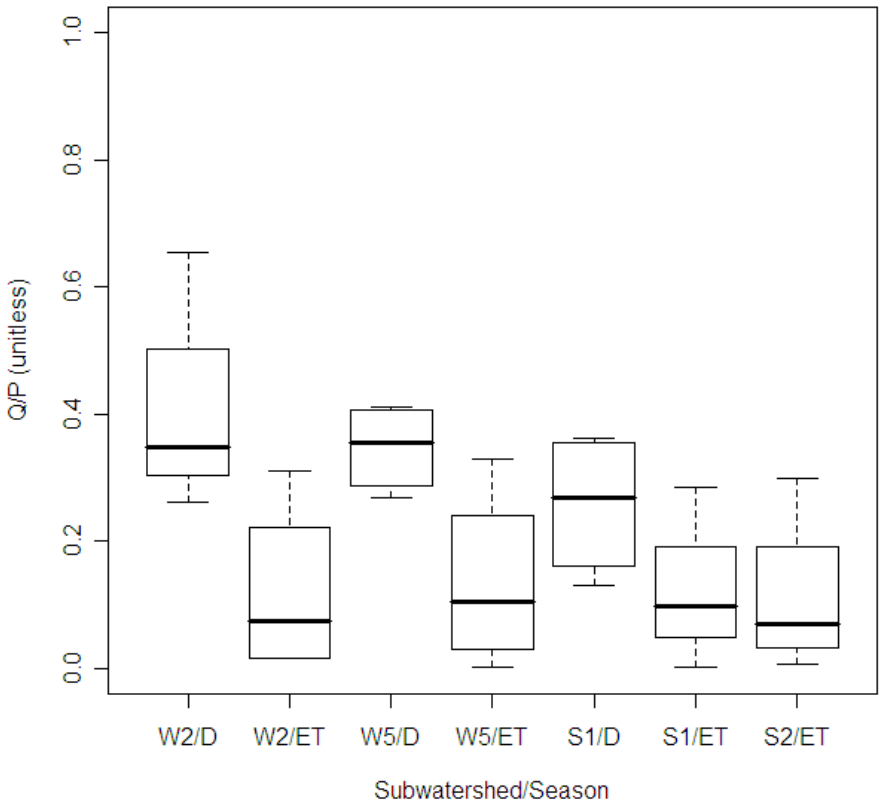

Figure 1.8 Seasonal Q/P ratios, box plot for 2005 - 2008
The plot displays the median, first quartile, third quartile, maximum value, and minimum value. Subwatershed W2 includes both surface runoff and subsurface tile flow. D = "Drainage Season" (April 14 to June 30), ET = "ET Season" (July 1 to September 30).

Next, the drainage season Q/P ratios for 2005 to 2008 were compared for the W2 (crop) and the W5 and S1 (crop/perennial/wetland) subwatersheds. Drainage season Q/P ratios (Figure 1.9) were analyzed statistically by performing a Student's two sample t-test, with $\alpha = 0.10$ and the alternative hypothesis (H_a) that the true difference in the four year means was not zero. No subwatershed was different from any other under this criterion. The largest difference was between subwatershed S1 and S2 (t=1.4021, df=5.235, p=0.2173). A paired t-test on the same dataset gave similar results.

For the ET season, the Q/P ratio for S2 was added to the analysis. The Student's t-test carried out on the ET season Q/P means (Figure 1.10) showed no significant difference between any pair-wise combination of the four subwatersheds.

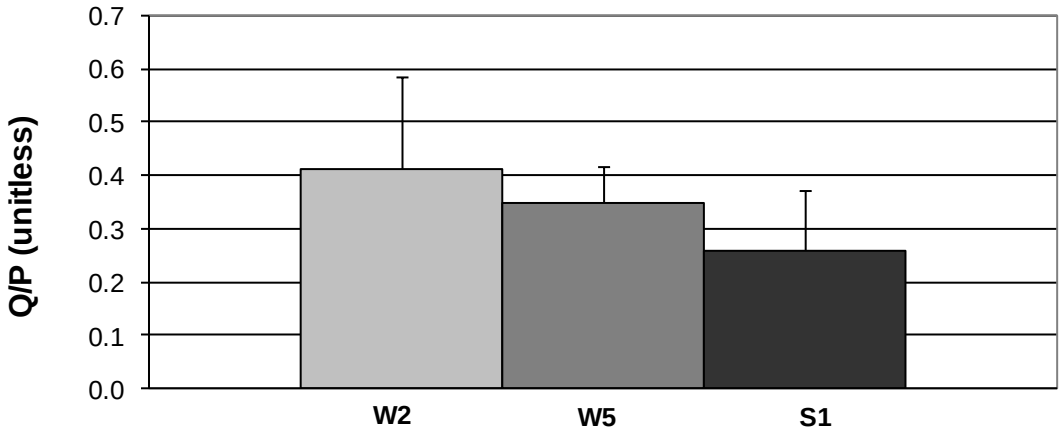

Figure 1.9 Drainage season Q/P ratio
The Q/P ratio represents the water yield of each subwatershed as a fraction of precipitation. Subwatershed W2 includes the sum of both surface runoff and subsurface tile flow.

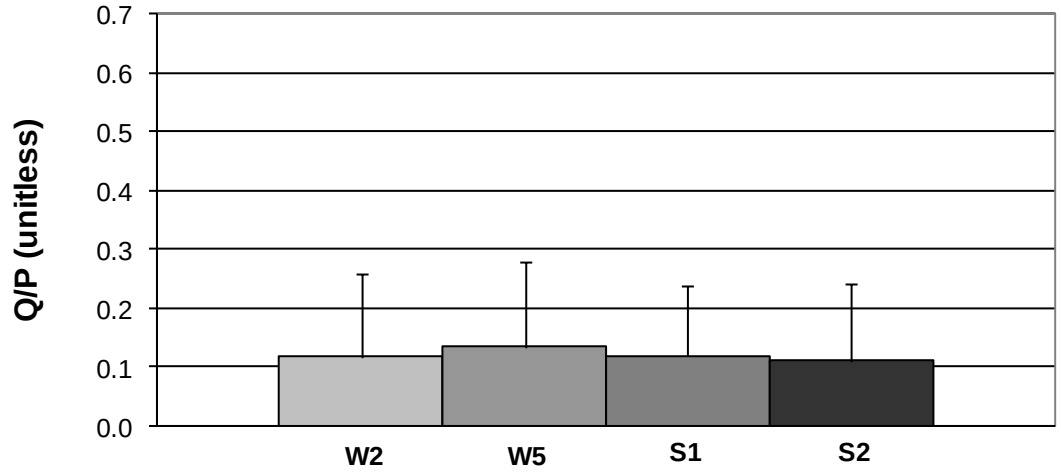

Figure 1.10 ET season Q/P ratio
The Q/P ratio represents the water yield of each subwatershed as a fraction of precipitation. Subwatershed W2 includes the sum of both surface runoff and subsurface tile flow.

1.4.3 Nitrate Response

The nitrate+nitrite-N (NN) response varied among the subwatersheds. For the crop subwatersheds W2 and W4, the NN concentration of surface runoff was highly variable, ranging from 1.43 mg·L^{-1} to 24.1 mg·L^{-1} (Figure 1.11, Figure 1.12). In contrast, the NN concentration of tile drainage from these subwatersheds varied little throughout the year (Figure 1.13, Figure 1.14). Very early season flows of 5.99 mg·L^{-1} and 4.26 mg·L^{-1} were recorded for tile drainage from W2 and W4, respectively, but most values were above 10 mg·L^{-1}. During the drainage season, W2 and W4 tile drainage mean NN concentrations were usually between 15 and 25 mg·L^{-1}. During the ET season, concentrations were slightly lower, 10 and 20 mg·L^{-1}. Samples taken from the wetland outlets had much lower NN concentrations and showed more variability over the course of the year. The NN levels for the W5 subwatershed (Figure 1.15) and the S1 subwatershed (Figure 1.16) were highest early in the drainage season, but in most years had dropped below the limits of detection by the beginning of July. The outflow of the S2 subwatershed (Figure 1.17) ranged from 0.73 mg·L^{-1} to 14.7 mg·L^{-1}.

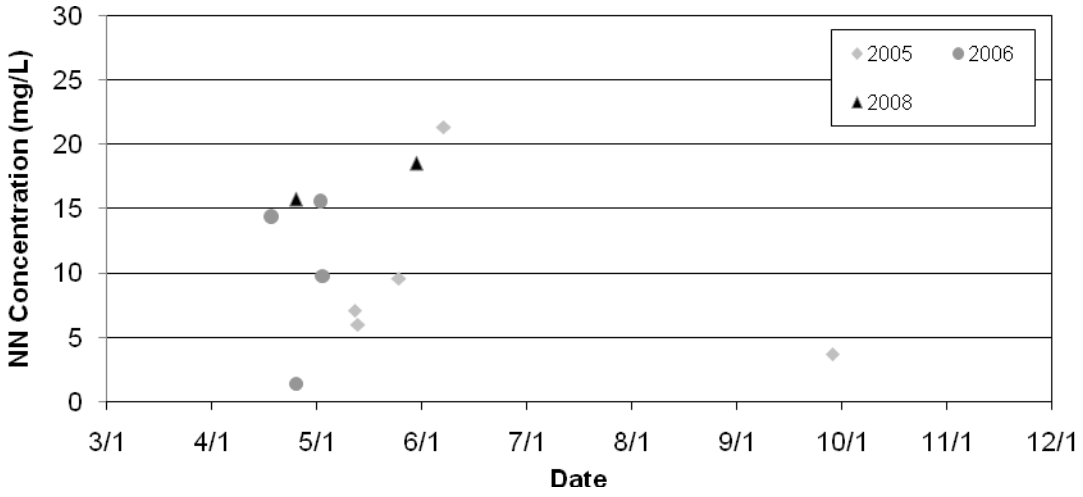

Figure 1.11 Subwatershed W2 surface channel nitrate+nitrite-N (NN) concentration
One liter grab samples were taken at the culvert passing under the road south of the Kittleson basin. Units are milligrams N·Liter-1 (parts per million).

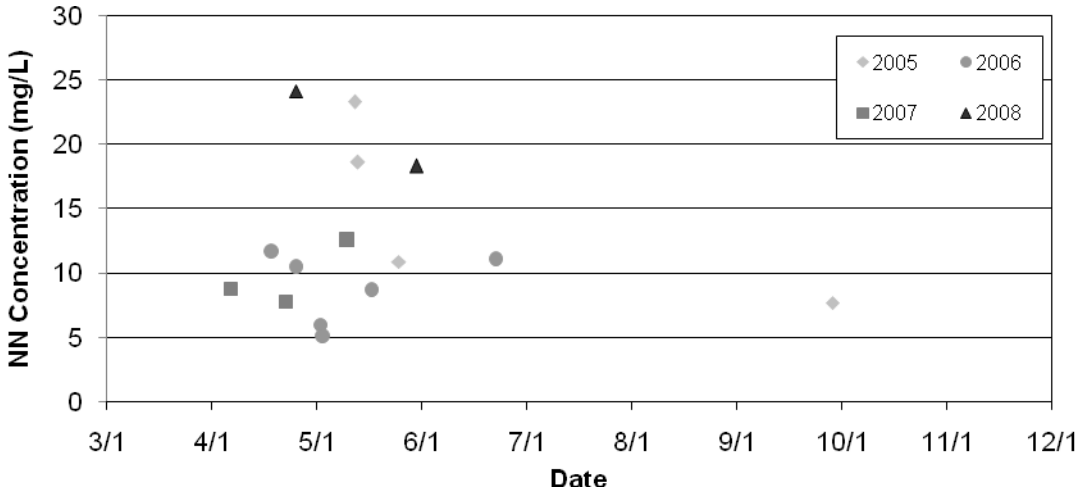

Figure 1.12 Subwatershed W4 surface channel nitrate+nitrite-N (NN) concentration
One liter grab samples were taken at the culvert passing under the road south of the Kittleson basin. Units are milligrams N·Liter^{-1} (parts per million).

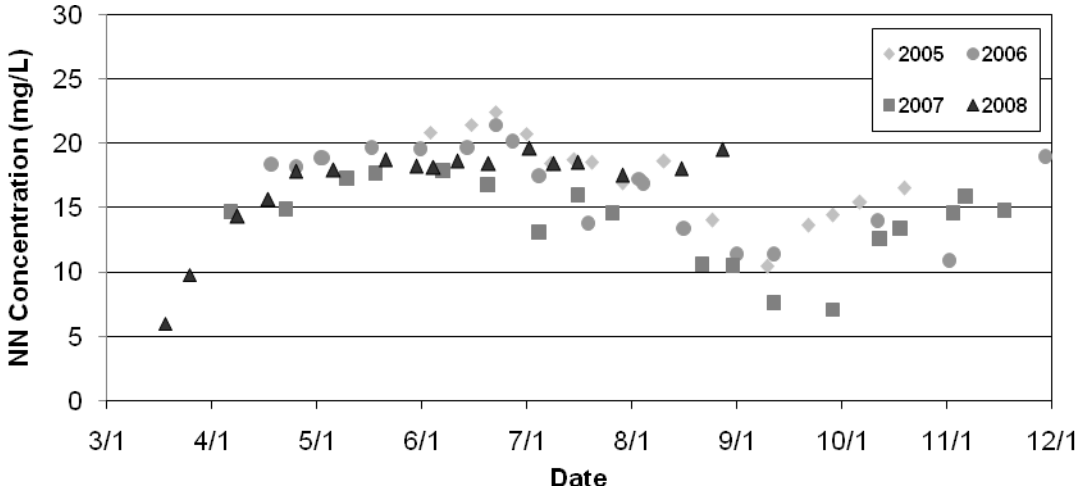

Figure 1.13 Subwatershed W2 tile drainage nitrate+nitrite-N (NN) concentration
One liter grab samples were taken at the tile drain outlet. Units are milligrams N·Liter^{-1} (parts per million).

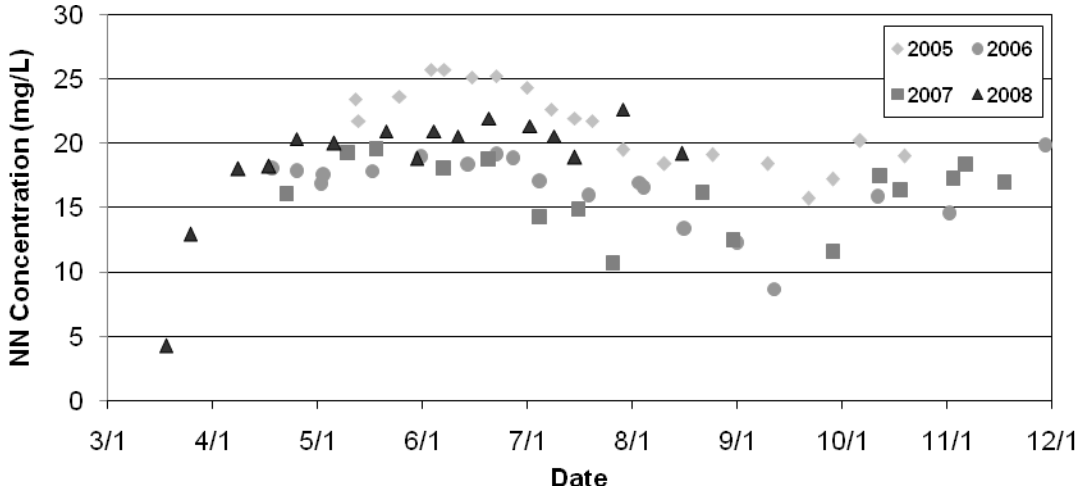

Figure 1.14 Subwatershed W4 tile drainage nitrate+nitrite-N (NN) concentration
One liter grab samples were taken at the tile drain outlet. Units are milligrams N·Liter^{-1} (parts per million).

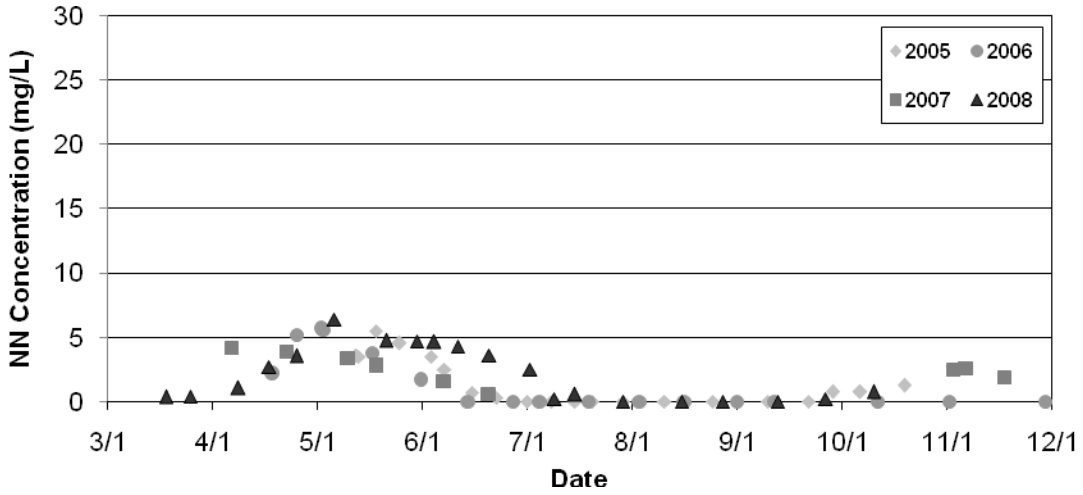

Figure 1.15 Subwatershed W5 nitrate+nitrite-N (NN) concentration
One liter grab samples were taken from water passing over the weir of the Kittleson basin outlet structure when flow was present. Samples were taken directly from wetland surface water during periods of zero flow. Units are milligrams N·Liter^{-1} (parts per million).

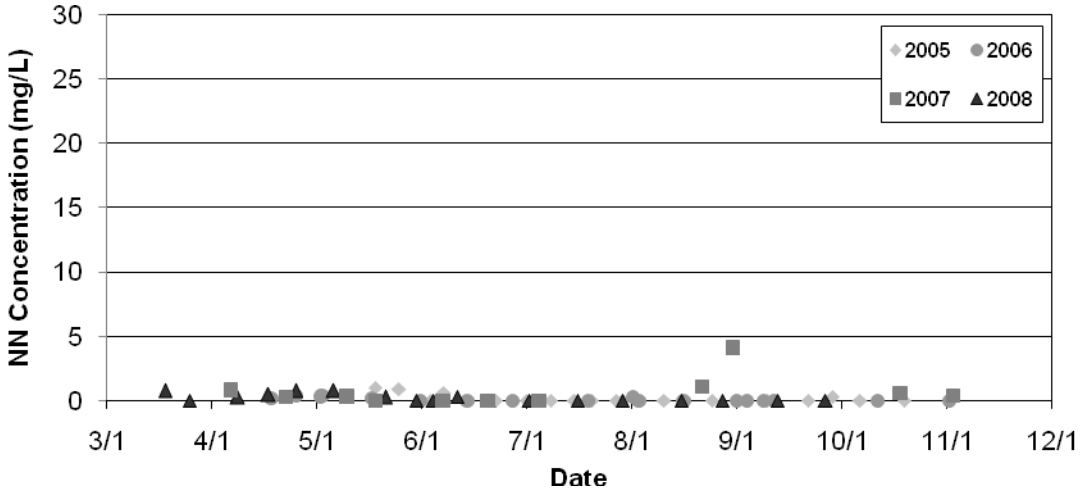

Figure 1.16 Subwatershed S1 nitrate+nitrite-N (NN) concentration
One liter grab samples were taken from water passing through the orifice of the lower SHEEK basin outlet structure when flow was present. Samples were taken directly from wetland surface water during periods of zero flow. Units are milligrams N·Liter^{-1} (parts per million).

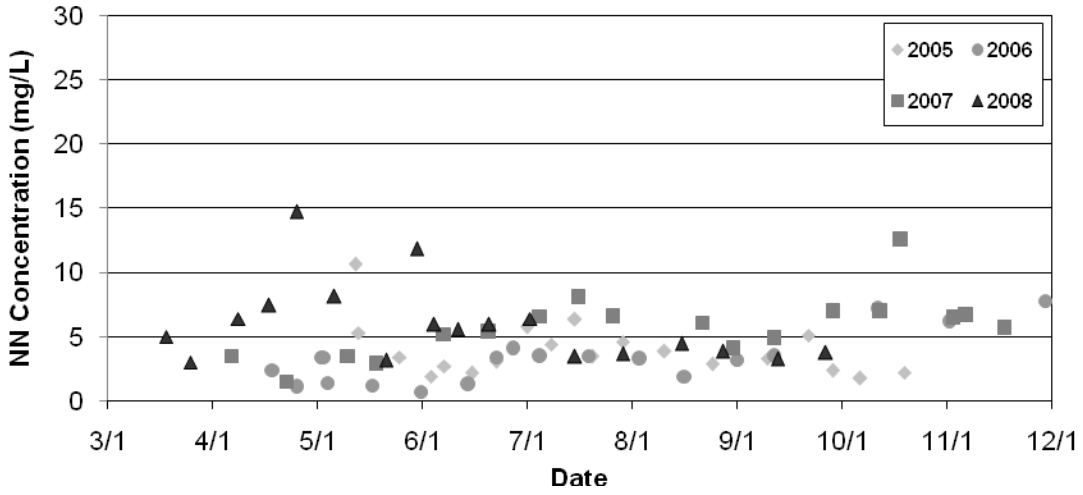

Figure 1.17 Subwatershed S2 nitrate+nitrite-N (NN) concentration
One liter grab samples were taken at the culvert passing under the road downstream from the JD37 tile drain outlet. Units are milligrams N·Liter^{-1} (parts per million).

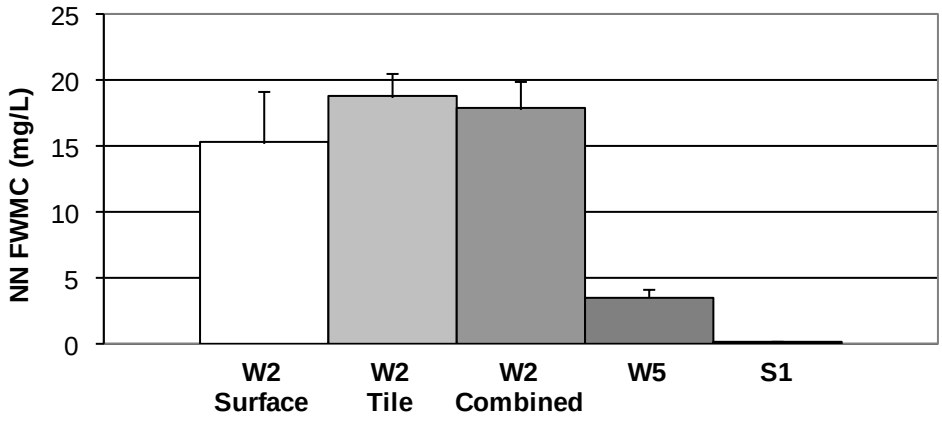

Figure 1.18 Drainage season nitrate+nitrite-N (NN) flow weighted mean concentration (FWMC)
FWMC was calculated by dividing total load by total flow volume over dates April 14 to June 30. Units are milligrams N·Liter^{-1} (parts per million). Error bars represent one positive standard deviation.

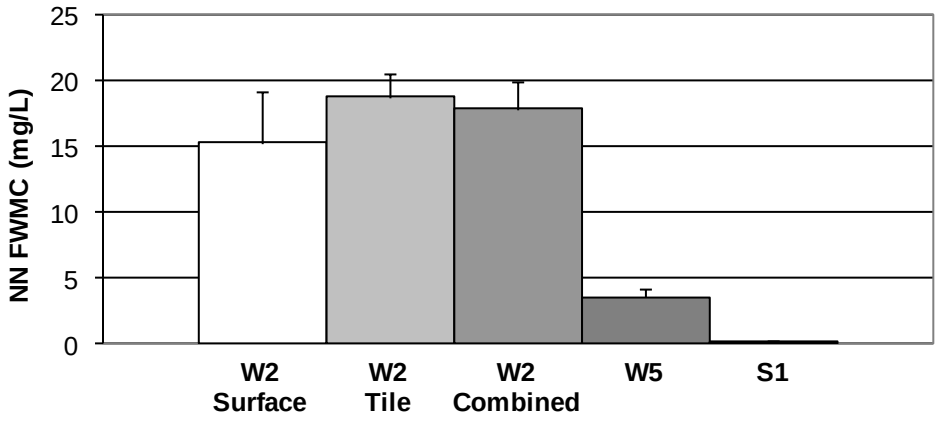

Figure 1.19 ET season nitrate+nitrite-N flow weighted mean concentration (FWMC)
FWMC was calculated by dividing total load by total flow volume for dates July 1 to September 30 of each year. Units are milligrams N·Liter^{-1} (parts per million). Error bars represent one positive standard deviation.

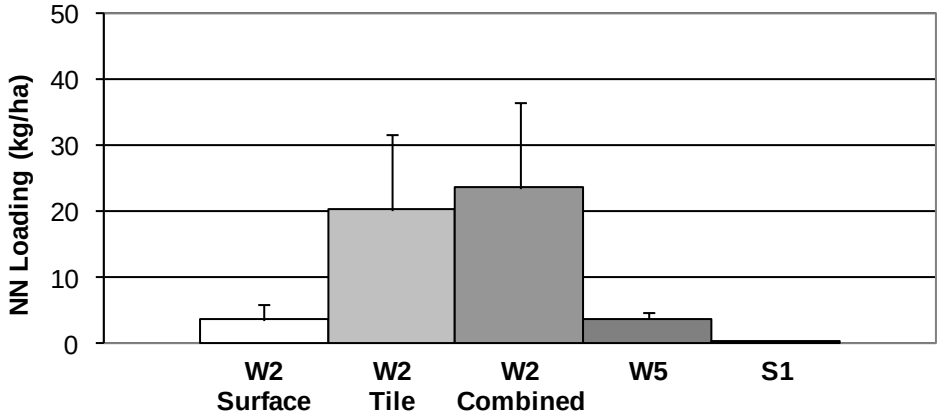

Figure 1.20 Drainage season area normalized nitrate+nitrite-N (NN) loading
Loading was calculated by dividing total load over dates April 14 to June 30 by subwatershed area. Units are kilograms N·hectare^{-1}. Error bars represent one positive standard deviation.

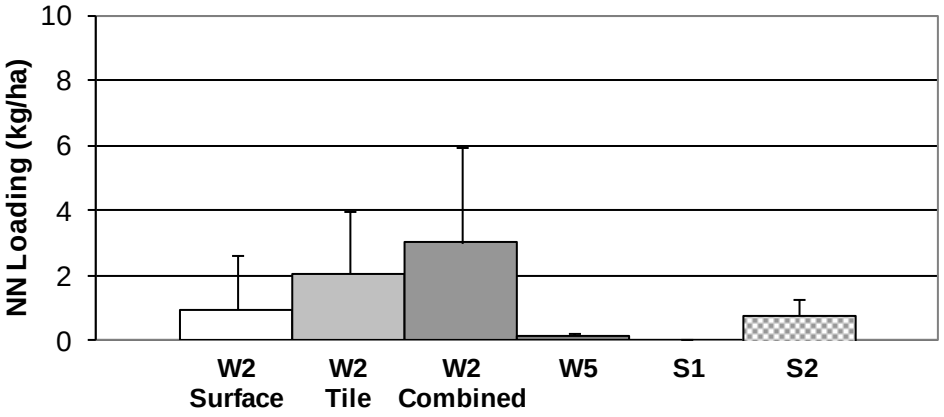

Figure 1.21 ET season area normalized nitrate+nitrite-N (NN) loading
Loading was calculated by dividing total load over dates July 1 to September 30 by subwatershed area. Units are kilograms N·hectare^{-1}. Error bars represent one positive standard deviation.

Because subwatershed discharge rate and NN concentration varied independently of one another, the flow weighted mean concentration (FWMC) (calculated by dividing the total load by the total discharge) was used to compare water quality. NN loading for each subwatershed were estimated with the computer program FLUX ((Walker 1996)).

The seasonal loads obtained from FLUX were divided by the total seasonal discharge measured at the flow monitoring stations to calculate the FWMC (Table A.1, Table A.3). The seasonal loads were also divided by the appropriate subwatershed area to obtain an area normalized loading rate in kilograms·hectare^{-1}. The results for both FWMC and area normalized loading were tested statistically for differences between subwatersheds.

We hypothesized that FWMC and specific yield would be higher in the crop subwatershed than the nested subwatersheds containing wetlands, due to loss of nitrogen through the process of denitrification within the wetlands. The relationship was first tested using the Student's two sample t-test with $\alpha = 0.05$. The W2 (crop) subwatershed NN FWMC was found to be significantly greater than the W5 or S1 subwatersheds during the drainage season ($p < 0.001$ in both cases) and during the ET season ($p=0.027$, $p=0.018$, respectively). The W2 NN specific loading was significantly greater than W5 or S1 specific loading during the drainage season ($p=0.027$, $p=0.018$, respectively) but not during the ET season ($p=0.073$, $p=0.068$, respectively).

A key assumption of the Student's t-test is that the data are normally distributed. Because the 2005 – 2008 dataset had only four points, normality was difficult to assess. Therefore the non-parametric Wilcoxon Rank Sum significance test was used to confirm the results. Once again, the FWMC for W2 was significantly greater than for W5 or S1 during either the drainage season or the ET season ($p=0.014$ in all cases). Specific loading for W2 was significantly greater than for W5 or S1 during the drainage season ($p=0.014$, $p=0.015$) and during the ET season ($p=0.014$).

We also hypothesized that the NN FWMC and specific yield would be greater for the W2 subwatershed when compared to the S2 subwatershed due to the presence of wetlands and a higher percentage of perennial cover in the S2 subwatershed. We were unable to compare the drainage season results due to the previously described lack of flow data for the S2 subwatershed during the drainage season. During the ET season, NN FWMC for W2 was significantly higher than for S2 by the Student’s t-test or the

WIlcoxon Rank Sum test (p=0.002, p=0.014, respectively), while specific loading was not significantly different by either test (p=0.114, p=0.243, respectively).

1.4.4 Phosphorus Response

Two forms of phosphorus, orthophosphate (OP) and total phosphorus (TP) were routinely measured in the study. TP is the form most commonly used as a measure of surface water quality, and therefore was the focus of our analysis.

Surface runoff TP concentrations were quite variable (Figure 1.22, Figure 1.23). Tile drainage TP concentrations were lower and more stable than surface runoff concentrations during both seasons (Figure 1.24, Figure 1.25). The tile drainage of subwatershed S2 (Figure 1.26) showed higher TP concentrations than the crop subwatersheds, but as with the tile drainage from the smaller W2 subwatershed, the concentrations were less variable than surface runoff.

The wetland outlet samples, in contrast, did show a high degree of seasonality (Figure 1.27, Figure 1.28). Somewhat elevated TP concentrations, approximately 0.2 $mg \cdot L^{-1}$, were observed at the beginning of the monitoring season probably due to detritus that accumulated in the wetlands over the winter. After the first flush, caused by snowmelt and spring rains, the concentration dropped slightly to less than 0.200 $mg \cdot L^{-1}$, where it remained until approximately June 1. Concentrations then began to rise, reaching maximums of approximately 0.800 $mg \cdot L^{-1}$ in the Kittleson wetland and 0.400 $mg \cdot L^{-1}$ in the Rosenberg wetland by the end of July. Between August 1 and August 15, the pattern was more variable from year to year, but generally by August 15 concentrations began to drop, decreasing steadily back to approximately 0.200 $mg \cdot L^{-1}$ by October 15th.

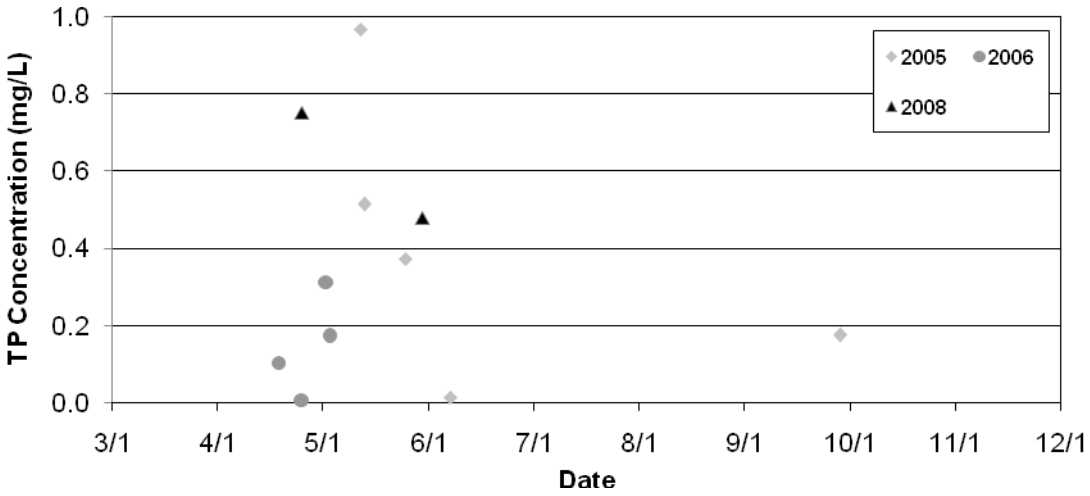

Figure 1.22 Subwatershed W2 surface channel total phosphorus (TP) concentration
500 milliliter grab samples were taken at the culvert passing under the road south of the Kittleson basin. Units are milligrams P·Liter $^{-1}$ (parts per million). There were no sample events in 2007.

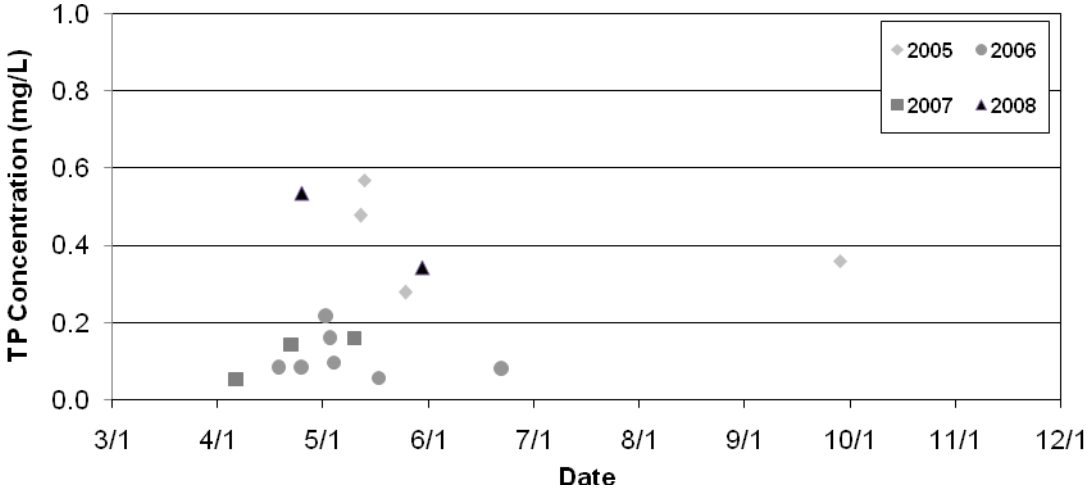

Figure 1.23 Subwatershed W4 surface channel total phosphorus (TP) concentration
500 milliliter grab samples were taken at the culvert passing under the road south of the Kittleson basin. Units are milligrams P·Liter $^{-1}$ (parts per million).

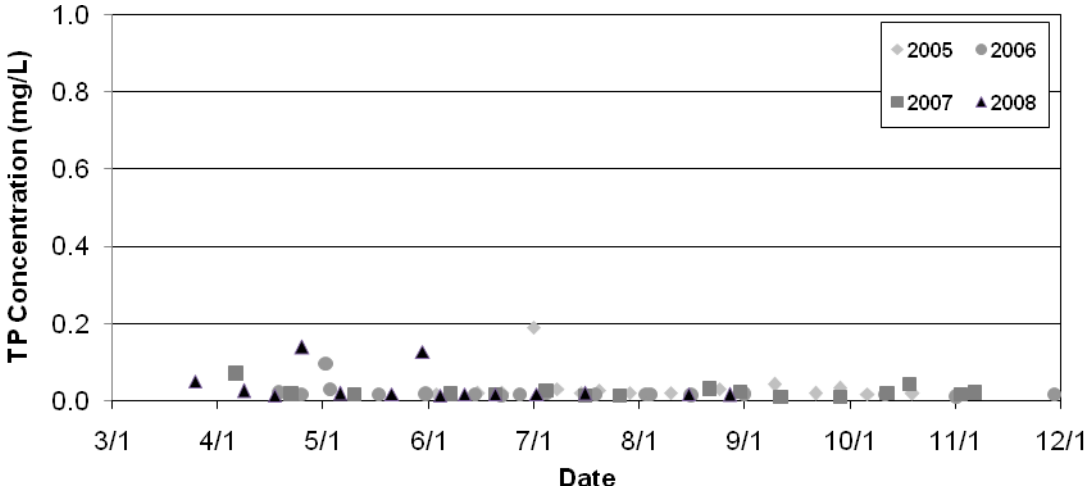

Figure 1.24 Subwatershed W2 tile drainage total phosphorus (TP) concentration 500 milliliter grab samples were taken at the tile drain outlet. Units are milligrams $P \cdot Liter^{-1}$ (parts per million).

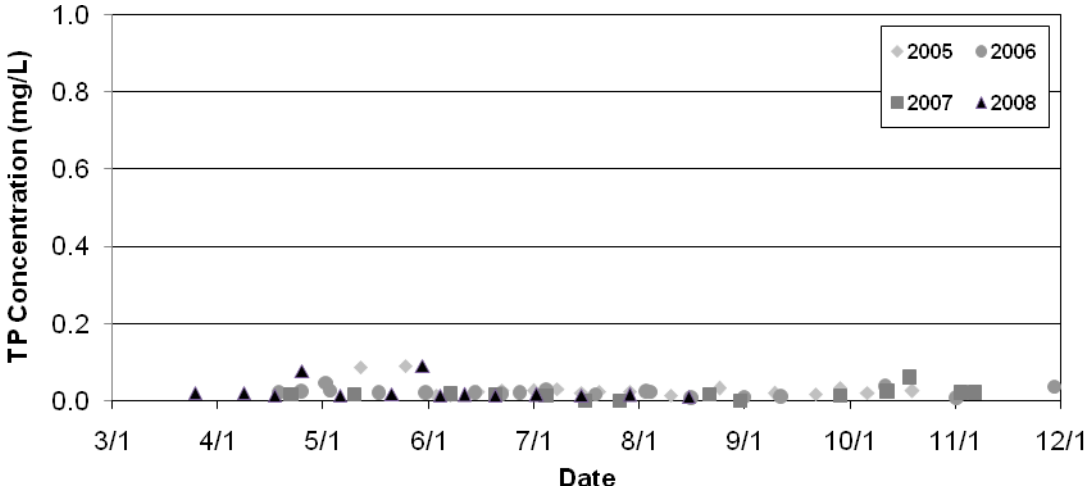

Figure 1.25 Subwatershed W4 tile drainage total phosphorus (TP) concentration 500 milliliter grab samples were taken at the tile drain outlet. Units are milligrams $P \cdot Liter^{-1}$ (parts per million).

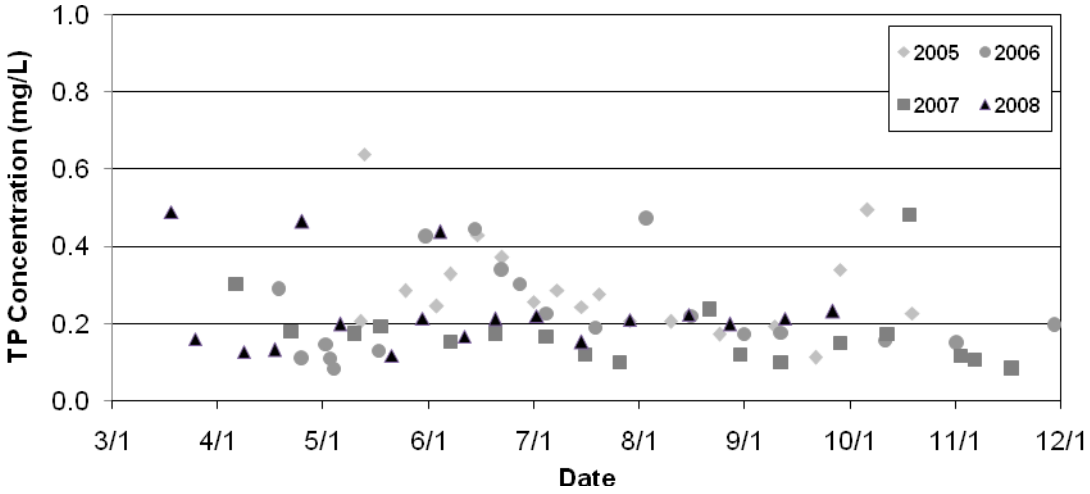

Figure 1.26 Subwatershed S2 total phosphorus (TP) concentration
500 milliliter grab samples were taken at the culvert passing under the road downstream of the JD37 tile drain outlet. Units are milligrams P·Liter $^{-1}$ (parts per million).

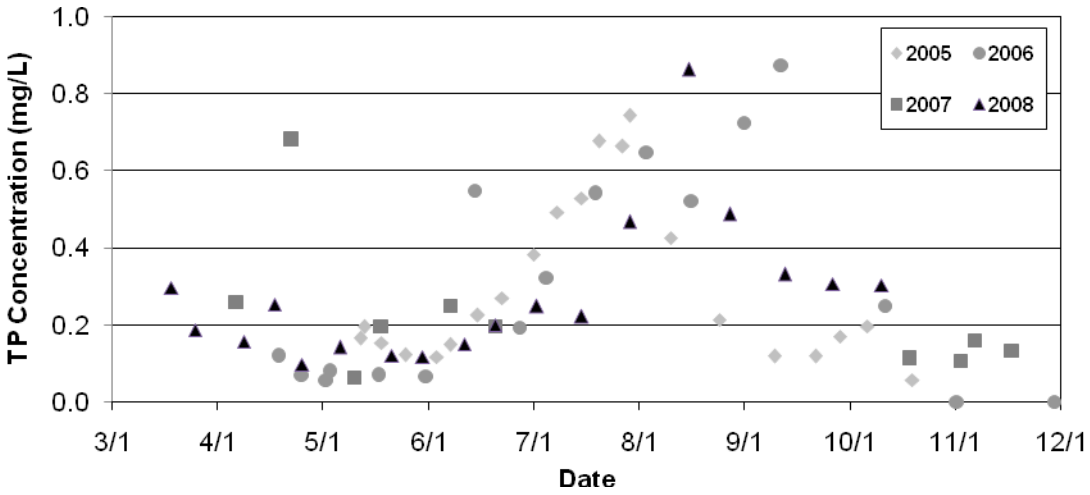

Figure 1.27 Subwatershed W5 total phosphorus (TP) concentration
500 milliliter grab samples were taken from water passing over the weir of the Kittleson basin outlet structure when flow was present. Samples were taken directly from wetland surface water during periods of zero flow. Units are milligrams P·Liter $^{-1}$ (parts per million).

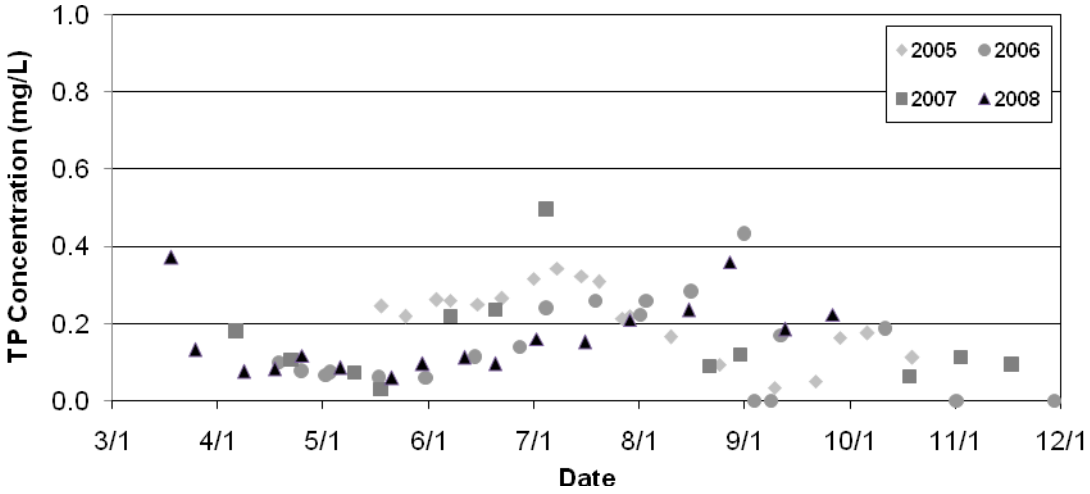

Figure 1.28 Subwatershed S1 total phosphorus (TP) concentration
500 milliliter grab samples were taken from water passing through the orifice of the Rosenberg basin outlet structure when flow was present. Samples were taken directly from wetland surface water during periods of zero flow. Units are milligrams P·Liter $^{-1}$ (parts per million).

We hypothesized that TP FWMC and loading from the W2 crop subwatershed would be higher than from the wetland subwatersheds due to the nutrient filtering effects of wetlands. However, we observed that the mean TP FWMC from the W5 subwatershed was greater than TP FWMC from the W2 subwatershed during both the drainage and the ET seasons and that TP FWMC from the S1 and S2 subwatersheds was greater than TP FWMC from the W2 subwatershed during the ET season (Figure 1.31, Figure 1.32). Similarly, TP loading from the W5 subwatershed was greater than TP loading from the W2 subwatershed, but only during the ET season (Figure 1.30).

For those series where the mean TP FWMC or area normalized loading were higher for W2 than the other subwatersheds, the results were tested for significance (α=0.05). Drainage season TP FWMC from W2 was not significantly greater than TP FWMC from S1 (Student's t-test, p=0.510; p=0.443, respectively). Drainage season TP loading for W2 was not significantly greater than W5 (Student's t-test, p=0.391, Wilcoxon Rank Sum test, p=0.443) or S1 (Student's t-test, p=0.133; Wilcoxon Rank Sum test, p=0.190).

Likewise, ET season TP loading for W2 was not significantly greater than S1 (Student's t-test, p=0.363; Wilcoxon Rank Sum test, p=0.845) or S2 (Student's t-test, p=0.333; Wilcoxon Rank Sum test, p=0.904).

Subwatershed TP responses were explored further by separating the surface runoff response from the subsurface tile response. The high TP concentrations of surface runoff dominated the response of the W2 subwatershed during both the drainage season and the ET seasons, despite the intermittent nature of surface flows (Figure 1.29 to Figure 1.32). Surface runoff FWMC during the drainage season was significantly higher than drain tile FWMC (Student's t-test, p=0.049; Wilcoxon Rank Sum test, p=0.029) and drainage season loading was also higher, but the difference was not significant at the α=0.05 level (Student's t-test, p=0.0985; Wilcoxon Rank Sum test, p=0.0571). Surface runoff FWMC and loading during the ET season were not significantly greater than tile drainage FWMC, however (Student's t-test, p=0.175; Wilcoxon Rank Sum test, p=0.204, respectively and Student's t-test, p=0.199; Wilcoxon Rank Sum test, p=0.310, respectively).

The influence of surface runoff was evident when subsurface tile discharge was compared to the wetland discharge. When surface runoff flows were excluded, drainage season W5 TP FWMC was significantly higher than W2 (Student's t-test, p=0.017; Wilcoxon Rank Sum test, p=0.0286), and S1 TP FWMC was higher than W2, but the difference was not significant at the α=0.05 level (Student's t-test, p=0.095; Wilcoxon Rank Sum test, p=0.10). ET season W5 TP FWMC was also significantly higher than W2 (Student's t-test, p=0.017; Wilcoxon Rank Sum test, p=0.013) and S1 and S2 TP FWMC were higher than W2 as well (Student's t-test, p<0.001; Wilcoxon Rank Sum test, p=0.013 in each case).

Wetland TP responses were also compared to each other. Although annual peak TP concentrations were higher in the Kittleson wetland than the Rosenberg wetland (Figure 1.27, Figure 1.28) loading differed significantly between the wetlands only during the drainage season (Student's t-test, p=0.03, Wilcoxon Rank Sum test, p=0.10), and

FWMC did not differ significantly in either season. This was probably because the peak concentrations of TP were measured during low or zero flow periods.

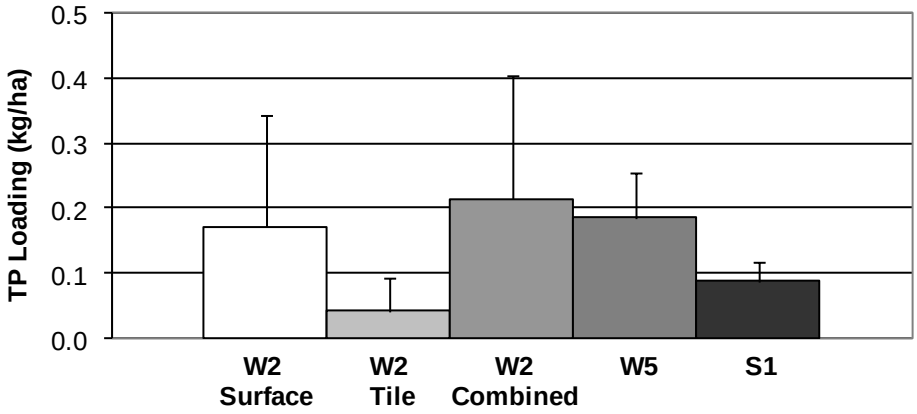

Figure 1.29 Drainage season area-normalized total phosphorus (TP) loading
Loading was calculated by dividing total load over dates April 14 to June 30 by subwatershed area. Units are kilograms P·hectare^{-1}.

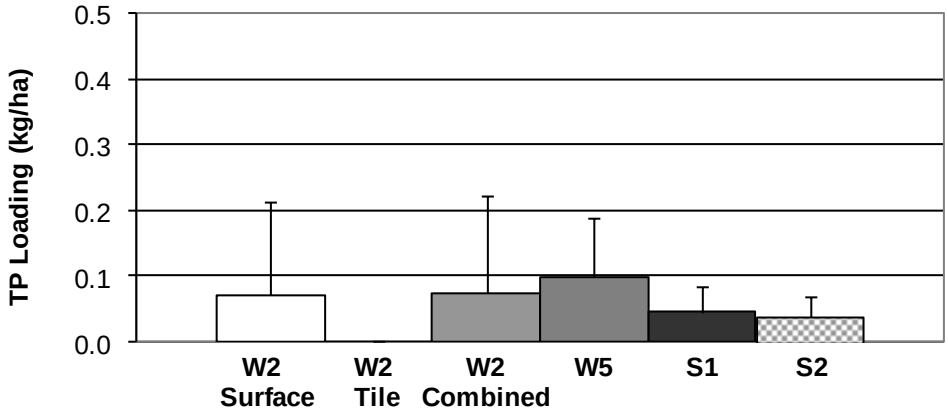

Figure 1.30 ET season area-normalized total phosphorus (TP) loading
Loading was calculated by dividing total load over dates July 1 to September 30 by subwatershed area. Units are kilograms P·hectare^{-1}.

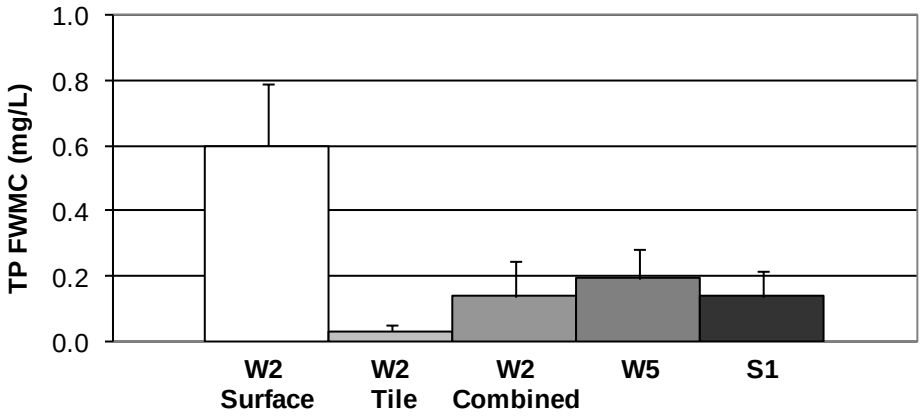

Figure 1.31 Drainage season total phosphorus (TP) flow weighted mean concentration (FWMC)
FWMC was calculated by dividing total load by total flow volume over dates April 14 to June 30. Units are milligrams P·Liter^{-1} (parts per million).

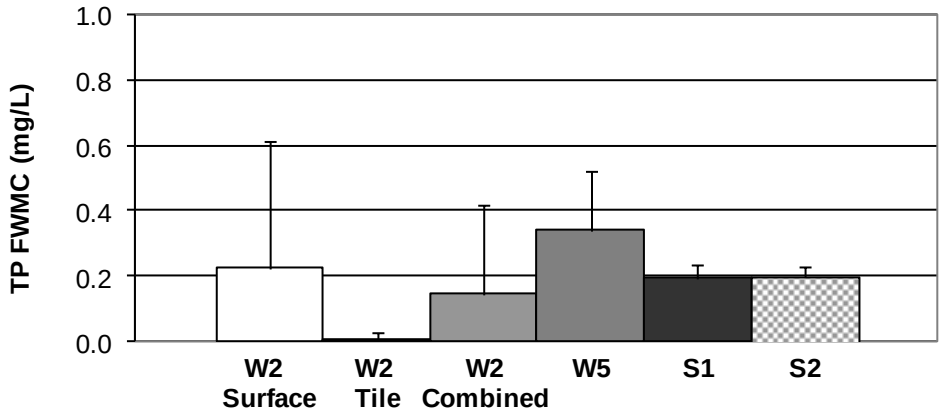

Figure 1.32 ET season total phosphorus (TP) flow weighted mean concentration (FWMC)
FWMC was calculated by dividing total load by total flow volume over dates July 1 to September 30. Units are milligrams P·Liter^{-1} (parts per million).

1.4.5 TSS Response

Total suspended solids (TSS) concentration measured in grab samples for the study years 2005 to 2008. Surface runoff TSS concentration was variable (Figure 1.33, Figure 1.34), but concentration was positively correlated with discharge for discharges above 0.2 cfs for W2 and 0.1 cfs for W4 (Figure 1.35, Figure 1.36).

In contrast to the surface channels, TSS concentration measured in the tile drains for the crop subwatersheds W2 and W4 was lower and much more stable. During the 2005 – 2008 study period, only one sample from subwatershed W2 (Figure 1.37) and two samples from subwatershed W4 (Figure 1.38) had TSS concentrations greater than 10 $mg \cdot L^{-1}$. There was no clear relationship between TSS concentration and season, or between TSS concentration and discharge.

The TSS concentrations measured at the wetland outlets W5 and S1 were generally higher than that measured at the tile drains. The W5 outlet series (Figure 1.39) exhibited more scatter and higher TSS concentrations than the S1 outlet (Figure 1.40). There was no clear relationship between discharge and TSS concentration for either site (not shown). The W5 outlet showed some seasonal differences, with TSS concentrations trending higher after approximately July 15 (Figure 1.39), likely due to the dense summer algal blooms that were observed in the Kittleson wetland each season from 2006 to 2008. The TSS concentration measured at subwatershed S2 was generally low and stable (Figure 1.41), as was seen in the drain tile flow from subwatersheds W2 and W4.

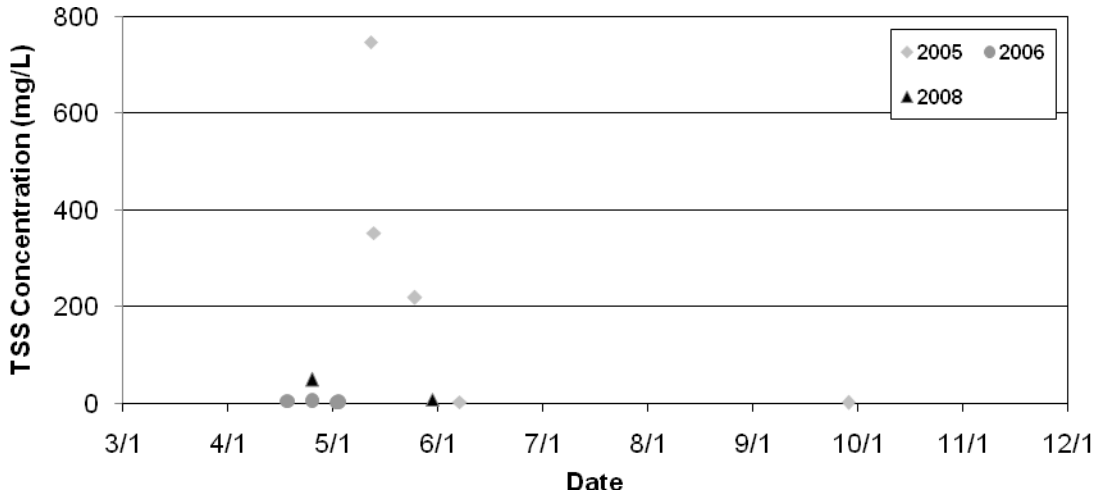

Figure 1.33 Subwatershed W2 surface channel total suspended solids (TSS) concentration
One liter grab samples were taken at the culvert passing under the road south of the Kittleson basin. Units are milligrams TSS·Liter^{-1} (parts per million).

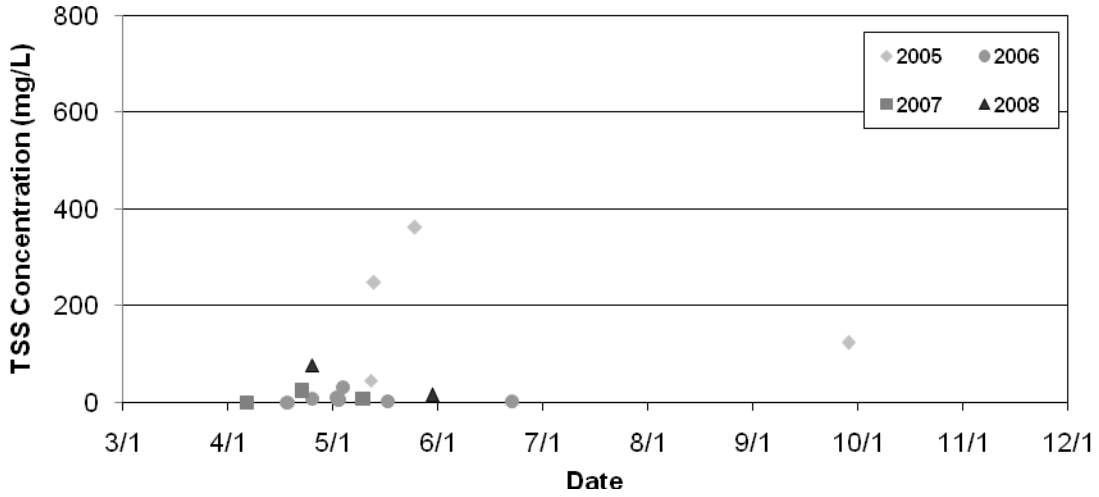

Figure 1.34 Subwatershed W4 surface channel total suspended solids (TSS) concentration
One liter grab samples were taken at the culvert passing under the road south of the Kittleson basin. Units are milligrams TSS·Liter-1 (parts per million).

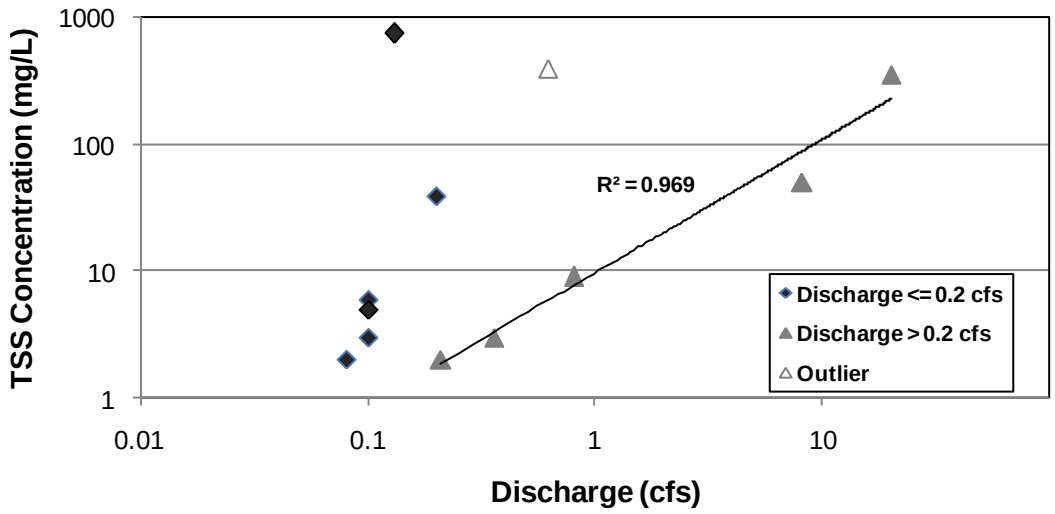

Figure 1.35 Discharge - TSS correlation for W2 surface channel.
One sample (0.62 cfs, 398 mg/L) was excluded from the regression series.

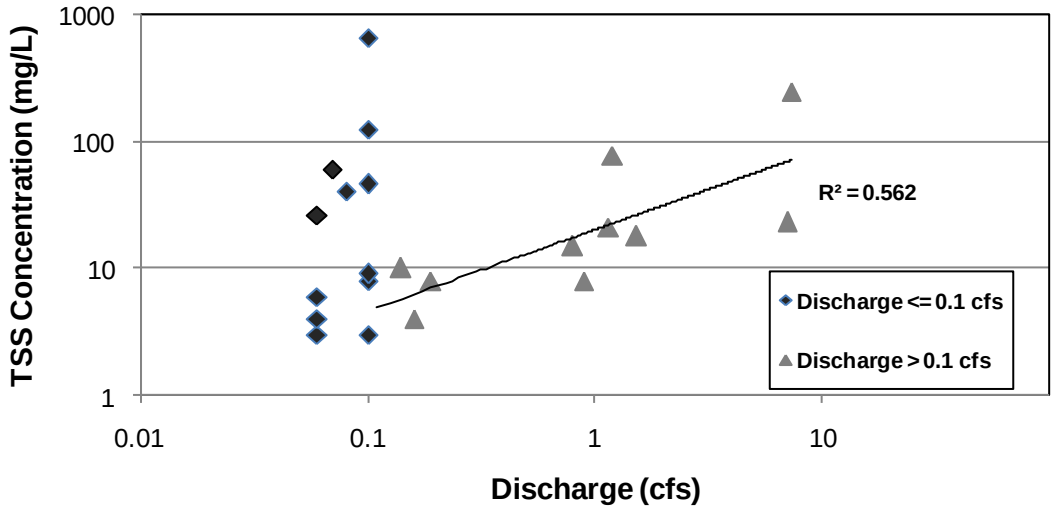

Figure 1.36 Discharge - TSS correlation for W4 surface channel.
No samples were excluded from the regression series.

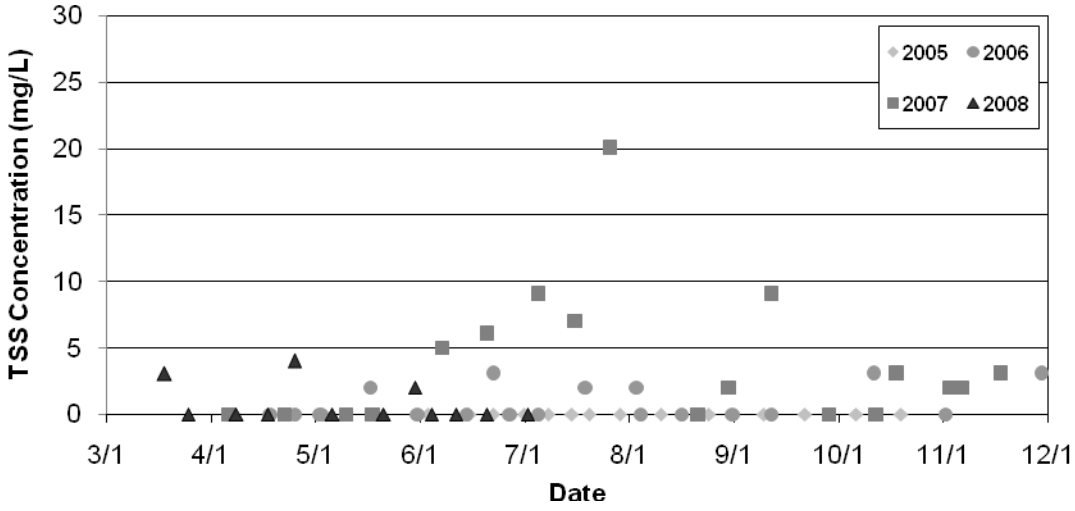

Figure 1.37 Subwatershed W2 tile drainage total suspended solids (TSS) concentration
One liter grab samples were taken at the tile drain outlet. Units are milligrams TSS·Liter^{-1} (parts per million).

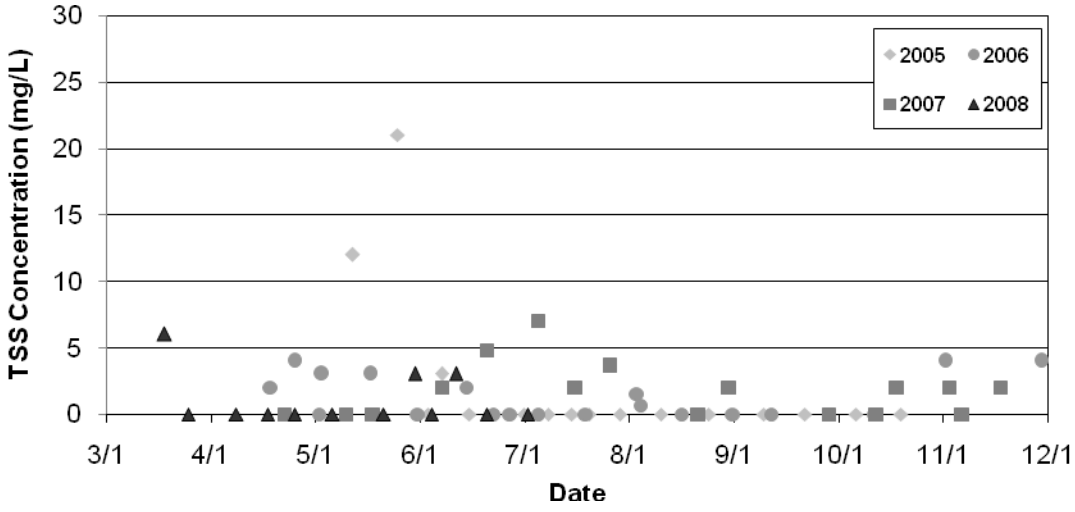

Figure 1.38 Subwatershed W4 tile drainage total suspended solids (TSS) concentration
One liter grab samples were taken at the tile drain outlet. Units are milligrams TSS·Liter^{-1} (parts per million).

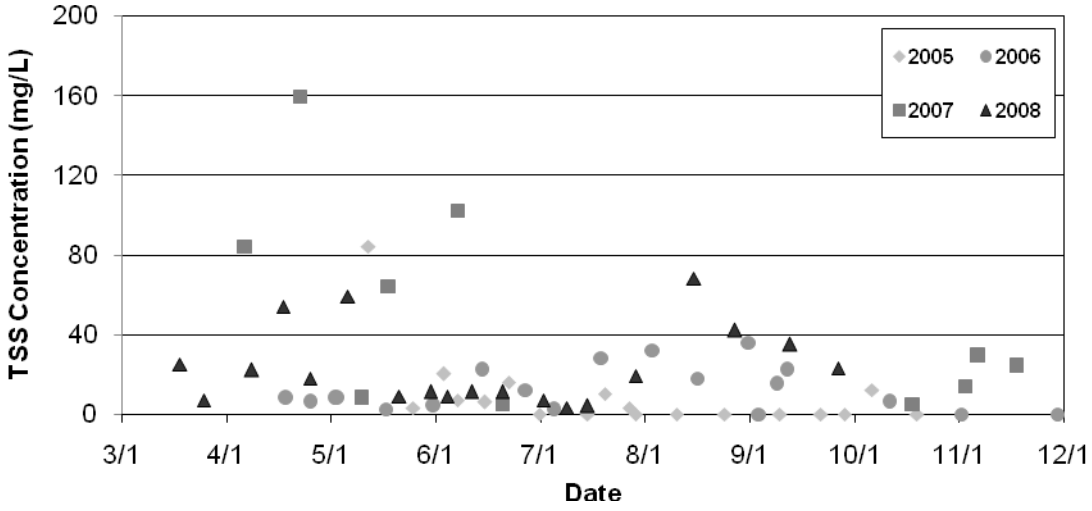

Figure 1.39 Subwatershed W5 total suspended solids (TSS) concentration
One liter grab samples were taken from water passing over the weir of the Kittleson basin outlet structure when flow was present. Samples were taken directly from wetland surface water during periods of zero flow. Units are milligrams TSS·Liter^{-1} (parts per million).

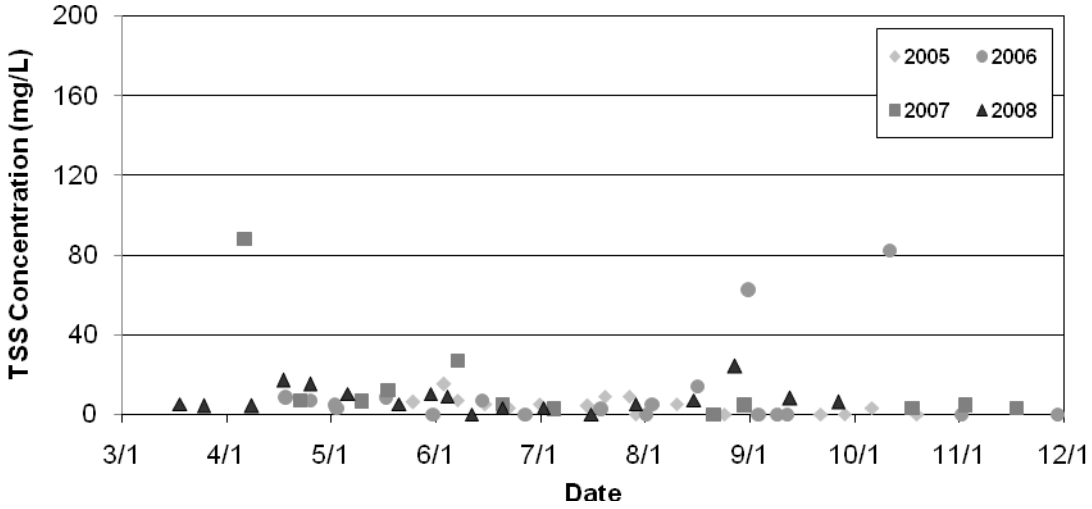

Figure 1.40 Subwatershed S1 total suspended solids (TSS) concentration
One liter grab samples were taken from water passing through the orifice of the lower SHEEK basin outlet structure when flow was present. Samples were taken directly from wetland surface water during periods of zero flow. Units are milligrams TSS·Liter^{-1} (parts per million).

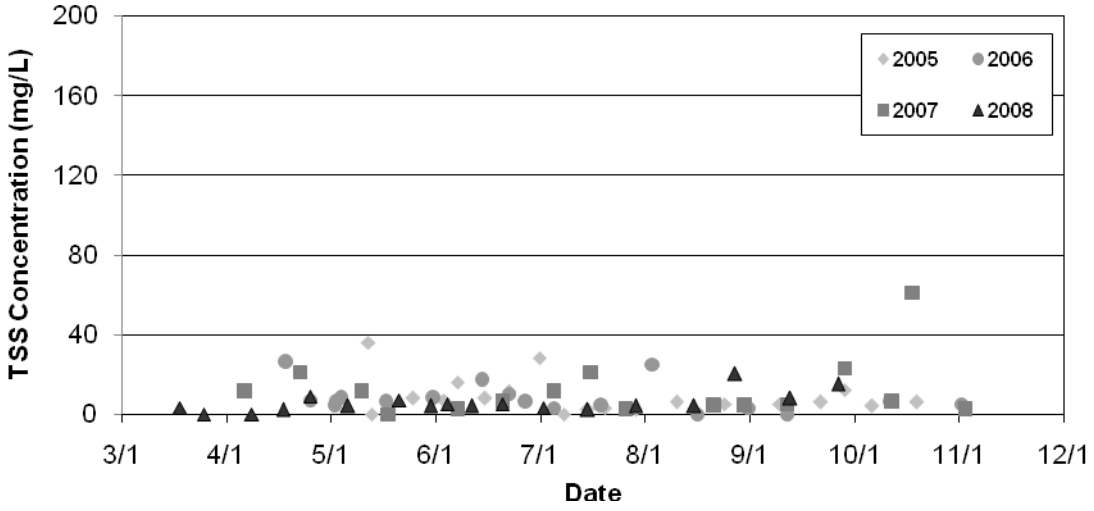

Figure 1.41 Subwatershed S2 total suspended solids (TSS) concentration
One liter grab samples were taken at the culvert passing under the road downstream of the JD37 tile drain outlet. Units are milligrams TSS·Liter^{-1} (parts per million).

We hypothesized that TSS FWMC and loading from the W2 crop subwatershed would be higher than from the wetland subwatersheds due to the settling of particles within the wetlands. However, statistical analysis using the Student's paired t-test and the Wilcoxon Rank Sum significance test showed that TSS concentration from the W2 subwatershed was not significantly higher than any of the other subwatersheds at the $\alpha = 0.10$ level during either the drainage season or the ET season. The absence of significant difference is explained by the high variance exhibited by the surface channel discharge, which dominates the W2 subwatershed response as seen previously with TP (Figure 1.42 to Figure 1.45).

When surface runoff contributions were excluded, drainage season W5 TSS FWMC and loading were significantly higher than W2 (Student's t-test, p=0.010, p=0.025; Wilcoxon Rank Sum test, p=0.014, 0.014), and drainage season S1 TSS FWMC and loading were significantly was higher than W2 (Student's t-test, p=0.017, p=0.009; Wilcoxon Rank Sum test, p=0.014, 0.014). This relationship held true for the ET season as well for both W5 (Student's t-test, p=0.038, p=0.038; Wilcoxon Rank Sum test,

p=0.029, 0.013) and S1 (Student's t-test, p=0.064, p=0.080; Wilcoxon Rank Sum test, p=0.029, 0.027).

Wetland TSS responses were also compared to each other. The Kittleson wetland TSS export was significantly greater than the SHEEK wetland TSS export during the drainage season as measured by FWMC (Student's t-test, p=0.026; Wilcoxon Rank Sum test, p=0.029), or loading (Student's t-test, p=0.044; Wilcoxon Rank Sum test, p=0.029). There was no significant difference between the two wetlands during the ET season.

It was hypothesized that the greater TSS export from the Kittleson wetland was due to a greater propensity to wind-aided sediment resuspension. The wind-TSS relationship is explored further in Chapter 2 of this thesis.

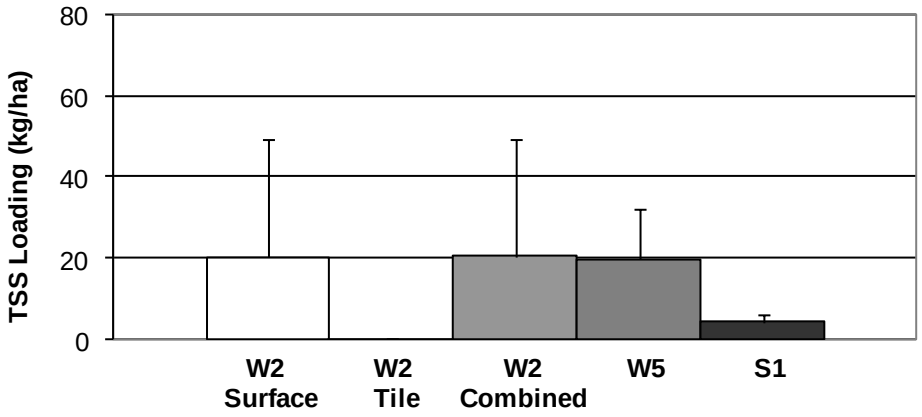

Figure 1.42 Drainage season area normalized total suspended solids (TSS) loading
Loading was calculated by dividing total load over dates April 14 to June 30 by subwatershed area. Units are kilograms TSS·hectare^{-1}.

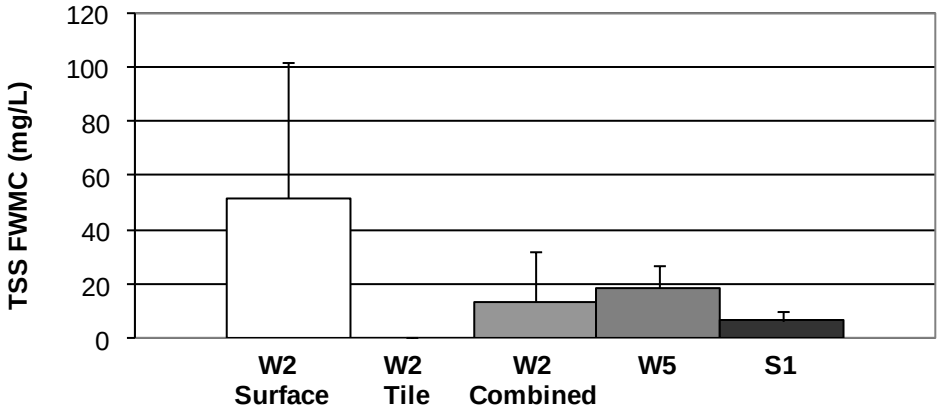

Figure 1.43 Drainage season total suspended solids (TSS) flow weighted mean concentration (FWMC)
FWMC was calculated by dividing total load by total flow volume over dates April 14 to June 30. Units are milligrams TSS·Liter^{-1} (parts per million). Error bars represent one positive standard deviation.

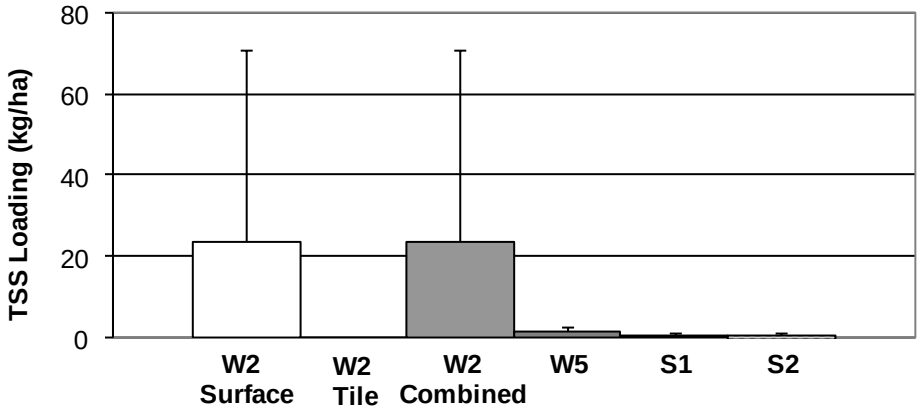

Figure 1.44 ET season area normalized total suspended solids (TSS) loading
Loading was calculated by dividing total load over dates July 1 to September 30 by subwatershed area. Units are kilograms TSS·hectare^{-1}.

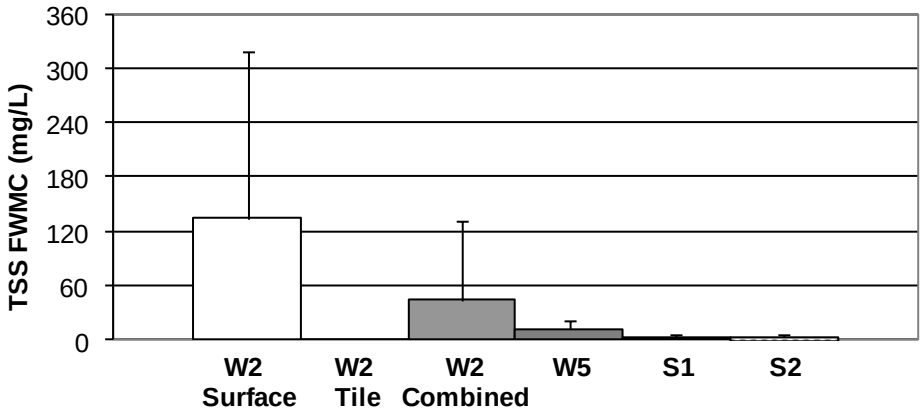

Figure 1.45 ET season total suspended solids (TSS) flow weighted mean concentration (FWMC)
FWMC was calculated by dividing total load by total flow volume over dates July 1 to September 30. Units are milligrams TSS·Liter^{-1} (parts per million). Error bars represent one positive standard deviation.

1.5 Discussion

The restored perennial vegetation/wetland complexes were expected to reduce water yield through increased transpiration during the early season. However, the water yield was not significantly different from the water yield from the crop subwatershed. This may be the result of the low transpiration rate of the warm season grasses used in the seed mix for the CREP land, as seen in the separate studies of Hutchinson and Hinck ((Hutchinson, Koelliker, Knapp 2008), (Hinck 2008)).

The wetlands were successful in reducing peak flows, as expected. Peak flow attenuation is desirable for Elm Creek in order to reduce the tendency of the creek to downcut within its channel and undercut its banks, both process which release sediment and phosphorus.

The restored wetlands were expected to act as sinks for nutrients and sediment. While the wetlands did act as sinks for nitrate, they did not perform as expected for phosphorus and sediment, due to a complex set of factors including biogeochemical characteristics, water elevations, and basin morphology.

With respect to nitrate, the wetlands were effective nutrient sinks. The Iowa CREP program recommends that wetlands be sized between 0.5% and 2% of their watershed area (Crumpton and others 2006). In this study, the area of each wetland complex was approximately 6% of its contributing watershed area. The data confirmed that the wetlands were appropriately sized to remove substantial amounts of nitrate through denitrification. Nitrate export was confined to the period from snowmelt until growth of denitrifying microorganisms were stimulated by warming water temperature; thereafter, NN concentrations in the wetlands decreased steadily after May 1 and were below the limits of detections by July 1 in most years.

With respect to TP, it was found that W5 subwatershed exhibited higher phosphorus export than the W2 watershed in every year except 2008 (Figure 1.46). TP export from subwatershed W5 was particularly high in 2005. The high transport rate in 2005 was the

result of high discharge acting in synergy with an early peak in TP concentration within the wetland. The cumulative export graph (Figure 1.47) shows that April to mid-June phosphorus export in 2007 was greater than phosphorus export in 2005, but abnormally dry conditions in the summer of 2007 caused the wetland to stop discharging by late June, before TP concentration in the wetland peaked. Similarly, during the 2008 season, high early season flows from the wetland due to above-normal April and May precipitation did not result in high TP export because TP concentration remained relatively low (approximately 200 $mg \cdot L^{-1}$) through July 15th. Only in 2005 did normal to above-normal precipitation fall throughout the summer, causing the wetland to discharge throughout the months of July and August, when TP concentration was at its peak (Figure 1.48).

Several other factors could impact the timing of the mid-summer phosphorus peak, including water temperature, the presence of alternate electron acceptors such as nitrate, and the presence of organic material. Comparison of the NN and P concentrations in grab samples taken from the wetlands showed that in every year, the rise of TP concentration in the Kittleson basin immediately followed the depletion of NN (data not shown). Water temperature and organic material availability were not examined as part of this study.

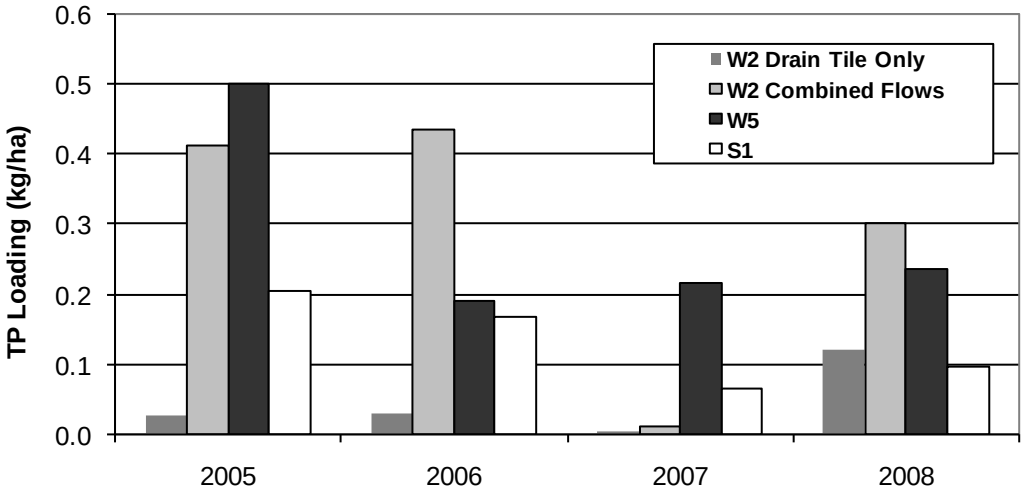

Figure 1.46 Subwatershed area-normalized total phosphorus (TP) loading
Loading is for dates April 14 to September 30. Subwatershed W2 is the sum of surface channel and drain tile loading. Units are kilograms P·hectare^{-1}.

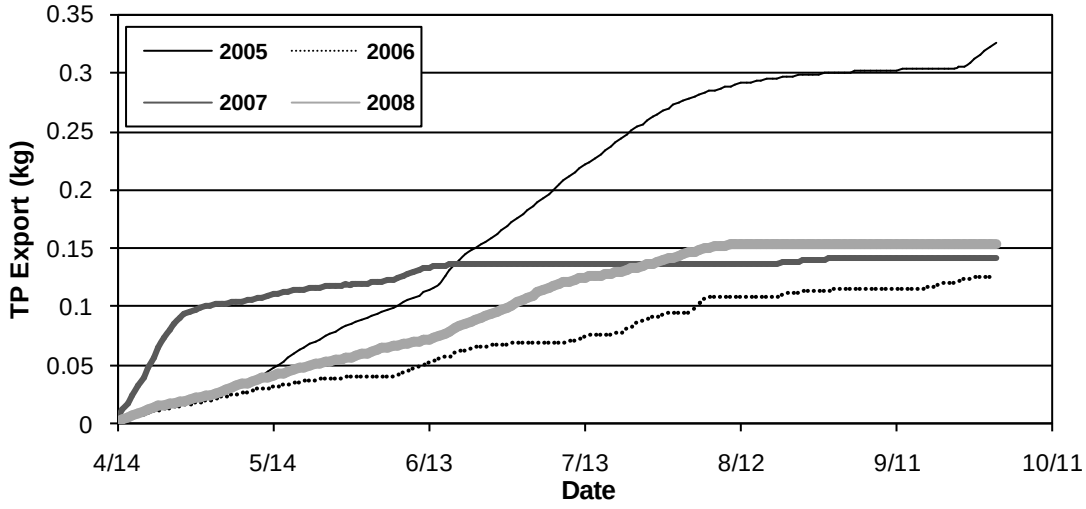

Figure 1.47 Subwatershed W5 cumulative total phosphorus (TP) export, 2005 - 2008
Daily loads were estimated using the 'Series' function in FLUX.
Units are kilograms of P.

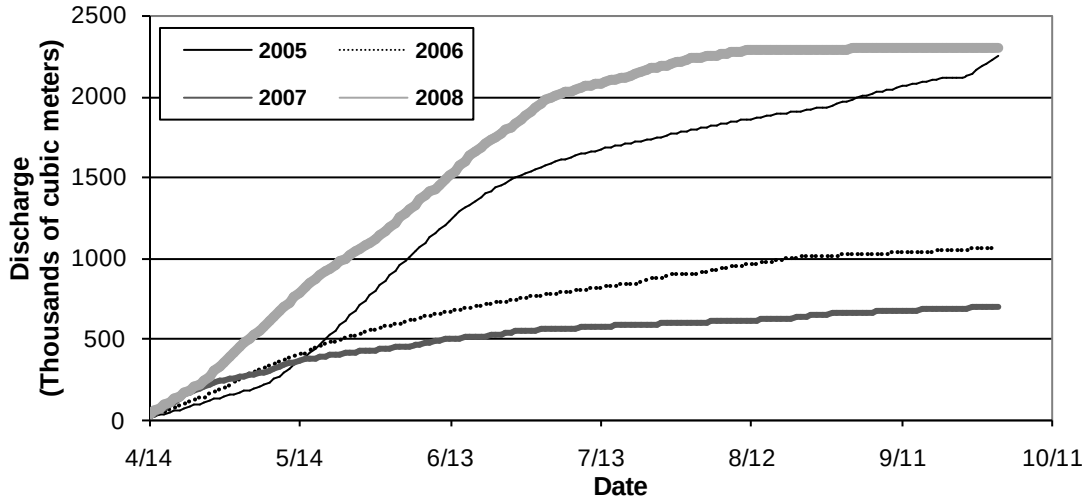

Figure 1.48 Subwatershed W5 cumulative discharge, 2005 - 2008
Daily flows were calculated from 15-minute flow data. Units are thousands of cubic meters.

The seasonal TP fluctuations displayed by both wetlands resemble the TP patterns in shallow lakes that are driven by internal phosphorus loading (Scheffer 1998). Lakes and wetlands located in southern Minnesota are often affected by the internal loading process, where phosphorus contributed by external sources and stored in bottom sediments is remobilized and returned to the water column.

The process begins when warm temperatures and large supplies of organic matter stimulate microbial growth along the sediment surface. Dissolved oxygen quickly becomes depleted by aerobic microbial processes, and anaerobic microbes then convert the oxidized form of iron (a strong phosphorus binder) to its reduced form (a weak phosphorus binder). Because the overlying water column is often aerobic in shallow, polymictic basins like the study wetlands, a redox gradient develops from deep, highly reducing sediments, where porewater phosphorus concentrations can reach concentrations as high as 13 mg/L (Gelbrecht and Lengsfeld 1998), to shallow, oxidative sediments with lower concentrations of dissolved P. Porewater phosphorus moves upward through the sediment by diffusion according to Fick's Law (Mulqueen,

Rodgers, Scally 2004). As the porewater phosphorus approaches the relatively oxic sediment-water interface, multiple factors including mineral content (Loeb, Lamers, Roelofs 2008; Zak, Gelbrecht, Steinberg 2004), mechanical perturbation by fish or wind (Scheffer 1998)and pH (Reddy 2008) determine whether phosphorus crosses the interface and enters the water column or reprecipitates in the sediment.

To verify that a reducing environment was present during the summer months, oxidative reductive potential (ORP) was measured in the wetlands beginning in August 2008. In the Kittleson wetland, ORP was in the reducing range (< 0 mV) during the late summer, then became oxidizing (> 0 mV) during the fall (Figure 1.49). The deeper transect sites (KB2, KB3, KB4, and KB5) were in the reducing range more often than the shallow sites, probably because they were less prone to mixing with oxygen-rich surface waters. Similar results were seen for the lower SHEEK wetland (data not shown).

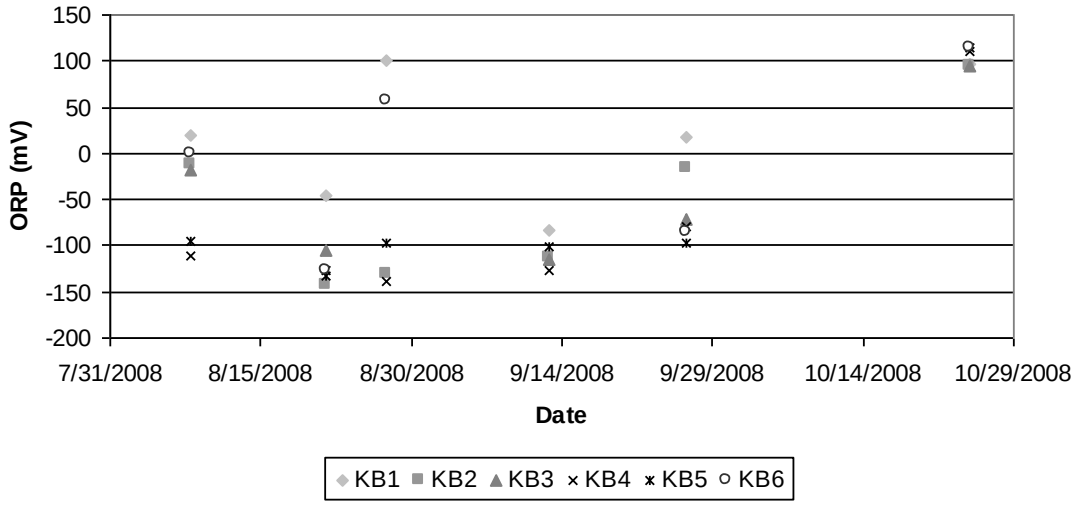

Figure 1.49 Kittleson wetland oxidative reduction potential (ORP)
ORP was measured by lowering a YSI multiparameter sensor to within approximately five centimeters of the sediment interface.

With respect to sediment export, the results were variable. Over the course of the four year study period, the sediment yield from the crop subwatershed was not significantly different from the sediment yield from the wetland watersheds. In years where there was significant surface runoff from the crop subwatershed surface channels, the wetlands may have acted as sinks for sediment. In years where there was little channelized runoff, the wetlands themselves – particularly the Kittleson basin – may have acted as sediment sources.

It is important to note that before the 2004 restoration, none of the subwatersheds contributing to the Kittleson basin were directly connected to Elm Creek. There were no surface ditch connections, nor were there any open standpipes which fed into JD73-2 within the Kittleson basin area. Therefore any sediment which was transported to the basin area before the wetland was restored was effectively trapped there and did not contribute to turbidity or TP concentration in the creek. The only sediment reaching the creek from these areas pre-restoration was carried by the subsurface tiles, which the study showed to be very low in TSS concentration. The wetland outlet to JD73-2 effectively opened a new route to transport sediment from the upper part of the watershed to Elm Creek. Because this is a new load, the W5 subwatershed has become a net source of sediment in all years. Wetlands which are restored along the flowpaths of existing intermittent channels or gullies which already flow directly into the creek are more likely to become net sinks for sediment.

We anecdotally noted that the highest TSS concentrations measured at the Kittleson basin outlet were coincident with windy conditions on the sampling day. We also noted that TSS concentrations in the Kittleson basin discharge were higher and more variable than TSS concentrations in the lower SHEEK basin discharge. We hypothesized that wind-aided resuspension played a role in the development of high TSS concentrations within the wetlands, and that the effect was greater in the Kittleson basin because it had a larger fetch than the lower SHEEK basin. The relationship between wind and sediment export was studied in detail in chapter two of this thesis.

Chapter 2 Sediment resuspension and export

2.1 Introduction

The bottom sediments of lakes are subject to resuspension whenever waves with sufficient shear force reach the sediment surface. Since all particles sink at a velocity related to particle size (a process known as sedimentation), particles in deep lakes can escape later resuspension when they are transported laterally to a deeper area and then sink to depths below the reach of resuspension waves. In this manner finer particles (those that suspend more easily and sediment more slowly) are sorted to deeper water, while areas that are more susceptible to resuspension become enriched in coarser particles that are more difficult to resuspend. However, particles in the shallow, polymictic lakes common to the PPR cannot sink to a depth beyond the reach of waves, and therefore remain susceptible to resuspension.

Flow-through wetlands restored along drain tile lines can export suspended solids under certain circumstances. When flooded soil is subjected to mechanical disturbances such as waves or the fish activity, sediment particles become suspended in the water column and can be exported during discharge periods. Anecdotal observations over four years of sampling at two wetland restoration sites suggested that suspended solids concentrations increased markedly during periods of high winds. Therefore, a flow-based model using grab samples taken at long intervals may be insufficient to accurately predict loading of suspended solids to Elm Creek.

This chapter details efforts to determine whether wind was a satisfactory explanatory variable for suspended solids export, and to build an empirical predictive model for the Kittleson basin site.

2.2 Literature Review

While the dynamics of wave movement are complex, a simple model has been used to successfully model resuspension in a shallow lake in Iowa(Carper and Bachman 1984). Formulae developed for coastal areas (US Army Coastal Engineering Research Center 1977)were applied to the shallow lake system, and sampling of inorganic total suspended solids (TSS) confirmed that resuspension occurred when winds passed a predicted critical velocity. Wavelengths roughly equal to twice the water depth were required to reach the bottom, and those wavelengths could be calculated by:

$$L_w = 1.56\left[0.77\,W\ \tanh\left[0.077\left(\frac{9.8F}{W^2}\right)^{0.25}\right]\right]^2$$

Equation 2

where L_w is the wavelength in meters, W is wind velocity in meters per second, and F is the fetch length in meters. Therefore, if bathymetry of a water body is known, the area contributing suspended sediment is defined as a function of wind velocity, wind direction, fetch and depth. Whether sediment is resuspended when waves touch the bottom depends on critical shear stress, a function of particle size and bottom consolidation.

The vertical flux of particles is represented by the resuspension rate minus the sedimentation rate

$$\upsilon = E - w_s C$$

where υ is the vertical flux, E is the resuspension rate ($g \cdot cm^{-2} \cdot s^{-1}$), *w* is the depth-averaged settling velocity ($cm \cdot s^{-1}$) and C is the depth-averaged concentration of suspended sediment ($g \cdot cm^{-3}$) (Sheng and Lick 1979). It follows then that given a steady wind velocity, the system will reach a steady state where vertical flux is 0:

$$C_e = \frac{E}{w_s}$$

If the body of water has a defined background concentration C_b of suspended sediment that sinks very slowly (fine particulates and phytoplankton), the total concentration C at a point is:

$$C = C_b + C_e$$

Empirical models of resuspension have been developed for specific water bodies using the above relationships. Kristensen et al. described a model to predict suspended solid concentration at a mid-lake station in a large shallow lake (Kristensen, Søndergaard, Jeppesen 1992). Their model was based on wind velocity, water depth and the mean particle settling velocity, but neglected horizontal particle gradients or transport. The model predicted that lake sediment was subject to resuspension approximately 50% of the time, with suspended solids reaching concentrations of up to 150 $mg \cdot L^{-1}$. Inclusion of fetch distance and wind direction did not significantly improve the model. A New Zealand study used bottom shear stress calculated by wave theory to build empirical models of shallow lakes (Hamilton and Mitchell 1996). Regression analysis of TSS concentration on predicted shear stress showed that the slope of the relationship varied 25-fold over the seven lakes of the study. Addition of macrophyte biomass and sediment settling velocity to the regression helped to explain most of this variation.

In addition to the vertical processes of resuspension and sedimentation, the concentration of suspended solids at a measuring station is also dependent on the effects of horizontal redistribution (Hamilton and Mitchell 1996). Once particles have been resuspended, they move horizontally in the direction of the wind at 1-2% of average wind speed (Bailey and Hamilton 1997). Therefore, the suspended solids concentration at a given point, under the influence of a wind blowing toward it at a constant velocity and direction, increases until it reaches a maximum at the time when sediment from the most distant contributing area reaches the station. An Australian shallow lake was modeled using a process-based 100 meter grid resuspension model coupled with a

hydrodynamic model to allow for horizontal transport and recirculation (Bailey and Hamilton 1997). The work showed that in areas with varying wind direction, changes in wind direction, and corresponding changes in fetch, were much more important that advection and diffusion in determining sediment distribution.

The prior modeling work suggests that suspended sediment concentration for a station located near the shore of a small lake may be relatively simple to model. A limited range of wind directions will have significant impact on the station, and the potential contributing area is significantly reduced.

2.3 Materials and Methods

Water samples were collected at the Kittleson wetland outlet using an ISCO Teledyne model 3700 automatic sampler and one liter wedge bottles, with the sampler port suspended in the upstream section of the water control structure. During the 2008 season the sampler was programmed for 6 hour intervals: 0400, 1000, 1600, and 2200. During the 2009 season the sampler was programmed for 8 hour intervals: 0800, 1600 and 2400. Sampling was limited to the relatively high flow period of the early season to minimize the possibility of particles settling within the box behind the weir or the inlet pipe from the wetland. At the end of the 24 bottle sequence, bottles were capped and mixed by inversion, then aliquots were poured into 500 mL storage bottles for laboratory analysis. Wedge bottles were rinsed and returned to the sampler.

Assays for total suspended solids (TSS) and suspended volatile solids (SVS) were done at the Saint Croix Watershed Research Station using methods similar to according to EPA method 160.2 and 160.4, respectively, except that samples were sometimes held beyond the seven-day holding period established by the methods because of sampling and equipment limitations. Briefly, glass fiber filters (Whatman type 934-AH, 1.5 micron pore diameter) were pre-burned in a muffle furnace overnight at 550 degrees Celsius. Each filter was then pre-weighed before being clamped into a vacuum filter apparatus. Water bottles were pre-weighed, then mixed thoroughly by inverting several times and a minimum of 100 mL was poured onto the filter. Vacuum was applied until all water had passed through the filter, then each filter was removed from the apparatus and placed individually into an aluminum tray. The filters were dried overnight (> 12 hours) at 105 degrees Celsius, then weighed. The difference between the pre-filtration weight and the 105 degree dried weight was taken as TSS. The filters were then placed in a muffle furnace and heated for two hours at 550 degrees Celsius. The difference between the 105 degree dried weight and the 550 degree weight was taken as SVS. The weight of the inorganic solids was obtained by subtracting SVS from TSS.

To measure wind velocity and direction, a Campbell Scientific model 03001 anemometer and wind vane sensor was installed near the southeast shore of the

Kittleson wetland. The sensor was placed on a two meter pole and placed so that it was not subject to sheltering from trees. Sensor measurements were scanned at one minute intervals, and the values were averaged and stored at twenty minute intervals on a Campbell Scientific CR10 datalogger.

2.4 Results

2.4.1 Suspended solids analysis

The date range for sampling the wetland discharge was from March 25, 2009 until June 12, 2009. Over that period, 174 samples were taken and subsequently analyzed for TSS and SVS. Early season sampling was intermittent because the sampling line occasionally froze at night, so only sample bottles that were completely filled were analyzed. The results from seven samples (12 AM on April 11 to 8 AM on April 12, 4 PM on April 25, and 8 AM on June 9) were discarded due to mishandling during testing, and the results from ten samples (June 2nd to June 4) were discarded because discharge was zero on those days. Wind velocity and direction records from the on-site weather station began at 6:20 PM on March 28.

The wetland was largely covered with ice until March 30, and samples taken before that time were assumed to reflect a background level of suspended solids. The six samples taken during this time averaged 12.6 $mg \cdot L^{-1}$ TSS and 5.5 $mg \cdot L^{-1}$ SVS. Most timepoints throughout the period of record showed TSS near the background levels that were recorded before ice-out. However, five peaks where the concentration exceeded 25 $mg \cdot L^{-1}$ were evident. TSS concentration had no discernible relationship with discharge (Figure 2.1) further supporting the presence of another determining factor for TSS concentration.

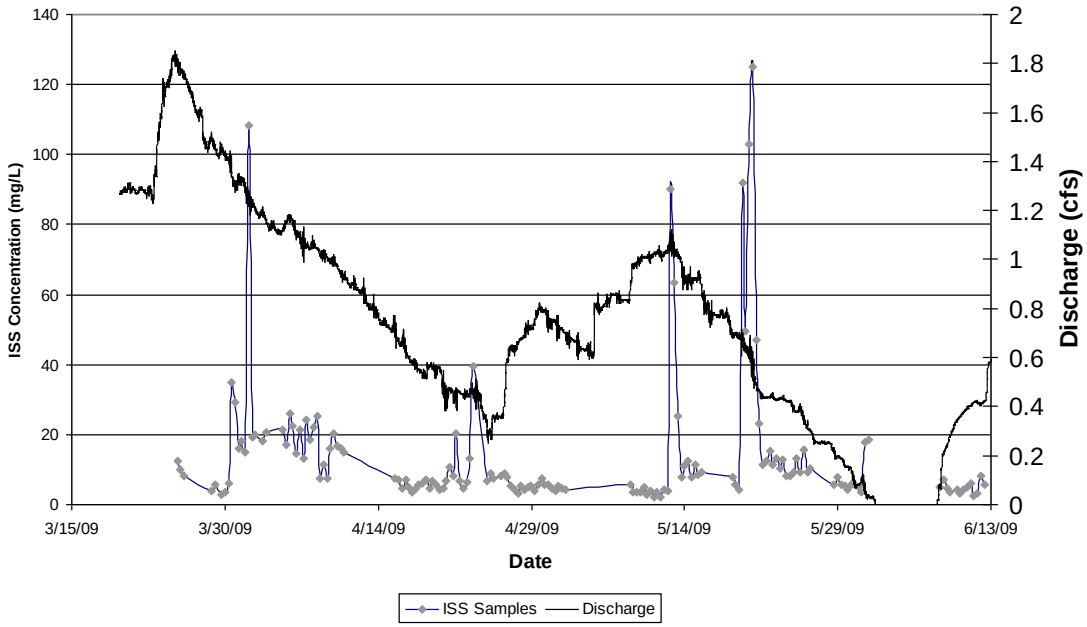

Figure 2.1 W5 discharge and inorganic suspended solids (ISS) concentration
Units are milligrams·Liter^{-1} for ISS concentration and feet^{3}·second^{-1} for discharge.

During the period that the wetland was free of ice, the TSS averaged 20.1 mg·L^{-1}, ranging from 4.81 to 160.4 mg·L^{-1}, and the SVS averaged 6.81 mg·L^{-1}, ranging from 3.93 mg·L^{-1} to 35.3 mg·L^{-1}. SVS averaged 40% of TSS, with a range from 0% to 78%. The proportion of SVS varied over the course of the sampling period; early season SVS was high, probably reflecting detritus accumulation over the winter months, then the concentration dropped before trending upward for the remainder of the period (Figure 2.2). In late May, an algal bloom was observed that corresponded to the peak values of SVS. To avoid confounding effects from phytoplankton growth, which is independent of wind velocity, the non-volatile, or inorganic suspended solid (ISS) fraction was chosen as the response variable for the model.

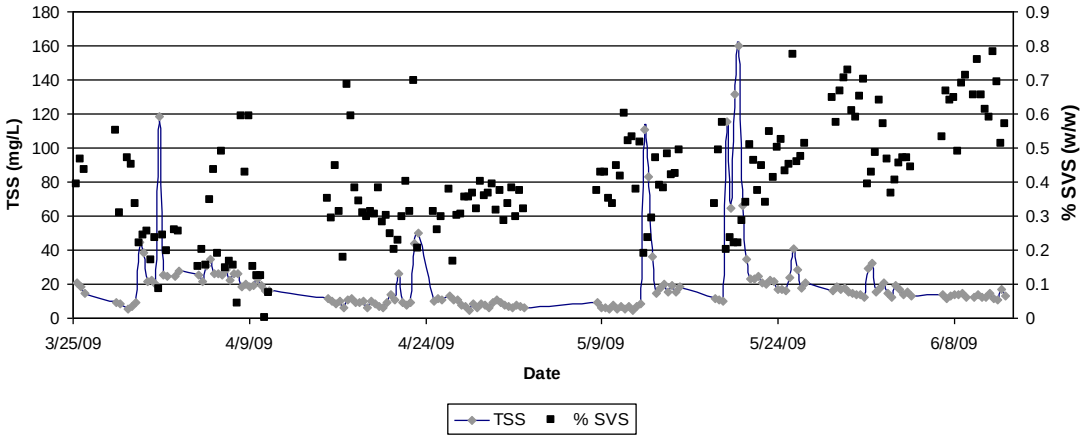

Figure 2.2 Total suspended solids (TSS) concentration and suspended volatile solids (SVS) proportion
Total suspended solids concentration for time based samples is shown on the left axis, with units of milligrams·L-1. SVS proportion of TSS is shown on the right axis (unitless).

2.4.2 Anemometer data analysis

Wind velocities varied widely over the monitoring period. The average velocity was 13.7 km/hour, and the maximum was 63.1 km/hour, recorded on May 13. Daily wind velocity ranged from 2.4 km/hour to 30.2 km/hour, with an average of 13.7 km/hour.

Since the concentration of wind-resuspended sediment at any specific time point was predicted to be based on the actions of wind during the recent past, average wind velocities calculated on trailing 24 hour windows were used to explore patterns in the relationship of wind to suspended sediment. All recorded peaks in ISS were associated with sustained high winds (Figure 2.3). However, the converse was not true; many wind velocity peaks were associated with background ISS, suggesting that another factor was involved.

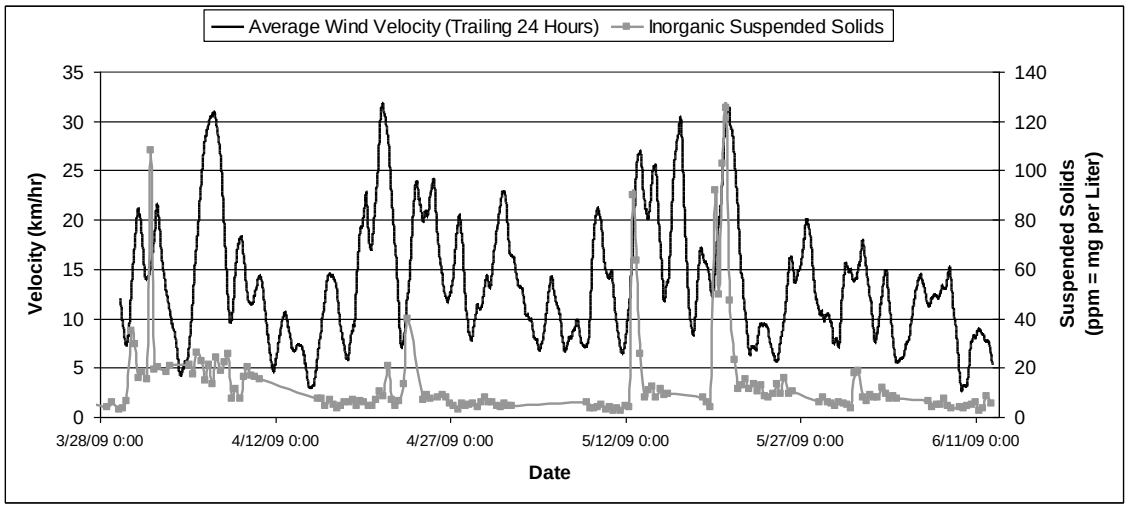

Figure 2.3 Trailing 24 hour wind velocity and ISS concentration

Suspended solids can travel in the direction of the wind at a velocity of 1%-2% of the wind velocity once they are suspended (Hamilton and Mitchell 1996), so the highest near-shore ISS concentrations would theoretically result from sustained high winds that resuspend sediment in upwind source areas and transport them towards the opposite shore. There, they would accumulate and remain in suspension due to the shallow bottom and long fetch. Because the outlet was located at the northern shore of the wetland, southerly winds were expected to have the strongest influence on ISS concentration of the discharge. To elucidate a mathematical relationship, vector formulas were used to assign numeric values to wind directions. The formula for the 'j' vector used the cosine of the wind direction to assign winds straight from the south (180 degrees) with a value of -1 per km/hr and winds from the north (0 degrees) with a value of +1. Likewise, a formula for the 'i' vector used the sine function to assign winds straight from the east (90 degrees) and west (270 degrees) with values of +1 and -1, respectively. The vectors were averaged over the trailing 6, 12, or 18 hour periods and multiplied by the average wind velocity over the corresponding period to obtain the magnitude of past wind effect for each 20-minute time point. The signs for the 'j' vector were swapped (180 degrees = +1, 0 degrees = -1) in order to reflect the predicted positive correlation between ISS and south winds.

Clear trends were seen in the plot of wind velocity, vector magnitudes and inorganic solids. Marked increases in ISS coincided with high velocity south winds, but not north winds (Figure 2.4). Winds from the east were generally low in magnitude during the monitoring period, and ISS concentrations were similarly low, even though the largest fetch is east of the outlet (Figure 2.5). Winds from the west were relatively high in magnitude, but were not associated with increased ISS, possibly due to geography, short fetch length or the tangential relationship of west winds with the north shore.

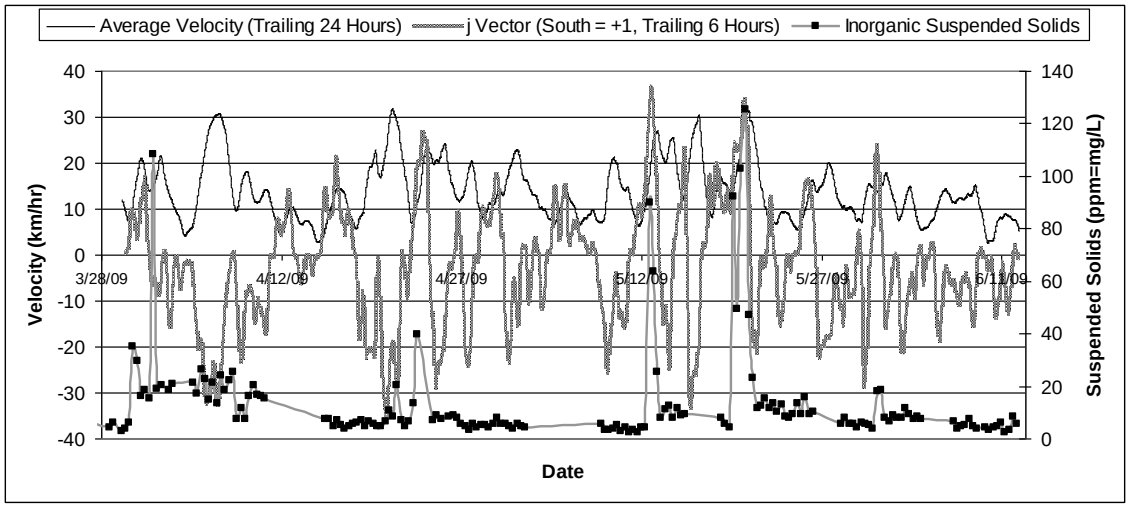

Figure 2.4 Trailing 24 hour wind velocity, trailing 6 hour j vector magnitude, and ISS.

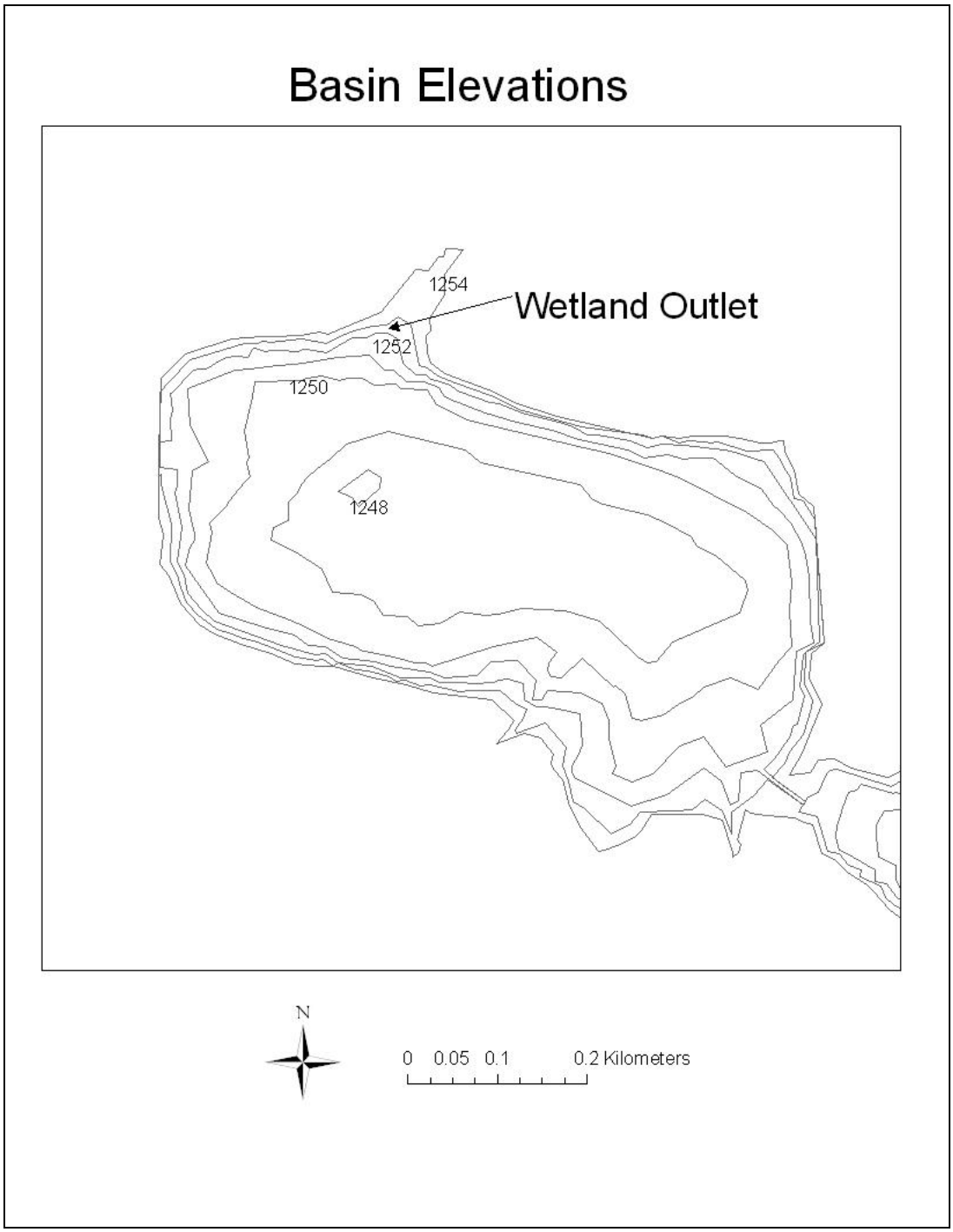

Figure 2.5 Basin Bathymetry
Elevations referenced to mean sea level (units of feet) were measured by BWSR in surveys prior to restoration. Depth at design elevation is calculated by subtracting the elevation from 1252.

2.4.3 Sediment resuspension modeling

The wind vector relationship was used to build a simple linear model to predict ISS loading based on wind velocity and direction measurements. The ISS concentrations were not normally distributed, so a log transformation was used (Figure 2.6). Wind and vector magnitudes were distributed approximately normally (not shown), and were not transformed.

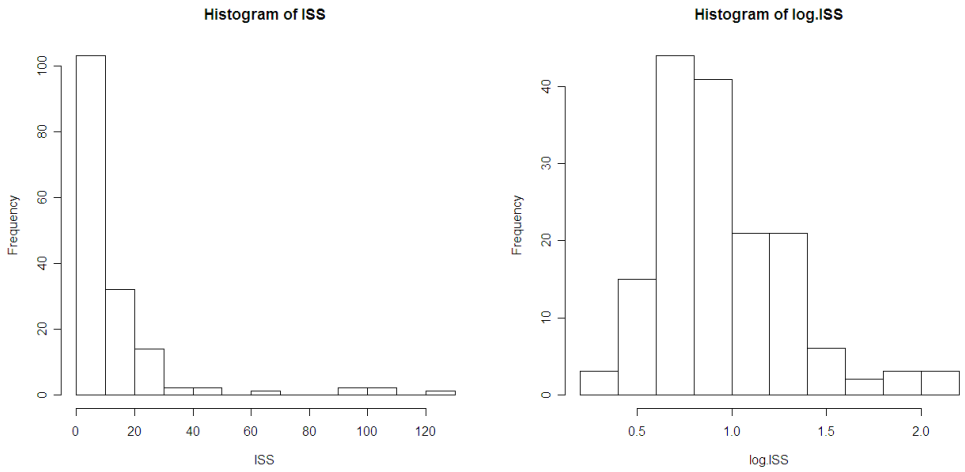

Figure 2.6 Distribution of ISS concentrations (left) and log10 ISS concentrations (right)

An attempt to fit all the data points to a linear model showed considerable scatter (Figure 2.7). A more successful model was achieved by limiting the data to only the points that were measured when the j vector was positive over the trailing 18 hours. This brought all the observed ISS peaks into the fit, and the resulting scatter plot was strongly suggestive of a correlation between wind velocity and the log10 of ISS concentration (Figure 2.8). A linear model between the log10 ISS and the trailing 12 hour average wind velocity gave the best fit, with an R^2 of 0.60.

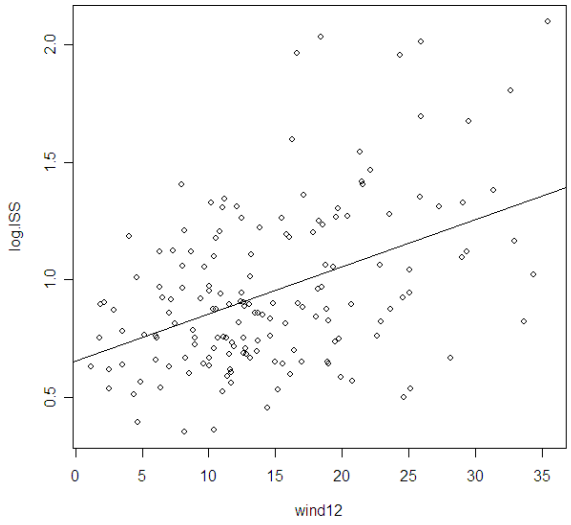

Figure 2.7 Model fit for log ISS concentration versus trailing 12 hour wind velocity

$$\log([\ ISS\ ]) = 0.6537 + 0.02015 \times 12\ \text{hour velocity}$$

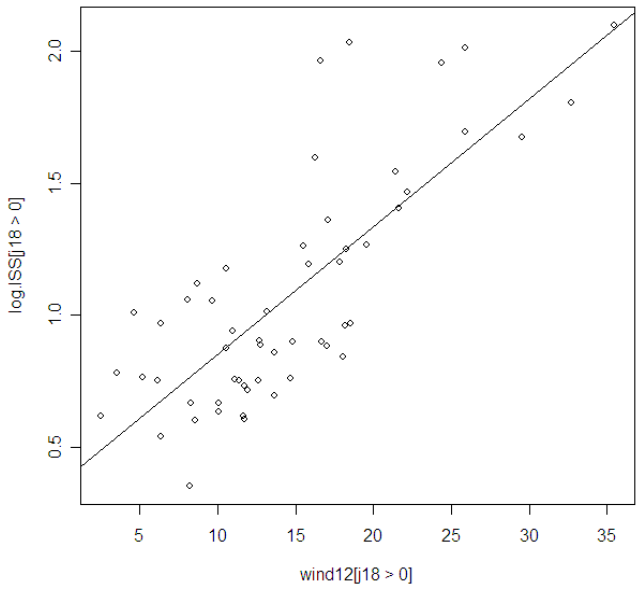

Figure 2.8 Model fit for screened log ISS concentration versus trailing 12 hour wind velocity

$$\log([\ ISS\ ]) = 0.367 + 0.048455 \times 12\ \text{hour velocity}$$

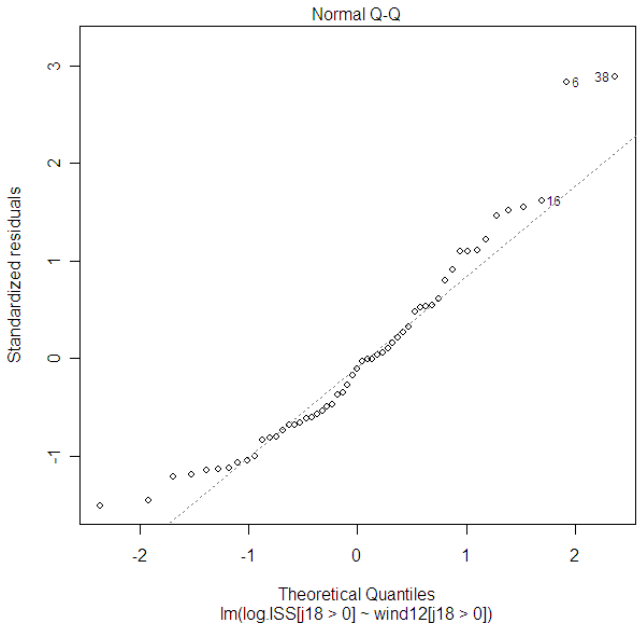

Figure 2.9 Normal Q-Q graph for model fit

While the model was a relatively good predictor of ISS for timepoints where the trailing 18 hour j vector is greater than zero, the remaining data points followed no clear trend (Figure 2.10). The solution chosen was to take the mean of these points: log(10) ISS = 0.883, or ISS concentration = 7.64 mg·L^{-1} where 18 hour j < 0. Therefore, the model becomes:

$$vectorj\ (18\ hour\ ) < 0 : \log\ ISS\ = 0.883$$

$$vectorj\ (18\ hour\ ) > 0 : \log\ ISS\ = 0.367093\ + 0.048455\ \times [12\ hourwindav\ erage\ ]$$

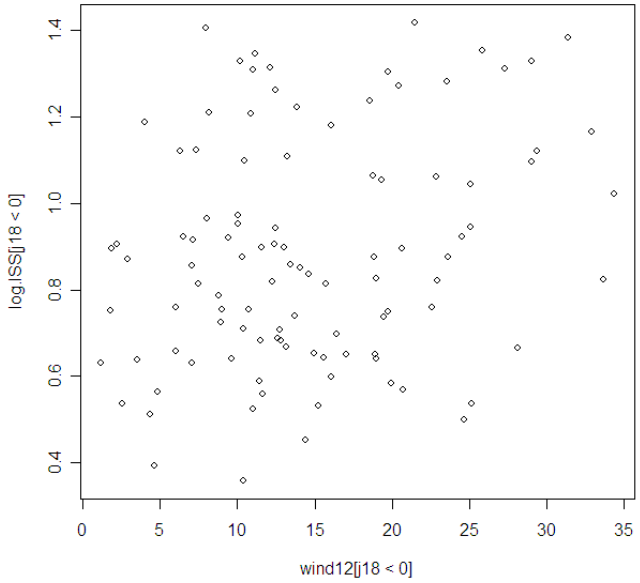

Figure 2.10 Trailing 12 hour wind velocity and rejected ISS data points

2.4.4 Comparison of 2009 season model and samples

The model was used to re-create the ISS response for the 2009 monitoring period, using the wind velocities collected on-site as input data. The predicted ISS values for timepoints corresponding to sample events were compared to the recorded ISS values. With the exception of an early season peak of 108 mg/L ISS on April 1 that was not predicted by the model, the model concentrations generally matched the sample concentrations.

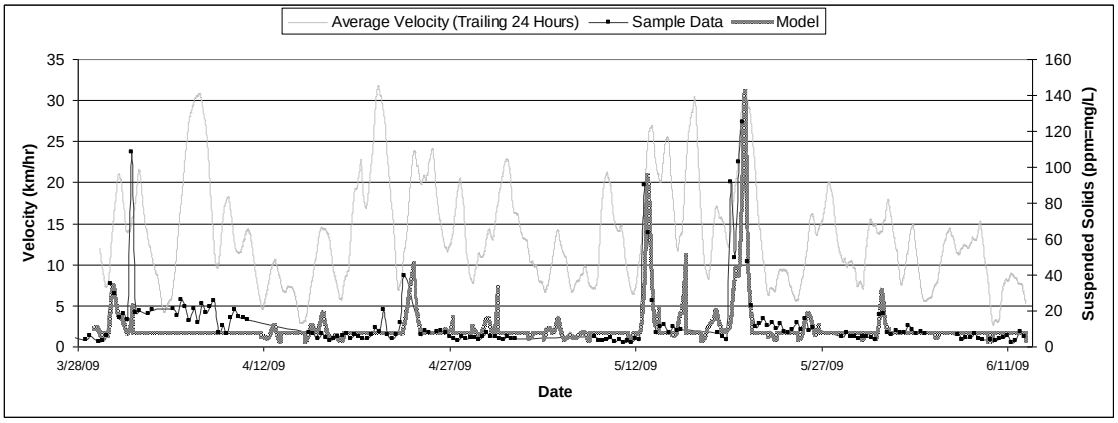

Figure 2.11 Modeled and actual ISS concentrations for 2009 sampling period

The April 1 ISS peak was associated with a period of rapidly shifting winds; beginning on March 30 the wind blew at 20-30 kph from the east for 20 hours, than shifted to the south at 15 kph for 10 hours, then shifted yet again, this time to the west, blowing at about 20-25 kph for the 8 hours preceding the sampling event. The series of changes may have mobilized sediment from many source areas and concentrated it in the southwest end of the wetland, where it was pushed towards the east and crossed the wetland outlet at the time of the sampling event. Although the wind continued to blow at 20-30 kph for the eight hours between the 8 AM sampling event and the 4 PM sampling event, the 4 PM ISS concentration was only 19 $mg \cdot L^{-1}$, a drop of 89 mg/L from the morning sample. This suggested that high concentrations of suspended inorganics at the wetland outlet were the result of sediment that was picked up in other parts of the wetland and transported by wave action towards the wetland outlet, supporting the use of the south wind vector as the best proxy for suspended load at the wetland outlet.

The relationship of suspended sediment with wind generally agrees with the empirical equation for bottom area activation, shown graphically in Figure 2.12. The fetch length for a south wind blowing towards the outlet is approximately 400 meters. South winds of 20 $km \cdot hr^{-1}$ reach a depths of 0.75 meters with 300 meters of fetch, and so can only activate the sediment in the shallow areas near the north shore. Winds of 30 km hr^{-1} are

sufficient to disturb the bottom sediment to depths of one meter with 200 meters of fetch length, activating approximately half of the area in the western lobe of the wetland, while winds of 40 km hr^{-1} activate virtually the entire lobe.

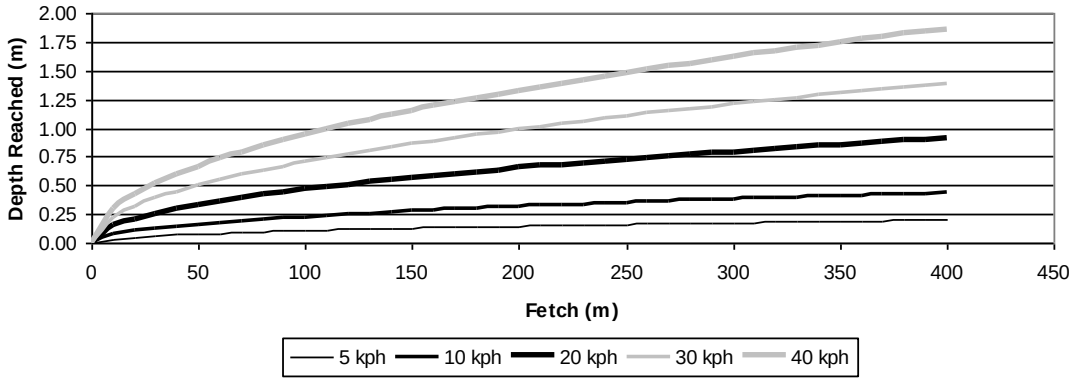

Figure 2.12 Bottom sediment activation curves
Curves are calculated using the formula for bottom activation where wavelength is equal to twice the depth (**Equation 2**).

The model was examined further by comparing estimates of daily ISS concentrations. Sample data was converted to a daily average by calculating the arithmetic mean of the ISS measured in the samples taken by the auto-sampler on that day. Model data was converted to a daily average by calculating the arithmetic mean of the 20-minute time step model estimates for that day. For days where the model concentration was not predicted by wind velocity, (j18 < 0), the daily concentration was generated using a normal distribution (mean=0.883, s.d.=0.263) that approximated the distribution of the log of background sample concentrations (Figure 2.13). The results were also compared to daily estimates calculated from the grab samples using the "Series" function in FLUX (Figure 2.14).

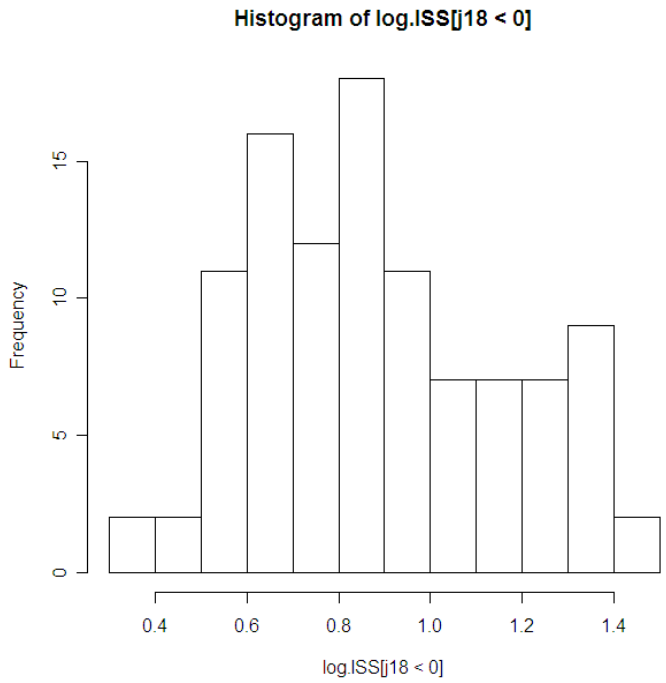

Figure 2.13 Background ISS distribution

A plot of the daily concentrations showed that the model often lags behind the actual concentrations by about a day. This suggests that even though the trailing 18 hour wind average was the best predictor for ISS with the available data, the response may actually be more rapid. More frequent sampling may define a more accurate relationship. The

modeled and actual datasets were compared using a paired t-test, and were found to be not significantly different (p=0.77).

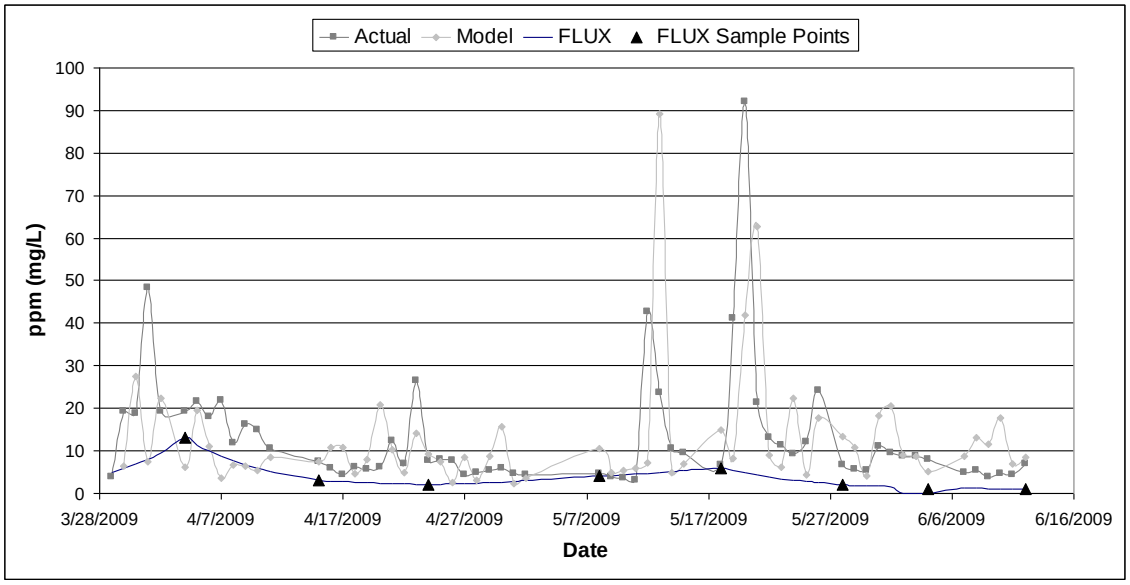

Figure 2.14 Inorganic suspended solids concentration, measured vs. modeled
"Actual" daily concentrations were calculated by averaging the ISS concentration of samples taken by the automatic sampler on that day. "Model" daily concentrations were calculated from the from FLUX values were interpolated using the series function.

Daily loading and total loading were also calculated for each of the three methods. Using the high density sampling, the total ISS loading for the 62 day sampling period was estimated to be 1,430 kg, while the wind-based model estimate was slightly lower at 1,200 kg. However, the FLUX model estimate, 480 kg, was much lower than the other methods. The corresponding FWMC values for the testing period were 15.2 $mg \cdot L^{-1}$, 12.8 $mg \cdot L^{-1}$, and 5.1 $mg \cdot L^{-1}$ for the auto-sampler estimate, wind-based model, and FLUX estimate, respectively. The low estimates of the FLUX model were due to very low inorganic solids concentrations in the grab samples compared to the automated samples, and also to the lack of samples during high wind events. The low concentrations may have been caused by differences in the time of sampling, sampling method or testing method.

2.4.5 Modeling 2007 and 2008 TSS loading

The model was then used to re-construct the Kittleson basin ISS export for the 2007 and 2008 seasons. Wind velocity records with a 20 minute time step were obtained from the Fairmont Municipal Airport, about 20 kilometers to the east of the test site. These tables recorded direction only as one of 8 quadrants: N, NE, etc., so the quadrants were converted to their corresponding degree measurements and assigned a vector as before. To account for site-based differences, airport velocity was scaled according to relationships established by paired readings from April-June 2009. A graph of the wind data and predicted ISS concentrations for the 2007 and 2008 drainage seasons (April 1 to June 30) are shown in Figure 2.15 and Figure 2.16, respectively. The 2007 model underestimated two April peaks that were measured with grab samples as well as one peak in mid-May. The first April peak and the May peak occurred during periods of high north winds, a condition that is modeled as background concentration. The second April peak was during a period of south winds following north winds, and may have been elevated by redistribution of sediment brought into suspension by the earlier peak.

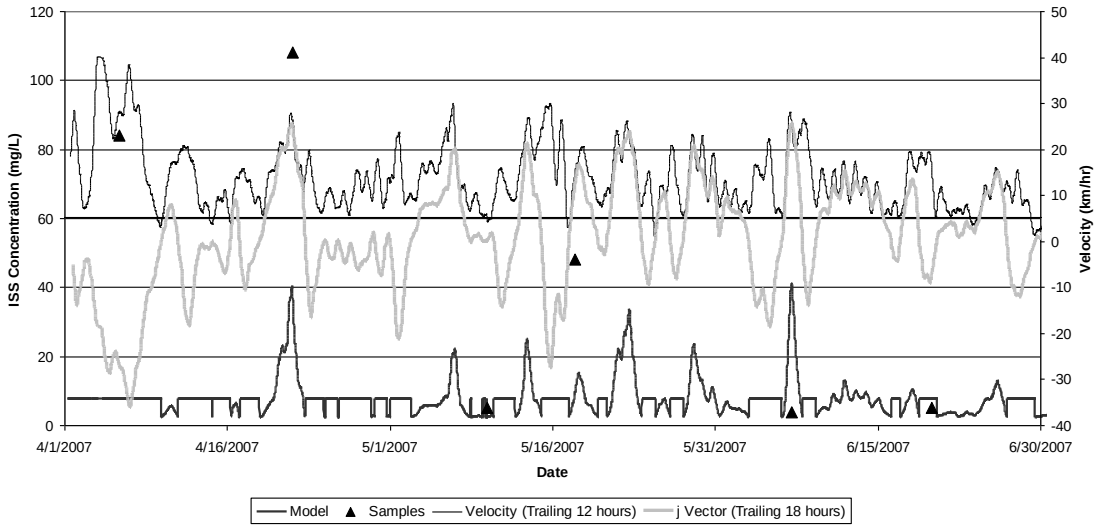

Figure 2.15 2007 season inorganic suspended sediment (ISS) wind model
Model predicted by twenty minute time step wind velocity and wind direction measurements at the Fairmont, Minnesota Municipal Airport. ISS concentration in units of milligrams·Liter^{-1} (parts per million) is shown on the left axis. Wind velocity averaged over the past 12 hours and j vector (180 degrees south = +1) averaged over the past 18 hours are shown on the right axis in kilometers·hour^{-1}.

The 2008 graph shows an underestimated sample event on May 6th. The wetland was very high at the time, approximately 0.6 feet above the level of the control structure trash guard. It is reasonable to assume that high velocity currents flowing over the shallow area near the structure were able to entrain additional sediment. No flows over the level of the trash guard (elevation 1253 feet) were observed during the high density sampling of 2009.

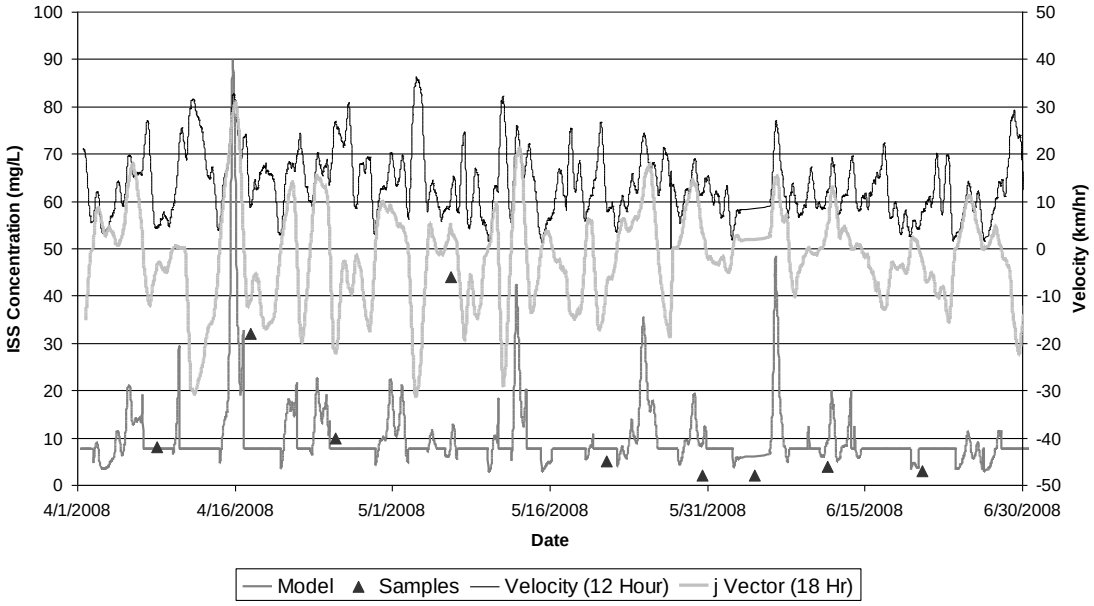

Figure 2.16 2008 season inorganic suspended sediment (ISS) wind model
Model predicted by twenty minute time step wind velocity and wind direction measurements at the Fairmont Municipal Airport. ISS concentration in units of milligrams·Liter^{-1} (parts per million) is shown on the left axis. Wind velocity averaged over the past 12 hours and j vector (180 degrees south = +1) averaged over the past 18 hours are shown on the right axis in kilometers·hour^{-1}.

Daily ISS loads and FWMC the drainage season (April 1 to June 30) were estimated for 2007 and 2008 using two methods: the FLUX software program based on grab samples taken every 10-14 days; and the empirical wind-based model based on data from the Fairmont Municipal Airport. Daily loads were summed to obtain the seasonal loading, then divided by the total discharge volume to obtain FWMC (Figure 2.18). The differences in model results varied from year to year; while FWMC obtained by the FLUX model was 233% higher than the wind based model for year 2007, it was 14% lower in 2008 and 58% lower in 2009. This variation likely arises from interpolation of concentration between widely spaced samples in the FLUX model, making it sensitive to single elevated data points, particularly when the samples are taken during high flow conditions.

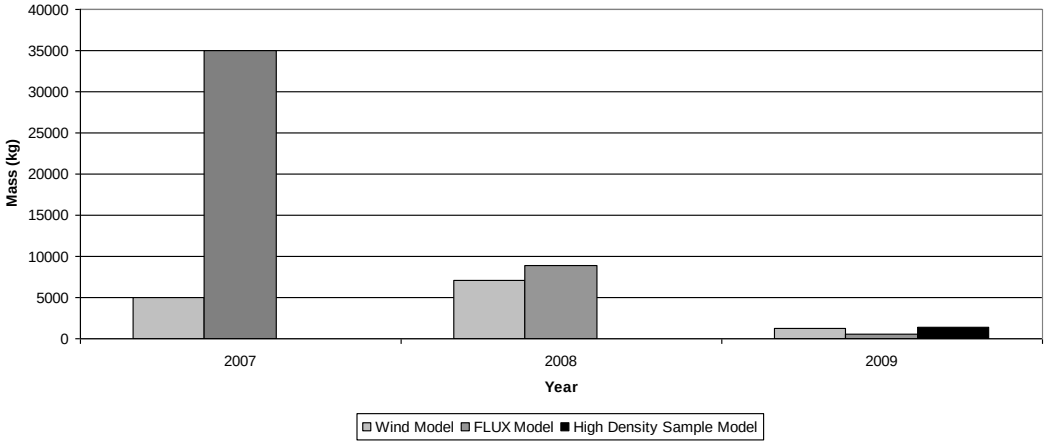

Figure 2.17 Estimated inorganic suspended solids (ISS) seasonal loading
ISS loading was estimated using the wind-based model, the FLUX model, or the high density auto-sampler data. Date ranges are April 1 to June 30 for years 2007 and 2008, and March 30 to June 12 for year 2009. Units are kilograms P.

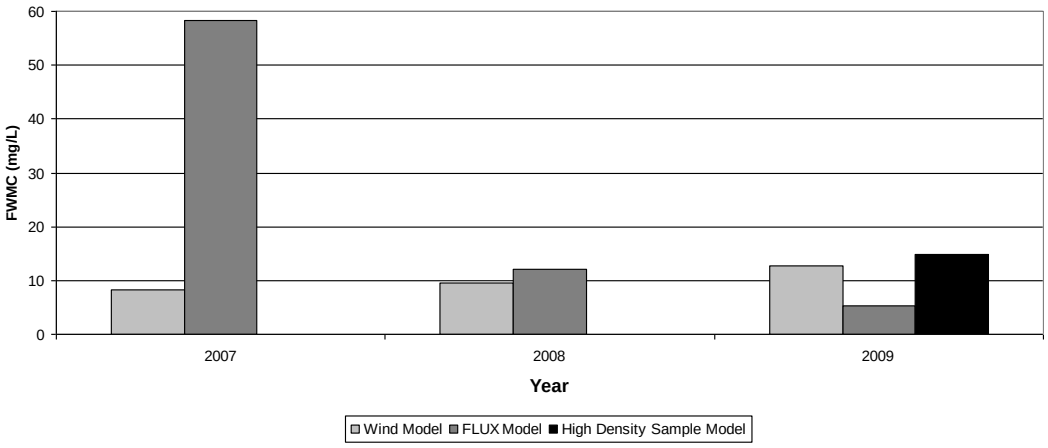

Figure 2.18 Estimated seasonal inorganic suspended solids (ISS) flow weighted mean concentration (FWMC)
ISS loading was estimated using the wind-based model, the FLUX model, or the high density auto-sampler data, then divided by the total flow volume for the period. Date ranges are April 1 to June 30 for years 2007 and 2008, and March 30 to June 12 for year 2009. Units are milligrams P·Liter^{-1} (parts per million).

The high density sample data from 2009 showed that the outflow ISS concentrations were characterized by sharp peaks which were unrelated to discharge, so collecting grab samples at widely spaced intervals is unlikely to produce accurate results. A graph of the daily concentrations for 2007 (Figure 2.19) shows the impact of interpolation on the FLUX model. The April 21 sample was collected on a day when south winds exceeded 50 kilometers·hour^{-1}, influencing ISS concentrations for the periods both before and after the sample date.

Although the 2008 seasonal FWMC estimates were similar for the FLUX and wind-based models, the daily concentration time series (Figure 2.20) shows that this is largely coincidental, as a missed wind event in April was balanced by a sampled event in May.

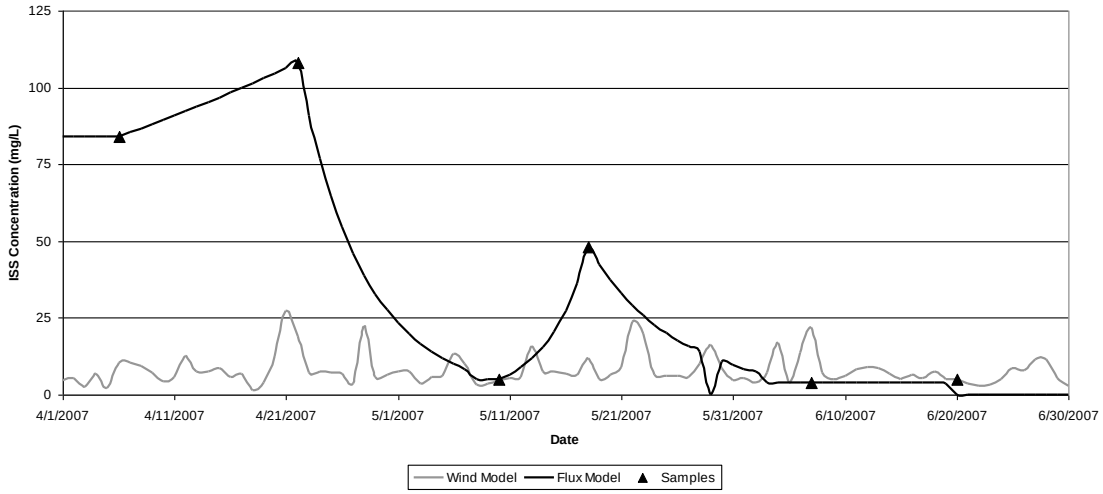

Figure 2.19 Predicted 2007 drainage season ISS (inorganic suspended sediment) Concentrations were modeled with FLUX or the wind-based model using a daily time step. Sample points shown are the grab samples used as input for the FLUX model. Wind-based model was based on velocity readings at the Fairmont airport. Units are milligrams·Liter^{-1}.

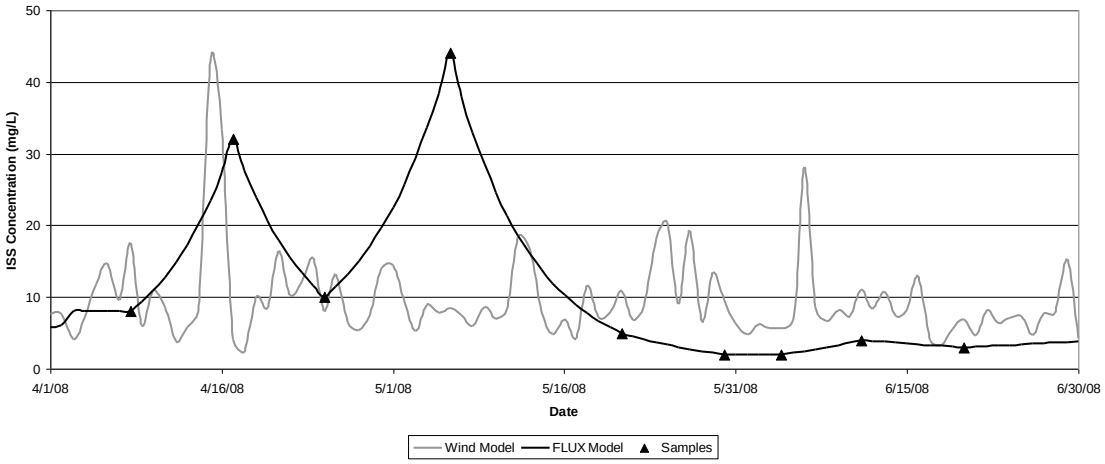

Figure 2.20 Flux and wind-based modeling for 2008 season
Concentrations were modeled with FLUX or the wind-based model using a daily time step. Sample points shown are the grab samples used as input for the FLUX model. Wind-based model was based on velocity readings at the Fairmont airport. Units are milligrams·Liter^{-1}.

2.5 Discussion

Through high-density sampling, we confirmed the anecdotal observations that ISS concentrations were related to wind speed. We found that ISS concentration was heavily influenced by wind direction as well. However, we lacked sufficient data for appropriate model validation, and therefore it was decided to use the TSS estimates obtained from FLUX to compare loading between subwatersheds. It should also be noted that other variables such as the degree of sediment consolidation or the presence of aquatic vegetation can influence the effect of waves on sediment resuspension. Effective use of the wind-based model for other years depends on the existence of similar sediment and vegetation conditions. Since no data on sediment consolidation or aquatic vegetation were recorded as part of the study, we could not assume that these conditions remained constant throughout the study period.

We noted anecdotally that TSS concentrations in the lower SHEEK basin did not seem to be as affected by wind resuspension. It is likely that the irregular shape of the lower SHEEK basin made it less susceptible; although there is sufficient fetch length to allow westerly winds to develop waves that can touch the bottom, the basin is also quite narrow to the west of the outlet. Only winds that blow in the direction parallel to this "arm" of the basin are expected to generate waves sufficient to resuspend sediment and carry it all the way to the outlet.

Because the prairie pothole region is windy and wetlands are not commonly sheltered by trees, other restoration sites are also likely to be influenced by wind in the same fashion. It is clear from this study that unprotected basins are highly susceptible to sediment resuspension, and steps should be taken during the design and restoration process to minimize sediment transport out of the basin.

Summary and Recommendations

The nutrient and sediment dynamics of restored wetlands are complex and subject to natural forces such as precipitation, temperature, and wind, as well as anthropogenic influences such as artificial drainage, tillage, and fertilization practices. Because crop and land prices have risen in recent years due to increased demand for corn and soybean products, it is unlikely that significant portions of the row crop fields on the subwatersheds feeding to the wetlands will be converted to other land uses in the near future. Therefore, the best alternative to minimize sediment and nutrient loading from these or future restorations is to establish a set of "best practices" based on typical weather and land management scenarios.

Emergent vegetation is effective in decreasing sediment resuspension and early season orthophosphate release due to wind (Horppila and Nurminen 2001). However, emergent species such as cattails do not establish well by seed in submerged conditions. During the study period, water levels in the Kittleson basin remained high even during drought years; therefore, emergent vegetation is not likely to become established beyond the littoral zone ((Van der Valk and Davis 1978)). Submerged and floating aquatic species have become established the basin, but these are most abundant in mid to late summer, and are not a significant factor in stabilizing sediment in windy conditions during the critical drainage season, when discharge is highest.

The Kittleson basin was used as a corn field immediately prior to flooding, and although the uplands surrounding the basin were planted with native grasses and shrubs as part of their conversion to CRP lands, no attempt was made to establish wetland vegetation within the basin. In contrast, the associated basin to the southeast had been managed as hunting land, and before flooding, emergent vegetation was able to establish within the basin itself. That vegetation has remained intact to date, even under five years of stable water levels.

Our data suggests that the magnitude of phosphorus export depends on spring temperature and precipitation. In order to minimize phosphorus export, discharge

should be minimized during the period between June 15 (the earliest observed date of TP internal loading) and September 1.

Taken together, improved control of nitrogen, phosphorus, and sediment export in the Kittleson basin could be achieved by a program of water level control. The program should be initiated with a partial drawdown to 1251 feet after September 30. Then, during the June decline of NN and before the late June increase in TP, the wetland should be drawn down further to 1248 or 1248.5 feet. This will expose large mud flat areas to the south of the outlet structure (the most critical source area for wind-aided sediment resuspension). Cattails or other emergent species that can survive in persistently high water levels can then be planted as plugs in that zone. Following an appropriate period to allow establishment, the wetland could then be allowed to fill again. Once emergent vegetation has been established, it will spread via rhizomes and increase in density.

In subsequent years, regular water level management should continue. Regular drawdowns after September 30 will provide additional storage volume for snow melt and for the high water flows of the drainage season. A partial summer drawdown should be initiated in June, but only to 1250 feet, when the boards can be replaced so that summer flows high in phosphorus are prevented. The drawdowns will help to maintain high density emergent vegetation, which will stabilize bottom sediments and increase water loss through evapotranspiration.

References

Atwood D, Bratkovich A, Gallagher M, Hitchcock G. 1994. Papers from NOAA's nutrient enhanced coastal ocean productivity study: Spcial issue. Estuaries 17(4):729-911.

Bailey MC and Hamilton DP. 1997. Wind induced sediment resuspension: A lake-wide model. Ecological Modelling 99(2-3):217-28.

Busman L, Lamb J, Randall G, Rehm G, Schmitt M. 1997. The nature of phosphorus in soils. Saint Paul MN: University of Minnesota, Minnesota Extension Service FO-6795-B .

Carper G and Bachman A. 1984. «Wind resuspension in a small prairie lake». Can J Fish Aquat Sci 41:1763-7.

Crumpton W. 2001. Using wetlands for water quality improvement in agricultural watersheds; the importance of a watershed scale approach. Water Science & Technology 44(11):559-64.

Crumpton W, Stenback G, Miller B, Helmers M. 2006. Potential benefits of wetland filters for tile drainage systems: Impact on nitrate loads to mississippi river subbasins. US Department of Agriculture, CSREES Project Completion Report.Washington, DC: USDA CSREES .

Gachter R, Ngatiah JM, Stamm C. 1998. Transport of phosphate from soil to surface waters by preferential flow. Environ Sci Technol 32(13):1865-9.

Galatowitsch SM and Van der Valk AG. 1998. Restoring prairie wetlands: An ecological approach. Iowa State Pr.

Gelbrecht J and Lengsfeld H. 1998. Phosphorus in fens adjacent to surface waters. Berlin, ISSN-Nr 1432:94-100.

Gentry LE, David MB, Royer TV, Mitchell CA, Starks KM. 2007. Phosphorus transport pathways to streams in tile-drained agricultural watersheds. J Environ Qual 36(2):408.

Goolsby DA, Battaglin WA, Lawrence GB, Artz RS, Aulenbach BT, Hooper RP, Keeney DR, Stensland GJ. 1999. Flux and sources of nutrients in the mississippi-atchafalaya river basin. Task Group 3 Report, Gulf of Mexico Hypoxia Assessment .

Hamilton DP and Mitchell SF. 1996. An empirical model for sediment resuspension in shallow lakes. Hydrobiologia 317(3):209-20.

Helmers M. J., Lawlor P., Baker J. L., Melvin S. and Lemke D. 2005. Temporal subsurface flow patterns from fifteen years in north-central iowa. ASAE meeting paper.

Hinck PJ. 2008. Evapotranspiration measurement and modeling for annual and perennial crops in south-central minnesota. University of Minnesota.

Horppila J and Nurminen L. 2001. The effect of an emergent macrophyte (typha angustifolia) on sediment resuspension in a shallow north temperate lake. Freshwat Biol 46(11):1447-55.

Hutchinson S, Koelliker J, Knapp A. 2008. Technical note: Development of water usage coefficients for a fully watered tallgrass prairie. Trans ASAE 51(1):153-9.

Jin C and Sands G. 2003. The long-term field-scale hydrology of subsurface drainage systems in a cold climate. Trans ASAE 46(4):1011-21.

Kladivko EJ, Grochulska J, Turco RF, Van Scoyoc GE, Eigel JD. 1999. Pesticide and nitrate transport into subsurface tile drains of different spacings. J Environ Qual 28(3):997-1004.

Kristensen P, Søndergaard M, Jeppesen E. 1992. Resuspension in a shallow eutrophic lake. Hydrobiologia 228(1):101-9.

Lenhart CF. 2008. The influence of watershed hydrology and stream geomorphology on turbidity, sediment and nutrients in tributaries of the blue earth river, minnesota, USA. Thesis (Ph. D.)--University of Minnesota, 2008. Major: Water resources science.

Loeb R, Lamers LPM, Roelofs JGM. 2008. Prediction of phosphorus mobilisation in inundated floodplain soils. Environmental Pollution 156(2):325-31.

Lorenz DL, G.H. Carlson, C.A. Sanocki. 1997. Techniques for estimating peak flow on small streams in minnesota. USGS Water-Resour. Investigations Rep. 97-4249 .

Lowrance RR, Todd RL, Asmussen LE. 1984. Nutrient cycling in an agricultural watershed: II. streamflow and artificial drainage. J Environ Qual 13(1):27.

Luo HR, Smith LM, Allen B, Haukos DA. 1997. Effects of sedimentation on playa wetland volume. Ecol Appl 7(1):247-52.

Macrae ML, English MC, Schiff SL, Stone M. 2007. Intra-annual variability in the contribution of tile drains to basin discharge and phosphorus export in a first-order agricultural catchment. Agricultural Water Management, 92(3):171-82.

Magette WL, Brinsfield RB, Palmer RE, Wood JD. 1989. Nutrient and sediment removal by vegetated filter strips. Trans ASAE 32(2):663-7.

Magner J. and Steffen L. 2004. Stream morphological response to climate and land-use in the minnesota river basin. ASCE.

Magner J, Payne G, Steffen L. 2004. Drainage effects on stream nitrate-N and hydrology in south-central minnesota (USA). Environ Monit Assess 91(1):183-98.

Mao D and Cherkauer KA. 2009. Impacts of land-use change on hydrologic responses in the great lakes region. Journal of Hydrology 374(1-2):71-82.

Minnesota Board of Water and Soil Resources. 2004a. Engineer's report for elm creek and rosenberg wetlands. .

Minnesota Board of Water and Soil Resources. 2004b. Engineer's report for kittleson wetland. .

Minnesota Board of Water and Soil Resources. 2004c. Minnesota river CREP fact sheet. .

Minnesota Pollution Control Agency. 2008. 303(d) total maximum daily load (TMDL) list. .

Minnesota Pollution Control Agency. 1998. Phosphorus in the minnesota river. St. Paul, Minn.: [St. Paul, Minn.] : Minnesota Pollution Control Agency : Minnesota River Basin Joint Powers Board.

Mulqueen J, Rodgers M, Scally P. 2004. Phosphorus transfer from soil to surface waters. Agricultural Water Management 68(1):91-105.

Payne G. 1994. Sources and transport of sediment, nutrients, and oxygen demanding substances in the minnesota river basin, 1989-1992. Minnesota River Assessment Project Report.Physical and Chemical Assessment 2.

Quade H. 2000. BLUE EARTH RIVER MAJOR WATERSHED DIAGNOSTIC REPORT. .

Randall GW, Iragavarapu TK, Evans SD. 1997. Long-term P and K applications. I. effect on soil test incline and decline rates and critical soil test levels. Journal of Production Agriculture (USA) .

Raymond PA, Oh NH, Turner RE, Broussard W. 2008. Anthropogenically enhanced fluxes of water and carbon from the mississippi river. Nature 451(7177):449-52.

Reddy KR. 2008. Biogeochemistry of wetlands. Crc Press.

Riedel MS, Verry ES, Brooks KN. 2005. Impacts of land use conversion on bankfull discharge and mass wasting. Journal of Environmental Management, 76(4):326-37.

Sands G, Song I, Busman L, Hansen B. 2008. The effects of subsurface drainage depth and intensity on nitrate loads in the northern cornbelt. Trans ASAE 51(3):937-46.

Scheffer M. 1998. Ecology of shallow lakes. Springer.

Schilling KE. 2005. Relation of baseflow to row crop intensity in iowa. Agriculture, Ecosystems and Environment 105(1-2):433-8.

Senjem N. 1997. Minnesota river basin information document. Minnesota Pollution Control Agency, St.Paul .

Sheng YP and Lick W. 1979. The transport and resuspension of sediments in a shallow lake. Journal of Geophysical Research 84:1809-26.

Sondergaard M, Kristensen P, Jeppesen E. 1992. Phosphorus release from resuspended sediment in the shallow and wind-exposed lake arreso, denmark. Hydrobiologia 228(1):91-9.

Stamm C, Fluhler H, Gachter R, Leuenberger J, Wunderli H. 1998. Preferential transport of phosphorus in drained grassland soils. J Environ Qual 27(3):515.

Turner RE, Rabalais NN, Justic D. 2008. Gulf of mexico hypoxia: Alternate states and a legacy. Environ Sci Technol 42(7):2323-7.

Twine TE, Kucharik CJ, Foley JA. 2004. Effects of land cover change on the energy and water balance of the mississippi river basin. J Hydrometeorol 5(4):640-55.

United States Congress. 1985. The food security act of 1985 (title XII, subtitle C). 198(99).

US Army Coastal Engineering Research Center. 1977. Shore protection manual. U.S. Army Coastal Engineering Research Center 1.

Van der Valk AG and Davis CB. 1978. The role of seed banks in the vegetation dynamics of prairie glacial marshes. Ecology 59(2):322-35.

Walker WW. 1996. Simplified procedures for eutrophication assessment & prediction: User manual instruction report W-96-2. USAE Waterways Experiment Station, Vicksburg, Mississippi .

Wetzel RG. 1975. Limnology. Saunders Philadelphia.

Zak D, Gelbrecht J, Steinberg C. 2004. Phosphorus retention at the redox interface of peatlands adjacent to surface waters in northeast germany. Biogeochemistry 70(3):357-68.

Appendix A. Water Quality Summary

Table A.1 Drainage season nitrate+nitrate-N (NN) flow weighted mean concentration (FWMC)

	FWMC ($mg \cdot L^{-1}$)						
Year	W2 Surface	W2 Tile	W4 Surface	W4 Tile	W5	S1	S2
2005	19.3	21.2	14.1	24.2	2.9	0.2	3.9 [a]
2006	10.1	18.9	15.5	18.0	3.6	0.1	NA[b]
2007	14.9	16.7	13.9	18.0	3.3	0.2	3.5[c]
2008	16.9	18.1	NA	20.4	4.3	0.3	7.3

[a]Flow monitoring began on 4/29

[b]Flow monitoring began on 7/5

[c]Flow monitoring began on 5/18

Table A.2 Drainage season nitrate+nitrate-N (NN) loading

	Load (kg)						
Year	W2 Surface	W2 Tile	W4 Surface	W4 Tile	W5	S1	S2
2005	694	3143	268	3838	2767	56	5418[a]
2006	860	3237	919	751*	2180	77	NA[b]
2007	43	1117	3528	519*	1416	58	434[c]
2008	679	5672	0	1318*	3002	99	14054

*Underestimated due to water loss at tile leak

[a]Flow monitoring began on 4/29

[b]Flow monitoring began on 7/5

[c]Flow monitoring began on 5/18

Table A.3 ET season nitrate+nitrate-N (NN) flow weighted mean concentration (FWMC)

	FWMC ($mg \cdot L^{-1}$)						
Year	W2 Surface	W2 Tile	W4 Surface	W4 Tile	W5	S1	S2
2005	9.7	17.1	14.1	19.8	0.1	< 0.1	4.1
2006	0.0	16.3	18.0	15.2	0.0	< 0.1	3.5
2007	13.3	11.4	9.1	13.7	3.3	1.7	6.5
2008	0.0	18.4	0.0	20.6	0.8	0.0	4.4

Table A.4 ET season nitrate+nitrate-N (NN) loading

	Load (kg)						
Year	W2 Surface	W2 Tile	W4 Surface	W4 Tile	W5	S1	S2
2005	571	511	609	888	50	4	2289
2006	0	107	250	272*	0	2	905
2007	43	44	25	51*	160	7	244
2008	0	687	0	450*	119	0	1582

*Underestimated due to water loss at tile leak

Table A.5 Drainage season orthophosphate (OP) flow weighted mean concentration (FWMC)

	FWMC ($mg \cdot L^{-1}$)						
Year	W2 Surface	W2 Tile	W4 Surface	W4 Tile	W5	S1	S2
2005	0.592	0.022	0.564	0.056	0.118	0.198	0.254[a]
2006	0.157	0.026	0.195	NA	0.006	0.041	NA[b]
2007	NA	0.007	0.114	NA	0.026	0.046	0.091[c]
2008	0.744	0.035	NA	0.008	0.150	0.094	0.223

[a]Flow monitoring began on 4/29

[b]Flow monitoring began on 7/5

[c]Flow monitoring began on 5/18

Table A.6 Drainage season orthophosphate (OP) loading

	Loading (kg)						
Year	W2 Surface	W2 Tile	W4 Surface	W4 Tile	W5	S1	S2
2005	34.4	3.2	10.8	8.8	113.8	51.9	351.4[a]
2006	3.9	4.5	5.2	0.0*	3.8	27.8	NA[b]
2007	0.0	0.5	18.8	0.0*	11.2	15.3	11.2[c]
2008	42.0	10.9	NA	0.5*	29.4	12	311.3

*Underestimated due to water loss at tile leak

[a]Flow monitoring began on 4/29

[b]Flow monitoring began on 7/5

[c]Flow monitoring began on 5/18

Table A.7 ET season orthophosphate (OP) flow weighted mean concentration (FWMC)

	FWMC ($mg \cdot L^{-1}$)						
Year	W2 Surface	W2 Tile	W4 Surface	W4 Tile	W5	S1	S2
2005	0.171	0.039	0.563	0.026	0.326	0.154	0.191
2006	NA	0.000	0.202	0.000	0.359	0.163	0.210
2007	NA	0.000	NA	0.000	0.061	0.142	0.332
2008	NA	0.000	NA	0.000	0.199	0.112	0.157

Table A.8 ET season orthophosphate (OP) loading

	Loading (kg)						
Year	W2 Surface	W2 Tile	W4 Surface	W4 Tile	W5	S1	S2
2005	10.4	1.2	24.4	1.2	134.8	35.7	107.3
2006	0.0	0.0	2.8	0.0*	36.2	23.6	54.7
2007	0.0	0.0	0.0	0.0*	4.8	0.7	16.9
2008	0.0	0.0	0.0	0.0*	50.5	19.6	70.0

*Underestimated due to water loss at tile leak

Table A.9 Drainage season total phosphorus (TP) flow weighted mean concentration (FWMC)

	FWMC ($mg \cdot L^{-1}$)						
Year	W2 Surface	W2 Tile	W4 Surface	W4 Tile	W5	S1	S2
2005	0.434	0.022	0.440	0.056	0.182	0.260	0.351[a]
2006	0.782	0.028	0.409	0.000	0.087	0.088	NA[b]
2007	0.432	0.007	0.436	0.000	0.321	0.110	0.142[c]
2008	0.749	0.062	NA	0.008	0.150	0.094	0.223

[a]Flow monitoring began on 4/29

[b]Flow monitoring began on 7/5

[c]Flow monitoring began on 5/18

Table A.10 Drainage season total phosphorus (TP) loading

	Loading (kg)						
Year	W2 Surface	W2 Tile	W4 Surface	W4 Tile	W5	S1	S2
2005	15.6	3.2	8.4	8.8	175.1	68.1	486.6[a]
2006	66.5	4.8	24.2	0.0*	52.6	59.4	NA[b]
2007	1.24	0.5	110.4	0.0*	136.6	36.2	17.4[c]
2008	30.1	19.4	0	0.5*	103.6	34.5	431.1

*Underestimated due to water loss at tile leak

[a]Flow monitoring began on 4/29

[b]Flow monitoring began on 7/5

[c]Flow monitoring began on 5/18

Table A.11 ET season total phosphorus (TP) flow weighted mean concentration (FWMC)

	FWMC ($mg \cdot L^{-1}$)						
Year	W2 Surface	W2 Tile	W4 Surface	W4 Tile	W5	S1	S2
2005	0.806	0.039	0.655	0.434	0.363	0.205	0.213
2006	NA	0.000	0.224	0.375	0.514	0.240	0.243
2007	0.095	0.000	NA	0.221	0.122	0.166	0.161
2008	NA	0.000	NA	0.000	0.323	0.167	0.194

Table A.12 ET season total phosphorus (TP) loading

	Loading (kg)						
Year	W2 Surface	W2 Tile	W4 Surface	W4 Tile	W5	S1	S2
2005	47.4	1.2	28.4	18.8	150.4	47.4	119.7
2006	0	0.0	3.1	5.2*	51.8	34.7	63.4
2007	0.31	0.0	0.0	0.6*	4.8	0.7	6.0
2008	0	0.0	0.0	0.0*	50.5	19.6	70.0

*Underestimated due to water loss at tile leak

Table A.13 Drainage season total suspended solids (TSS) flow weighted mean concentration (FWMC)

	FWMC ($mg \cdot L^{-1}$)						
Year	W2 Surface	W2 Tile	W4 Surface	W4 Tile	W5	S1	S2
2005	46.2	0.0	198.1	0.0	24.1	5.3	10.0[a]
2006	122.7	0.0	143.1	1.3	6.7	3.7	NA[b]
2007	6.1	0.7	203.7	7.9	23.4	11.9	2.4[c]
2008	32.7	0.2	NA	0.1	21.3	6.3	4.8

[a]Flow monitoring began on 4/29

[b]Flow monitoring began on 7/5

[c]Flow monitoring began on 5/18

Table A.14 Drainage season total suspended solids (TSS) loading

	Loading (kg)						
Year	W2 Surface	W2 Tile	W4 Surface	W4 Tile	W5	S1	S2
2005	1660	0	3780	0.6	23213	1379	13824[a]
2006	10436	2	8468	56*	4070	2526	NA[b]
2007	17	46	51619	229*	9963	3938	293[c]
2008	1313	65	0	6.6*	14700	2335	9267

*Underestimated due to water loss at tile leak

[a]Flow monitoring began on 4/29

[b]Flow monitoring began on 7/5

[c]Flow monitoring began on 5/18

Table A.15 ET season total suspended solids (TSS) flow weighted mean concentration (FWMC)

	FWMC ($mg \cdot L^{-1}$)						
Year	W2 Surface	W2 Tile	W4 Surface	W4 Tile	W5	S1	S2
2005	265.0	0.0	202.8	0.0	0.5	2.5	4.1
2006	NA	0.1	78.5	0.5	20.9	6.8	3.5
2007	4.0	0.0	23.2	4.0	17.3	1.3	8.5
2008	NA	0.1	NA	0.0	9.6	1.0	3.0

Table A.16 ET season total suspended solids (TSS) loading

	Loading (kg)						
Year	W2 Surface	W2 Tile	W4 Surface	W4 Tile	W5	S1	S2
2005	15586	0	8784	0	223	567	2287
2006	0	< 1	1088	9*	2107	987	909
2007	13	< 1	63	15*	679	5	316
2008	0	4	0	0*	1493	118	1076

*Underestimated due to water loss at tile leak